(19) Europäisches Patentamt
European Patent Office
Office européen des brevets

(11) **EP 3 222 350 A1**

(12) **EUROPEAN PATENT APPLICATION**

(43) Date of publication:
27.09.2017 Bulletin 2017/39

(51) Int Cl.:
B01L 3/00 *(2006.01)*

(21) Application number: **16161648.7**

(22) Date of filing: **22.03.2016**

(84) Designated Contracting States:
AL AT BE BG CH CY CZ DE DK EE ES FI FR GB GR HR HU IE IS IT LI LT LU LV MC MK MT NL NO PL PT RO RS SE SI SK SM TR
Designated Extension States:
BA ME
Designated Validation States:
MA MD

(71) Applicant: **ETH Zurich**
8092 Zurich (CH)

(72) Inventors:
- **VÖRÖS, Janos**
  8050 Zurich (CH)
- **ZAMBELLI, Tomaso**
  8044 Zürich (CH)
- **MARTINEZ, Vincent**
  8002 Zurich (CH)

(54) **FLEXIBLE HOLLOW NEEDLES AND CANTILEVERS AND METHOD FOR MAKING THEREOF**

(57) The present invention relates to a device comprising a flexible shank, and the shank comprises a microfluidic channel having an aperture, particularly a hollow flexible needle, more particularly a flexible micropipette or a flexible, hollow cantilever, and a method for manufacturing thereof, wherein the method comprises a layer-by-layer deposition and curing, wherein the microfluidic channel is formed by means of a sacrificial filing body layer made of metal. Hereby are described the production of complex tip shapes in parallel and additionally, the integration of force sensing onto the devices.

Fig. 15

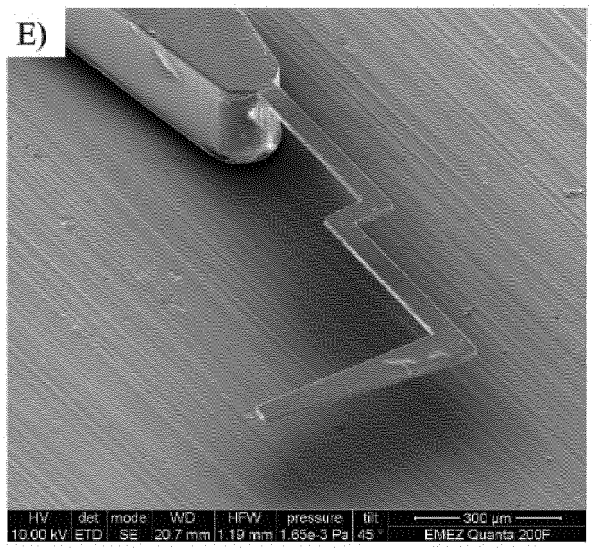

EP 3 222 350 A1

Description

[0001] The present invention relates to flexible, hollow devices, particularly microneedles or hollow cantilevers with complex tip shape and integrated force sensor, and methods of manufacture and uses thereof.

[0002] Micropipette-based technologies represent still today the simplest approach for cell injections and manipulations in general. Most techniques for the fabrication of micopipettes are low throughput and rely on heating and pulling principles. They are limited to tubular and straight tips and are therefore not compatible with the realization of tips with complex geometries such as comers, high curvature and several cm in length. Furthermore, conventional micropipettes are usually fabricated of brittle materials (e.g. glass).

[0003] A further technology targeting single-cell applications evolved from the Atomic Force Microscopy (AFM) technology. Integrating a microchannel into an AFM cantilever allowed broadening the spectrum of AFM applications in liquid towards a force-controlled nanopipette enabling novel range of applications such as controlled spatial manipulation, local injection and dispensing, selective and massive force spectroscopy, and serial perturbation experiments.

[0004] AFM cantilevers are usually made of silicon or silicon nitride, which exhibit high Young's moduli (190 and 385 GPa, respectively). For biological applications, cantilevers are mostly operating in liquid environment with contact mode where a low spring constant is desirable to be less invasive on fragile biomaterials. Replacing silicon by soft polymeric material would allow higher sensitivity for the same considered channel and cantilever thicknesses. On the other hand, thicker channel and cantilever dimensions could potentially enable a larger range of microfluidic applications with similar force detection sensitivity to conventional silicon-based AFM cantilevers.

[0005] SU-8 (IBM) is known as the negative-tone photoresist with the highest available epoxide functionality for its eight epoxy sites per monomer component. Thanks to the strongly cross-linked nature of this photoplastic material, SU-8 exhibits important mechanical stability as well as chemical resistance to a multitude of solutions, which makes it a good candidate for robust microfluidic systems. SU-8 does not only present advantages in terms of surface chemistry with the possibility of multiple surface functionalisations but also, physical surface modification by laser or plasma treatment among others.

[0006] Furthermore, the SU-8 presents other interesting features: low Young's modulus of 4.5 GPa, transparent material, ease to tailor the thickness down to 500 nm simply by spin-coating, and high aspect-ratio structuring (> 18). Finally, SU-8 can be also directly photo patterned allowing complex designs and potential mass fabrication. After optimization of a working fabrication process, it is rather simple to adapt the design of the device directly by changing the photolithography masks. If one takes into account the formula for the spring constant of a cantilever, geometrical dimensions of the cantilever contribute more to the final stiffness in the case of SU-8 because of its lower Young's Modulus compared to silicon. This provides the possibility for the fabrication of devices with a wider spectrum of spring constants on the same wafer.

[0007] First polymer-based AFM cantilevers were fabricated in 1999 by means of a simple batch process where the integrated tip and the lever were obtained in one photolithography step (IBM). They showed a resolution comparable to that of standard silicon cantilevers. Later on, polymer-based cantilevers were used as highly sensitive stress sensors.

[0008] In addition, for a gentle single-cell patterning by a micropipette or a hollow cantilever, the use of a force sensor within or at the micropipette or the hollow cantilever is advantageous to avoid the application of too excessice forces on the single cell. Similarly for single-cell injection, a force sensor can help to rupture gently the membrane, maximizing therefore the rate of cell recovery. However, most force sensors are based on laser reflective methods, which are therefore invasive and nonusable in surgical environment.

[0009] Based on this background it is the objective of the present invention to provide flexible hollow micropipettes or cantilevers that are particularly suitable for manipulating microscopic objects, particularly single cells, in the submicrometer range, as well as methods for making those.

[0010] The objective is attained by the subject matter of the independent claims. Preferred embodiments of the invention are further specified in the dependent claims and described below.

[0011] The present invention is particularly based on the on the novel concept that metal may be used as sacrifial filling material in a photolithographic process using photoresists for the manufacturing of devices in the micrometer scale with microfludic channels. Furthermore, the concept of fabricating a thick hollow needle layer-by-layer, from a side to another, is newly introduced. Thereby, it is possible to provide new designs of flexible hollow needles that particularly overcome the limitations of glass micropipettes in terms of tip geometry, fluidic robustness and fabrication throughput.

[0012] According to a first aspect of the invention, a method for manufacturing a device comprising a flexible shank is provided, wherein the shank comprises a microfluidic channel and an aperture, which is in fluid communication with microfluidic channel.

[0013] The method comprises the steps of:

- providing a support covered by a sacrificial release layer;
- depositing a bottom layer of a first photoresist onto said sacrificial release layer;
- partially curing the bottom layer within a first defined pattern, thereby yielding a bottomside or a first sidewall of the device comprising the flexible shank,

wherein the bottomside optionally comprises the aperture;

- depositing a metal seed layer onto the bottom layer, and particularly onto the sacrificial layer not covered by the bottom layer;
- depositing a mould layer of a second photoresist onto the metal seed layer,
- curing the mould layer within a second defined pattern, thereby yielding a cured mould layer, wherein a part of the metal seed layer covering the bottom layer is not covered by the cured mould layer, and the cured mould layer forms the mould that later defines the microfluidic channel and optionally the aperture and/or a reservoir in fluid communication with the microfluidic channel;
- depositing an additional metal layer onto the part of the metal seed layer not covered by the cured mould layer, whereby particularly the additional metal layer defines the space of the microfluidic channel, and optionally of the aperture and/or of the reservoir in fluid communication to the microfluidic channel;
- dissolving the second photoresist or the mould layer, and the metal seed layer;
- depositing a cover layer of the first photoresist onto the bottom layer and the additional copper layer;
- completely curing the first photoresist comprised within the cover layer and the bottom layer within a third defined pattern, thereby forming sidewalls and a topside of the device or a bottomside, a second sidewall opposite to the first sidewall and a topside of the device, whereby the topside or the second sidewall opionally comprises an opening, the cover layer merge with the bottom layer such that at least one part of the first photoresist delimiting the microfluidic channel is integrally formed in one piece, and the bottomside, the sidewalls and the topside embrace the additional metal layer optionally with the exception of the opening or the aperture;
- dissolving the additional metal layer yielding the microfluidic channel and optionally the aperture and/or the reservoir, wherein optionally the opening comprised within the topside or the second sidewall of the device is in fluid communication with the microfluidic channel, or optionally with the reservoir; and
- dissolving the sacrificial release layer releasing the device from the support.

[0014] Advantageously, the method of the invention enables the access to new designs of flexible hollow needles, whose tip can be made of a complex shape by mass production. By the method of the invention, a high throughput fabrication of needles with complex tip shape (corners or high curvature) is enabled, on the contrary of individually made glass micropipettes. The fabrication relies on a layer-by-layer photolithography process where bottom or side layer, channel and top or second side layer are accordingly patterned in a three-step protocol.

[0015] Advantageously, the device of the invention may be produced with the method of the invention from bottom to top or it may be fabricated sideways from a side to another. The sideways fabrication offers more possibilities to get a sharp tip with high curvature, e.g. for single-cell injection or for biopsy-like applications.

[0016] The term "shank" in the context of the present specification particularly refers to a structural element that houses a microfluidic channel and an aperture being in fluidic communication with the microfluidic channel. The shank may be designed as a beam of a hollow cantilever or a shank of a micropipette.

[0017] The term "photoresists" in the context of the present specification particularly refers to a viscous composition essentially consisting of, or comprising, a species of photoreactively polymerisable or depolymerisable compounds, and optionally comprising a solvent, wherein particularly the viscous composition is characterized by a viscosity of at least 100 cSt (centi Stokes), for example in range of 100 cSt to 500 cSt or 10,000 cSt to 60,000 cSt.

[0018] Such photoreactive compounds may polymerise or be cross-linked upon light expore, such as the monomers comprised within a negative photoresists. Such photoreactive compound may also depolymerise upon light exposure, for example by cleavage of cross-link bondings, such as compounds comprised within a positive photoresist.

[0019] The term "curing" is used in the context of the present specification in the meaning known to the skilled person. It particularly refers to the process of solidifying of the above-mentioned photoresists or the above-mentioned visous composition by means of light exposure (triggering cross-linking reactions) and/or heat (for evaporating a solvent optionally present in the photoresists or the viscous composition). Curing may also comprise the post-exposure bake, developing by contacting the cured photoresists with a solvent such as propylene glycol monomethyl ether acetate, and rising with an organic solvent such as isopropanol or acetone, thereby removing unpolymerised photoresists. In case of a negative photoresist, a post exposure bake may be important to complete the photo-activation process.

[0020] Furthermore, "curing within a defined pattern" means in the context of the present specification that the photoresist layer is exposed to light (particularly light in the ultraviolet region) within the defined pattern resulting in polymerization of the photoresist within the pattern, in case of a negative photoresist, or in case of a positive photoresist in depolymerisation of the photoresist within the pattern and curing of the photoresist outside of the pattern.

[0021] The term "partly curing" in the context of the present specification particularly means that the respective photoresist layer is cured in such a manner that only a fraction of the photoresist is cured, or in other words, that part of the photoresist monomers remains reactive for further polymerisation. Avantageously, a partly cured photoresists layer may be connected with another pho-

toresist layer such that both layer are integrally formed in one piece.

[0022] Particularly, such partly curing of the bottom layer may be achieved by limited light exposure and/ or reduced baking time of the bottom layer.

[0023] By forming the part of the device of the invention delimiting the microfluidic channel intergrally in one piece, the microfluidic channel is characterized by complete tightness or perfect sealing while applying pressure to the channel, particularly up to 6 bar. Additionally, the integrally one-piece design of the device avoids problems such as delamination of the device or adhesion issues.

[0024] In certain embodiments, the first photoresist comprised within the partly cured bottom layer and the cover layer is completely cured such that at least a part of the cured photoresist delimiting the microfluidic channel exhibits a homogenous structure.

[0025] The above-mentioned metal seed layer has the advantage that the metal seed layer effectively separates the partly cured bottom layer of the device from the mould layer, thereby avoiding undesired interaction between the aforementioned layers. Additionally, in case of the bottom layer in made of a negative photoresist and the mould layer is made of a positive photoresist, the bottom layer is shielded by the metal seed layer from light exposure during the curing of the mould layer, thereby avoiding complete curing of the bottom layer.

[0026] An advantage of using the metal layer as sacrifical filing body that later defines the microfluidic channel and optionally the aperture and/or the reservoir is that the deposition of the additionally metal layer can be performed under conditions, under which a complete curing of the bottom layer can be avoided, in contrast to the use of, for example, expoxy or polydimethylglutaridimide as sacrifical filing material, wherein the high temperatures being applied to evaporate the solubilizing solvent can lead to an undesired complete curing of the bottom layer. Additionally, the additional metal layer does not exhibit any undesired interactions with the first photoresist and is furthermore easily removable. Particularly, the metal doesn't dissolve into the freshly spin-coated cover photoresist, which may comprise a solvent, particularly when the photoresist layer hasn't undergone baking until complete solvent evaporation. Without the additional metal layer, the freshly spin-coated mould layer may directly dissolve the patterned and only partly cured bottom layer.

[0027] Alternatively, instead of metal any material, for example a viscous ink or a liquid plastic, may be used as sacricial filling body that does not interact with the first photoresist and optionally can be cured under condition that avoids complete curing of the bottom layer and/or shields the bottom layer form light exposure during curing of the mould layer and/or is easily removable.

[0028] Particularly, the mould layer is cured such under such conditions that a complete curing of the bottom layer is avoided, e.g. by reducing the baking time of the mould layer.

[0029] Particularly, the second defined pattern defines the shape of mould that later defines the shape and space of the microfluidic channel and optionally of the aperture and/or of the reservoir.

[0030] In certain embodiments, the first defined pattern defines the shape of the bottomside of the device of the invention and optionally the position and size of the aperture. In certain embodiments, the first defined pattern defines the shape of a first sidewall of the device of the invention.

[0031] In certain embodiments, the third defined pattern defines the shape of the topside of the device of the invention and optionally the position and size of an opening in the topside. In certain embodiments, the third defined pattern defines the shape of a second sidewall opposite to the first sidewall of the device of the invention and optionally the position and size of an opening in the second sidewall.

[0032] In certain embodiments, the third defined pattern is identical to the first defined pattern, optionally with the exception of the opening comprised within the topside or second sidewall of the device of the invention.

[0033] In certain embodiments, the first photoresist is a negative photoresist. Non-limiting examples for negative photoresists include SU-8 and phenol formaldehyde resins (CAS Nr. 9003-35-4) such as Novolac.

[0034] In certain embodiment, the second photoresist is a positive photoresist. Non-limiting examples for positive photoresists include AZ 4620 AZ 4533, AZ 4562, and PMMA.

[0035] In certain embodiments, a handling block layer or a handling block is attached onto the cover layer, the topside or the second sidewall of the device of the invention, wherein the handling block layer or the handling block comprises a through hole that is in fluid communication with the microchannel. Particularly, the handling block layer or the handling block is attached to a part of the topside or second sidewall of the device that does not comprise the flexible shank. In certain embodiments, the through hole in the handling block layer or the handling block has the same diameter as the opening in the topside or the second sidewall. In certain embodiments, the handling block layer or the handling block is characterized by a thickness in the range of 100 μm to 300 μm. In some embodiments, the handling block layer is characterized by a thickness of 250 μm.

[0036] In certain embodiments, the handling block layer consists of or comprises the first photoresist, is deposited onto the top layer, and the handling block layer is cured. In this case, the cover layer may be only partly cured before deposition of the handling block layer, and after deposition of the handling block layer, the first photoresit comprised within bottom layer, the cover layer and the handling block layer is completely cured such the device is integrally formed in one piece.

[0037] In certain embodiments, the bottom layer is characterized by a thickness in the range of 0.5 μm to 100 μm. In certain embodiments, the bottom layer is characterized by a thickness in the range of 4 μm to 10 μm.

In certain embodiments, the bottom layer is characterized by a thickness in the range of 5 μm.

[0038] In certain embodiments, the cover layer is characterized by a thickness in the range of 0.5 μm to 100 μm. In certain embodiments, the cover layer is characterized by a thickness in the range of 5 μm to 12 μm. In certain embodiments, the cover layer is characterized by a thickness of 7 μm. The aforementioned thickness of the cover layer particularly refers to the thickness of the part of the coverlayer covering the additional metal layer.

[0039] In certain embodiments, the additional metal layer is characterized by a thickness in the range of 0.1 μm to 50 μm. In certain embodiments, the additional metal layer is characterized by a thickness in the range of 0.5 μm to 23 μm. In certain embodiments, the additional metal layer is characterized by a thickness of 3 μm.

[0040] Alternatively, thicker channels may be manufactured using the method of the invention for a different range of applications e.g. 3D printing, dispensing of micro-objects such as single cells, or robust patch clamping.

[0041] In certain embodiments, the sacrificial release layer characterized by a thickness in the range of 5 nm to 500 nm. In certain embodiments, the sacrificial release layer characterized by a thickness in the range of 5 nm to 150 nm. In certain embodiments, the metal seed layer is characterized by a thickness of 150 nm.

[0042] In certain embodiments, the metal seed layer consisits of or comprises a metal selected from the group comprised of copper, aluminium, chromium, gold, silver, platinum, and zinc. In certain embodiments, the additional metal layer consists of or comprises a metal selected from the group comprised of copper, aluminium, chromium, gold, silver, platinum, and zinc.

[0043] In certain embodiments, the support is formed by a silicon wafer.

[0044] In certain embodiments, the sacrificial layer comprises a bottom sacrificial layer, a top sacrificial layer and optionally a sacrificial interlayer, wherein the top sacrificial layer is removed within the first defined pattern, particularly by etching, before the bottom layer is deposited onto the sacrifical layer. In certain embodiments, areas of the sacrificial layer lying outside of the first defined pattern are coated with a protective layer, particularly a cured photoresist, areas not coated by the protective layer are contacted with an etchant solution, and the protective layer is removed after etching. In certain embodiments, the top sacrifical layer and/or the bottom consit of or comprise chromium. In certain embodiments, the sacrifical interlayer consists of or comprises gold.

[0045] In certain embodiments, the bottom layer is deposited by spin coating. In certain embodiments, the mould layer is deposited by spin coating. In certain embodiments, the cover layer is deposited by spin coating.

[0046] In certain embodiments, the metal seed layer is deposited by thermal evaporation, particularly at low current for low UV radiation. In certain embodiments, the metal seed layer is deposited with an emission current of below 5 A, particulary below 1 A, more particular at 0.5 A.

[0047] In certain embodiments, the additional metal layer is electrochemically deposited in a bath comprising a solution with the respective metal ions, such as, for example, copper sulphate in case of the additional metal layer consist or comprises copper, accompanied by the application of a current.

[0048] In certain embodiments, the bottom layer and the cover layer are cured such with the first defined pattern and the third defines pattern, respectively, that the shaft of the device comprises a tip that extends along a first direction. In certain embodiments, the angle between the first direction a longitudinal axis of the shank or the microfluidic channel is in the range of 180° to 90°. In certain embodiments, the tip comprises a plurality of segments extending from the shank, wherein each segment is characterized by a tapered shape, and between each segment a portion of the tip is arranged, and wherein at least one of the portions arranged between the segments is designed as predetermined breaking point. Advantageously, the tip curvature, shape and/or length can directly be patterned with the method of the invention, e.g. by patterning with a respective photomask. Provided that the tip defines the bottomside of the device, the device is in this case manufactured sideways, meaning particulary that the bottom layer becomes the first sidewall of the device and the cover layer becomes the bottomside, the topside and the second sidewall of the device.

[0049] In certain embodiments, the bottom layer and the coverlayer are cured such with the first defined pattern and the third defined pattern, respectively, that the shaft exhibits a curved shape, a jagged shape, a zigzag shape or a shape comprising a step, or in other words, the shank comprises one or more corners.

[0050] The term "a shape comprising a step" particularly refers to the shape of a shank that comprises two parts each of them extending along a direction, respectively, wherein one of the two directions is arragned with respect to the other direction at an angle in the range of - 30° to 30°C, particularly in the range of -10°C to 10°C, more particular 0°, and the two parts are connected to each other by a intermediate part extending along a direction, which parallel to none of the aforementioned two direction.

[0051] In certain embodiments, the bottom layer and the cover layer are cured such with the first defined pattern and the third defines pattern, respectively, that the shaft of the device comprises a tip that extends along a first direction, the angle between the first direction a longitudinal axis of the shank or the microfluidic channel is in the range of 180° to 90, and the shaft exhibits a curved shape, a jagged shape, a zigzag shape or a shape comprising a step, wherein the curved shape, the jagged shape, the zigzag shape or the shape comprising a step extends within a plane being parallel to the first direction. Also in this embodiment, the device of the invention is manufactured sideways as described above. Advanta-

geously, the production of devices, particularly of cantilevers with complex shapes of the shank and the tip may be performed with the method of the invention, which additionally suitable for mass production.

[0052] According to a further aspect of the invention, a device is provided. The device has

- a flexible shank comprising a microfluidic channel and an aperture that is in fluid communication with the microfluidic channel, wherein the microfluidic channel extends through the shank along the longitudinal axis of the shank and is delimited by at least one surface being formed by a polymer
- a reservoir in fluid communication to the microfluidic channel, whereby the aperture is oriented at the end of the flexible shank opposite to the reservoir, and
- optionally a means for measuring a mechanical force acting on the flexible shank arranged on or within the flexible shank.

[0053] In certain embodiments, the polymer forming the at least one surface delimiting the microfluidic channel is integrally formed in one piece. In certain embodiments, the polymer forming the at least one surface delimiting the microfluidic channel is characterized by an elasticity in the range of 0.5 GPa to 20 Gpa, preferably in the range of 1 GPa to 10 GPa, more preferable in the range of 4 GPa to 5 GPa, even more preferable 4.5 GPa.

[0054] In certain embodiments, the microfluidc channel is configured to pass a fluid stream with pressure of up to 6 bar, and and particularly is fluid tight up a pressure of 6 bar(a).

[0055] In certain embodiments, the flexible shank is characterized by a spring constant in the range of 0.01 $N*m^{-1}$ to 1,000 $N*m^{-1}$, preferably in the range of 0.5 $N*m^{-1}$ to 80 $N*m^{-1}$.

[0056] Advantageously, by the one-piece design of the polymer, the microfluidic channel is completely fluid tight up to a pressure of 6 bar(a), when applied to the microfluidic channel.

[0057] In certain embodiments, the device of the invention is manufactured by a method according to the first aspect of the invention or any embodiment thereof.

[0058] In certain embodiments, the polymer forming the at least one surface delimiting the microfluidic channel exhibits a homogenous structure.

[0059] In certain embodiments, the device of the invention is integrally formed in piece, and particularly exhibits a homogenous structure.

[0060] In certain embodiments, the device further comprises a handling means with a through hole in fluid communication with the reservoir, wherein particularly the handling means is arranged above the reservoir such that the shank is deformable without be obstructed by the handling means. Particularly, the reservoir extends to the through hole.

[0061] In certain embodiments, the polymer is cured photosensitive polymer, in other words a polymer formed by curing, wherein oligomers are cross-linked upon exposure of light. In certain embodiments, the polymer is SU-8.

[0062] In certain embodiments, the polymer is a blend of at least two photosensitive polymers that are cured such that the blend is integrally formed in one piece.

[0063] In certain embodiments, the microfluidic channel has a length in the range of 0.05 mm to 50 mm. In certain embodiments, the microfluidic channel has a length in the range of 0.1 mm to 0.5 mm. In certain embodiments, the microfluidic channel has a length in the range of 1 mm to 5 mm. In certain embodiments, the microfluidic channel has a width in the range of 1 μm to 50 μm, particulary from 1 μm to 30 μm. In certain embodiments, the microfluidic channel has height in the range of 0.1 μm to 30 μm.

[0064] In certain embodiments, the shank has a thickness in the range of 10 μm to 50 μm. In certain embodiments, the shank has a thickness of 12 μm. In certain embodiments, the shank has a width in the range of 20 μm to 80 μm.

[0065] In certain embodiments, the aperture is characterized by a diameter in the range of 1 μm to 50 μm, particularly in range of 5 μm to 35 μm, more particular in the range of 20 μm to 30 μm.

[0066] In certain embodiments, the handling means is characterized by a height in the range of 100 μm to 300 μm, particularly 250 μm.

[0067] In certain embodiments, the through hole comprised within the handling means is characterized by a diameter in the range of 100 μm to 500 μm.

[0068] In certain embodiments, the means for measuring a mechanical force acting on the flexible shank is formed by a metal layer consisting of at least one noble, non-toxic metal, whereby the metal layer is able to changes its resistance in dependence of a mechanical force acting on the metal layer and thereby on the shanks. In certain embodiments, the noble, non-toxic metal is gold.

[0069] In certain embodiments, the means for measuring a mechanical force acting on the flexible shank is formed by a sensing layer comprising a plurality of nanowires made of metal, wherein the nanowires are partially coated with an isolator such that at least a part of the nanowires are in conductive contact to each other when no mechanical force is acting on the shank, and the at least one part of the nanowires in conductive contact to each other decreases with increase of the mechnical forces acting on the shank. Such means is particularly suitable to detect mechanical forces in the range of pN to nN. In certain embodiments, the nanowires are characterized by a thickness in the range of 40 nm to 60 nm and/or a length in the range of 5 μm to 20 μm. In certain embodiments, the nanowires consist of or comprise silver. In certain embodiments, the isolator is aluminium oxide. In certain embodiments, the sensing layer is characterized by a thickness in the range of 2 μm to 3 μm, wherein the nanowires comprised within the sensing layer are characterized by a length of 5 μm to 10 μm and

a diameter of approx. 60 nm. The above described means is also disclosed in the patent application EP 15171419.3.

[0070] In certain embodiments, the means for measuring a mechanical force acting on the flexible shank is formed by a sensing layer comprising a plurality of nanowires made of metal, wherein the nanowires are arranged such within the sensing layer that at least a part of the nanowires are in conductive contact to each other when no mechanical force acts on the shank, and the at least one part of the nanowires in conductive contact to each other decreases with increase of an mechnical forces acting on the shank. Such means is particularly suitable to detect mechanical forces in the range of 100 nN and higher. In certain embodiments, the nanowires are characterized by a thickness in the range of 40 nm to 60 nm and/or a length in the range of 5 μm to 50 μm. In certain embodiments, the nanowires consitst of or comprise silver.

[0071] In certain embodiments, the means for measuring a mechanical force acting on said flexible shank is formed by a part of the shank being optically transparent, wherein the part of the shank is configured to change its optical properties, particularly its refractive or diffractive properties, in dependence of a mechanical force acting on the part of the shank.

[0072] In certain embodiments, the aperture is comprised within a tip of the shank. In certain embodiment, the tip extends along a first direction from the shank, wherein the angle between the first direction and the longitudinal axis of the shank is in the range of 180° to 90°C. In certain embodiments, the tip is characterized by a cylindrical shape or a tapered shape, particularly a conical or pyramidal shape. Such device may advantageously be used as cantilever for single-cell injections or imaging of soft tissues with high sensitivity.

[0073] In certain embodiments, the shank is characterized by a curved shape, a jagged shape, a zigzag shape or a shape comprising a step, wherein particularly the curved shape, the jagged shape, the zigzag shape or the shape comprising a step extends within a plane being parallel to the first direction along which the tip extends from the shank.

[0074] In certain embodiments, a tip comprising a plurality of segments extends from the shank, each segment is characterized by a tapered shape, and between each segment a portion of the tip is arranged, and wherein at least one of the portions arranged between the segments is designed as predetermined breaking point. Advantageously, clogging possibly occuring within the tip can be overcome by removing the clogged segment, e.g. by breaking off the clogged segment with a tweezer.

[0075] In certain embodiments, the device is designed as a cantilever or a micropipette. In certain embodiments, the micropipette comprises a re-usable tip such as a tip comprising a plurality of segments extends from the shank, each segment is characterized by a tapered shape, and between each segment a portion of the tip is arranged, and wherein at least one of the portions arranged between the segments is designed as predetermined breaking point.

[0076] Advantageously, the device of the invention is particularly suitable for for fine surgical applications.

[0077] According to a further aspect of the invention, a method for spatially manipulating a microscopic object, particularly a single cell, is provided. The method comprises the steps of:

- providing a device having a flexible shank with a microfluidic channel and an aperture in fluidic communication with said microfluidic channel according to any one of the above aspects or embodiments of the invention, and
- capture the microscopic object at or within the microfluidic channel or release the microscopic object from or out of the microfludic channel by applying or altering a fluidic current within the microfluidic channel.

[0078] In certain embodiments, the microscopic object is located at first postion and captured, and the captured microscopic object is released at a second position, wherein particularly

a) the device of the of the invention is positioned such that the microscopic object is capturable at the first position,
b) the microscopic object is captured at the first position,
c) the device of the invention comprising the captured microscopic object is positioned such that the captured microscopic object is releasable at the second position, and
d) the captured microscopic object is released at the second position.

[0079] In certain embodiments, the microscopic object is captured by attaching the microscopic object at the aperture. In certain embodiments, the microscopic is released by detaching the microscopic object from the aperture.

[0080] In certain embodiments, the microscopic object is captured by sucking the microscopic object into the microfluidic channel. In certain embodiments, the microscopic object is released by pumping the microscopic object out of the microfluidic channel.

[0081] In certain embodiments, the microscopic object is capture by sucking the microscopic object through the microfluidc channel into a reservoir in fluid communictation with the microfluid channel and released by pumping the microscopic object out of the reservoir through the microscopic channel.

[0082] The invention is further illustrated by the following examples and figures, from which further embodiments and advantages can be drawn. These examples are meant to illustrate the invention but not to limit its

scope.

Description of the figures

[0083]

Fig. 1 shows the microfabrication process for producing micro-channeled SU-8 cantilevers with A) deposited Cr/ Au/ Cr release layer on a silicon wafer and patterned SU-8 bottom layer with definition of a circular aperture, B) deposited copper seed layer, C) patterned positive AZ sacrificial photoresist, D) electroplated copper growth layer, E) dissolved positive photoresist and copper seed layer, F) patterned SU-8 top layer with definition of an inlet, G) patterned SU-8 chip layer for handling and H) etching of the channel sacrificial layer and release from the wafer.

Fig. 2 shows the characterization of the SU-8 devices with A) optical picture of a cantilever after copper plating, B) and C) SEM views of a cantilever of 12 μm thickness for channel thickness of 3 μm (flipped upside down compared to Figure 1), D) fluorescent microscopy top view with fluorescent liquid coming out at the aperture, E) apparent liquid meniscus reaching the transparent cantilever and F) flow rate as a function of pressure applied on the chip with linear fit in red dash line. Uncertainty measured in the flow rate was at most 4% for the same applied pressure. It is not represented on the graph for more clarity.

Fig. 3 shows the force adhesion measurements of S. *cerevisiae.* The yeast cells were measured on bare glass and PDA-coated glass substrates with A) an optical picture of a cantilever with a 6 μm diameter aperture before and B) during force spectroscopy of single targeted yeast. In C), a typical force spectroscopy curve of a yeast cell on glass substrate showed adhesion forces of 15.8 nN (distance of detachment of 240 nm) as a difference between approach curve in blue and retract curve in red. In D), adhesion forces on the 2 substrates were compared exhibiting forces of 15 ± 7.6 nN on glass and 33 nN ± 11.9 nN on PDA, averaged respectively, over 21 and 26 force curves for 10 and 12 different yeasts and performed with the same cantilever. On the graph, the mean is represented as a square, the median as a line separating two boxes with each box determined by the 25th and 75th percentiles and whiskers determined by the 5th and 95th percentiles.

Fig. 4 shows examples of forces curves obtained with a SU-8 cantilever in A) air and B) liquid environment on glass substrate. In this configuration, only the end of the cantilever was touching the substrate.

Fig. 5 shows schematics illustrating the main approaches developed for single-cell patterning using a hollow cantilever. A) A micropipette-like configuration for a best cell placement resolution of 250 μm (configuration 1). B) Controlled direct deposition by mechanical squeezing and physical confinement of individual cells (configuration 2). C) The same cantilever was used for fine negative or subtractive patterning with the possibility of single-cell detachment if cell sitting on an adhesive substrate (configuration 3) or coarse negative patterning if cell on a repulsive substrate (configuration 4).

Fig. 6 shows the precise deposition of single C2C12 cells using configuration 2 with A) a grid pattern of 4 single cells deposited frame after frame from top left to bottom right and B) a grid pattern of six spots with varying number of cells per spot. Green circles represent the aperture of the cantilever during deposition, while the numbers of the bottom panel correspond to the order of deposition.

Fig. 7 shows the negative patterning of C2C12 mammalian myoblast cells using configurations 3 and 4, corresponding respectively to top and bottom panels. In the configuration 3, where C2C12 were seeded on a PDL-coated adhesive surface, the cantilever was approached A) on the cell of interest. A large underpressure of -800 mbar was applied to the cantilever for 10 sec to detach the cell in B). In the configuration 4, where cells were seeded on a PLL-g-PEG coated repulsive surface,

the cantilever was brought 10 μm away from the surface-level C). Low underpressure of-10 mbarwas applied for 1 sec D), thus removing the cells roughly contained within a perimeter of 300 μm diameter around the aperture.

Fig. 8 shows the subtractive patterning of primary hippocampal neurons on a fully PDL-coated adhesive surface (configuration 3). Optical pictures of the area of interest are displayed before patterning in A), after patterning in B) and after 5 DIV in C). After longer time in vitro, the pattern became less obvious due to cell migration.

Fig. 9 shows the subtractive patterning of primary hippocampal neurons using configurations 3 (A to D) and 3-4 (E and F). A PDL pattern was locally dispensed in the form of a smiley before backfilling the remainder with PLL-g-PEG for a better adhesive to non-adhesive contrast. A) Neurons seeded on the surface before patterning, B) Neurons on the surface after removal of those sitting on the repulsive surface. Neurons viability was tracked by transfecting the culture visible in bright field in C), with adeno-associated virus (AAV) after 6 DIV, showing in D) spontaneous calcium activity expressed in GFP after 12 DIV and neurite outgrowth activity. Similarly, neurons were removed from PLL-g-PEG surface on a second pattern as well as the half-right of the PDL pattern shown by a bright field image of healthy neurons population with no apparent neuron adhering again on the half-right of the PDL-coated smiley in E) and in F) calcium activity expressed after 12 DIV in GFP.

Fig. 10 shows the *in situ* modifications of an existing pattern of neurons. In A), the pattern realized in Fig. 9C) is illustrated after 14 DIV in fluorescence light microscopy. The two white encircled areas were subject to removal in B) as well as an eye of the smiley in C), by applying with the cantilever high and constant suction for 10 sec onto each spot (pressure inferior to -800mbar). Another existing pattern is shown in bright field microscopy after 14 DIV before patterning in D), and additional deposition of 3 fresh primary neurons forming a second eye to the smiley, as pointed out in E).

Fig. 11 shows the upside down SEM images of A) a cantilever used in the micropipette-like configuration with the aperture defined in the front plane for a channel thickness of 22 μm (configuration 1) and B) a cantilever with the aperture designed at the bottom plane with same channel thickness for an aperture diameter varying from 20 to 35 μm (configurations 2 to 4).

Fig. 12 shows in A), B) and C) a layer-by-layer photolithography process, wherein bottom layer, channel and top layer are patterned in a three-step protocol; in D) a global view of the sketched device and in E) an optical image of the finalized device.

Fig. 13 shows optical pictures of four different designs of cantilevers microfabricated sideways, scalebar being identical for all. A) shows a curved tip, whereas B) and C) depict a triangle-like tip and D) a rectangle-like tip.

Fig. 14 shows optical pictures of five different micropipette designs. A) and B) depict a geometry of probe, which could act as an diffractometer upon mechanical force, C) and D) have a high and long tip to reach inaccessible locations, E) and F) a sliceable tip for several uses. G) and H) display a long tip with an additional corner.

Fig. 15 shows corresponding SEM images of figure 14.

Fig. 16 shows SEM images of the sliceable tip before in A) and after cutting in B) at the location represented by a dashed green line. C) depicts a close-up view of B) where the aperture is electrically charging because of the non-existing conductive coating while SEM imaging. Despite the charging effect, the dark hollow channel is apparent.

Fig. 17 shows SEM images of two different thick cantilevers (respectively at bottom and top panels) demonstrating a pillar-like structure at the aperture-level.

Fig. 18 shows the process flow for tube-like tips with in A) patterning of SU-8 bottom layer, B) copper seed layer deposition, C) AZ sacrificial patterning for channel definition, D) copper plating for thickness of 10 μm, E) etching of AZ and copper seed layer and patterning of SU-8 top layer and F) release of the probe.

Fig. 19 shows a scheme of the mode of action of one possible force sensor.

Fig. 20 schematically shows an embodiment of the force sensor comprised within shank (cantilever beam) of the device of the invention (here designed as cantilever), wherein the force sensor is formed by a composite structure in the shape of a cantilever beam.

Fig. 21 schematically shows a method for producing the composite structure depicted in fig. 20.

Figs. 22 to 23 show optical images of a cantilever equipped with the force sensor depicted in Figs. 20 and 21.

Fig. 24 shows an embodiment of the device of the invention characterized by a needle-like design made by sideways fabrication; (A) global view from different perspectives and (B) a section of the shank with the tip (upper panel) and a cross section thereof.

Fig. 25 shows an embodiment of the device of the invention characterized by a biopsy tool-like design; (A) global view from different perspectives and (B) a section of the shank with the tip (upper panel) and a cross section thereof.

Fig. 26 shows an embodiment of the device of the invention characterized by a biopsy tool-like design with light sensor; (A) global view from different perspectives and (B) a section of the shank with the tip (upper panel) and a cross section thereof.

Fig. 27 shows an embodiment of the device of the invention being a sealed and reusable micropipette with sliceable tips; (A) global view from different perspectives and (B) a section of the shank with the tip (upper panel) and a cross section thereof.

Fig. 28 shows an embodiment of the device of the invention characterized by a micropipette design with force sensor; (A) global view from different perspectives and (B) a section of the shank with the tip (upper panel) and a cross section thereof.

Fig. 29 shows an embodiment of the device of the invention characterized by a blunt (tipless) cantilever design; (A) global view from different perspectives and (B) a section of the shank with the aperture (upper panel) and a cross section thereof.

Fig. 30 shows an embodiment of the device of the invention characterized by a cantilever design with a triangle tip; (A) global view from different perspectives and (B) a section of the shank with the triangle tip (upper panel) and a cross section thereof.

Fig. 31 shows an embodiment of the device of the invention characterized by a cantilever design with a rectangle tip; (A) global view from different perspectives and (B) a section of the shank with the rectangle tip (upper panel) and a cross section thereof.

Fig. 32 shows an embodiment of the device of the invention characterized by a cantilever design with two sharp tips; (A) global view from different perspectives and (B) a section of the shank with the rectangle tip (upper panel) and a cross section thereof.

Fig. 33 shows an embodiment of the device of the invention characterized by a micropipette design for patch-clamp; (A) global view from different perspectives and (B) a section of the shank with the tip (upper panel) and a cross section thereof.

Examples

[0084] A novel fabrication method was established to produce flexible, transparent and robust tipless hollow atomic force microscopy (AFM) cantilevers made entirely from SU-8. Channels of 3 μm thickness and several millimeters length were integrated into 12 μm thick and 40 μm wide cantilevers. Connected to a pressure controller,

the devices showed robust sealing performance with no leakage up to 6 bars. Changing the cantilevers length from 100 μm to 500 μm among the same wafer allowed targeting various spring constants range from 0.5 to 80 N/m within a single fabrication run. Such hollow polymeric AFM cantilevers were operated using optical beam deflection method (OBD). To demonstrate the performance of the device, single-cell force spectroscopy (SCFS) experiments were carried out with a single probe detaching in a serial protocol more than 100 *Saccharomyces cerevisiae* yeast cells from glass and glass-coated with polydopamine measuring adhesion forces in the sub-nanoNewton range.

[0085] SU-8 now offers a new alternative to conventional silicon-based hollow cantilevers with more flexibility in terms of complex geometric design and surface chemistry modification.

[0086] As scope of this work, SU-8 hollow AFM tipless cantilevers were developed. The process for the realization of robust embedded microchannel is presented together with the corresponding integration into the final device, i.e. an AFM chip. Serial single-cell force spectroscopy (SCFS) with forces recorded in the sub-nanoNewton range validated the AFM feasibility and functionality of those flexible cantilevers.

[0087] As SU-8 has been standardly used in microfluidic applications, several processes have been developed in order to realize hollow structures. Nonetheless, it still remains challenging to fabricate entire SU-8 fluidic devices because SU-8 is a negative-tone resist: oligomers from bottom SU-8 of the microchannel must always be present in sufficient quantity to polymerize with top SU-8 covering the channel in order to ensure a watertight sealing at the interface.

[0088] Herein, a promising process for fabrication of 1 to 5 mm long and sub-μm to 10 μm thick hollow channels that show high fluidic robustness with resistance over 6 bars of pressure is provided.

Microfabrication Process for Tipless SU-8 Hollow AFM Cantilevers:

[0089] Figure 1 illustrates the process flow that was established for this fabrication. A novel "sacrificial-filling-material" approach based on electrochemical deposition was investigated. For easy handling of the devices as well as to limit their initial bending, 12-μm thick cantilevers were designed on a wafer- scale.

[0090] In the process, the first step consisted in depositing a sacrificial release layer 21 made of 5 nm chromium/ 50 nm gold/50 nm chromium on a silicon carrier substrate, known as enhanced sacrificial layer, to ensure a fast release of the probes from the wafer. Then, a 5-μm thick SU-8 bottom layer 22 was photolithographically patterned with the formation of a circular outlet aperture 13 having a diameter down to 4 μm (Fig. 1A). After development of the first layer 21, a copper seed layer 23 of 150 nm thickness was deposited on the wafer surface using thermally resistive evaporation for low UV radiation (Fig. 1 B). This layer 23 was consequently thick to support uniform electrical conductivity over the surface. As depicted in Fig. 1C, a positive photoresist 24 such as AZ4562 was then patterned to define the shape of the future hollow channel 12 as well as to guarantee straight walls during the sacrificial metal growth 25. Here, the use of a positive photoresist 24 was advantageously so that SU-8 areas 22 on the bottom plane supposed to polymerize subsequently with the cover layer 26 were spared from UV exposure while patterning the positive resist. Reduced baking time was also advantageous to prevent complete polymerization. Then, a sacrificial copper layer 25 was electrochemically deposited in a bath of copper sulfate for a thickness of 3 μm (Fig. 1 D). Prior to electroplating, the wafer was quickly plasma treated and dipped in sulfuric acid to ensure a better wetting. Next, the positive photoresist 24 was dissolved by immersing the wafer for 5 s in acetone followed by a quick dipping of 3-4 s in a hydrogen peroxide based etchant until the thin copper seed layer 23 disappeared, as seen in Fig. 1 E. Then, a 7 μm thick SU-8 top layer 26 of the probe was spin-coated over the existing structures and patterned accordingly as seen in Fig. 1 F. To improve mechanical stability of the assembly, a 250-μm thick block layer 28 of SU-8 was patterned to form the handling chip part 15 of the probe 100 making a cylindrical reservoir 14, 16 directly connected to the channel 12 (Fig. 1 G). The sacrificial layer 25 forming the channel 12 was then dissolved in a copper etching solution for several days depending on agitation (2-mm long channels). This versatile approach allowed fabricating several millimeter long channels 12 for thicknesses ranging from 100 nm to tens of micrometers. A ferric chloric based copper etchant was preferred over hydrogen peroxide based etchant because the latter one formed oxygen bubbles that stayed confined at the inlet's surface because of SU-8's hydrophobicity. Then, the fabricated probe 100 was released from the carrier wafer by using a chromium etching solution to dissolve the release layer 21 in two hours as shown in Fig. 1 H. Cantilevers showed maximal initial bending of 5° because of their consequently high thickness (> 10 μm). Therefore, there was no need to use a more complex dry release technique to further minimize such bending. Finally, probes 100 were squeezed on top of hydrophobic parafilm substrate for easy handling before gold deposition. A 10-nm thin layer was deposited onto the entire device to ensure a satisfactory laser reflection on top of the cantilever and by doing so, enabling optical beam deflection (OBD) method for force detection. Depending on the use, this thickness may be increased or decreased if one wanted to privilege AFM laser force signal or better visibility of surface objects through the transparent microlever. Finally, probes 100 could be gently peeled off with tweezers from the parafilm substrate.

[0091] A specific holder with many more conductive pins could also be designed to guarantee even better

copper growth uniformity.

Cantilever-like designs with tip

[0092] Most of current biological applications require a tip. This protrusion allows for sharper AFM imaging but also diverse fluidic applications such as single-cell injection and extraction, patchclamp or chemical stimulation. One of the biggest limitations commonly observed with silicon-based hollow cantilevers is the need for milling an aperture outlet individually for each probe. This is mostly done using the tedious focused ion beam (FIB), which cannot be multiplexed. Therefore, a human incertitude and an increase of the cost are necessarily introduced. Only one type of geometry with an aperture at the end of the pyramidal tip can be directly defined through photolithography processing. This important drawback can be circumvented by slightly adapting the process initially developed for blunt hollow probes described above. In the original version of the process, the layer-by-layer fabrication consisted in the sequential assembly of bottom 22, channel 25 and top layers 26. For the version of cantilevers equipped with tips, the process has been modified to fabricate the devices sideways with the sequential assembly of one side, channel and opposite side layers, as displayed in the corresponding schematics in Figure 12 A), B) and C). In Fig 12D) a global view of the device can be observed, which was slightly changed for the final version as shown on the optical image of the finalized device in E).

[0093] Using silicon-based technology, this was not developed mostly because of the necessary important thickness of all different layers. Indeed, it means for devices fabricated sideways that each layer is at least couple of microns thick to, once the device is tilted back, get any laser signal focused on the top of the cantilever. Despite the difficulties in term of fabrication, silicon-based cantilevers would be much stiffer. By considering Young's Modulus of silicon or silicon nitride, a nominal width of 4 μm for each layer (giving a total width of 12 μm) and conventional cantilever dimensions such as 400 μm in length and 15 μm in thickness, one can estimate the spring constant in the range of 10 $N*m^{-1}$. Since the device is tilted, width and thickness in this configuration are respectively equivalent to usual thickness and width. In comparison, the spring constant would be 40 times lower for identical dimensions using SU-8 polymer. Another significant advantage with this process is the possibility to give various shapes and lengths to the tips instead of a single pyramidal geometry in the case of a silicon-based hollow cantilever. The natural disadvantage with the following process is the unavoidable "fake" 3D of the tip since it is only a projection of a 2D design in the third dimension. This aspect can be minimized by adding some photolithography steps to obtain different step heights which could be rendered then probably smoother using high hard baking temperature. As depicted in Figure 13, cantilevers 100 with curved, triangle-like and rectangle-like tips 17 could be fabricated. All tips were "cut" following an angle of 10 degrees with the substrate in order to be compatible with the JPK AFM setup for monitoring force-deflection.

Micropipette-like designs

[0094] By the method of the invention, micropipettes with complex shapes can be manufactured, particularly in a high-through-put manner. In addition, SU-8 offers some advantages in terms of electrical isolation in the case of piezoresistive force sensing in comparison with force sensors known in the art. This latter electrical-based sensing only comes with 2 electrical wires to contact the sensing film (described below), limiting de facto the intrusion for surgical applications. Prototypes of SU-8 micropipettes with various designs were realized. Figure 14 depicts in A) and B) possible geometries of a pipette tip, which upon applied force will change the periodicity between the triangles. Thus, by passing light through the periodically arranged triangles, one could modulate the diffracted or refracted light depending on mechanical strain exerted at the tip-level. Also depicted in C) is a curved tip, in D) a straight tip, in E) and F) a sliceable tip (see further below) and in G) and H) a mm-long tip with an additional comer for sensing deflection within two axes if the sensor is coating the total surface of the probe. Figure 15 depict the SEM images of the same designs in B), D), E) and F) and others in A) and C).

[0095] Another common issue in micro- or nano-fluidics is the channel or aperture clogging. Because of particles, dust, cell residues or other unexpected events related to experiments, it is generally easy to obstruct such a small and hollow surface area. To overcome this problem, a prototype of sliceable tip has been developed. It consists in having several tips mounted together in series with higher mechanical weakening for the last tip. In our configuration, the latter tip is more susceptible to break off while touching it with tweezers. A worn-out tip could be broken and replaced by a new one in the middle of an experiment without many adjustments. The proof of concept is demonstrated in figure 18 depicting a sliceabletip before (A) and after breaking (B) a tip, wherein thereby created new tip exhibits an apparent channel (C). The tip may be breaken of by simply touching the last tip with tweezers. Figure 16 depicts the breakage of the last 3 tips.

Thick cantilevers

[0096] Thick cantilevers with integrated microchannels of 22 μm height were fabricated as well for single-cell patterning purposes. It is a very similar process to the one described above with the difference that the AZ4562 sacrificial photoresist is spin-coated and patterned at a higher thickness of 27 μm for control over the copper growth within the channel. Cantilevers show a total thickness of 50 μm. Interesstingly, some cantilevers randomly

selected for SEM imaging showed a perfectly cylindrical pillar formed in the center of the circular aperture, as for example, depicted in Fig. 19. This necessarily has to do with the copper growth during the electroplating process. One hypothesis to explain this phenomenon might result from the fact that the channel thickness is below expected. From the measurements on the profilometer before spin-coating of the top SU-8 layer, a few devices among the wafer show a channel thickness below 15 μm. As depicted by Figure 18, the hollow cylinder formed by the bottom SU-8layer gets filled during plating starting from the vertical walls and the horizontal bottom surface with a uniform thickness of about 10 μm thick copper (Figure 18 D). Considering the aperture is 30 μm wide, the hollow cylinder is not completely filled after deposition. A pillar structure can be left empty and subsequently formed by the spin-coating of the top SU-8 layer (Figure 17A and Figure 18 F). Figure 17 A) and B) show a 10 μm wide pillar structure, whereas width in C) and D) the pillar sturcture is 5 μm wide.

Force sensors

[0097] Depending on the design of the device of the invention and the application, for which it serves, mechanical strain can cause bending, compression or elongation on the surface of the device. This strain can be measured within 2 configurations based on piezoresistive sensing. The sensing layer is always located on the surface, as far as possible from the neutral axis of the cantilever or pipette for higher force sensitivity.

[0098] The different configurations can be classified as following (from low to higher strain):

1. A composite film of metallic nanowires coated with an insulator at the interface for force detection between pN and nN.
Here, a large network of silver nanowires 31 (AgNWs) is first deposited on a surface. A thin aluminum oxide coating (from few angstroms to few nm) is conformally deposited on the surface of the nanowires 31. The AgNWs network 31 with Al_2O_3 is then embedded in the SU8 polymer (Fig. 21). The Al_2O_3 coating does not alter the initial resistance R_0 of the network; at rest, R_0 is low since all wires are in contact (Fig. 19). However, upon bending of the cantilever the AgNW network is displaced and the single AgNWs slide along each other's insulator coating, causing a proportion of the wires not to be in contact with other wires anymore, but with the insulating Al_2O_3 layer. The latter results in a significant increase in resistance (ΔR) resulting in a higher GF and thus higher sensitivity. Once back at rest the wires have returned to their initial positions again where they contact each other at initial location, showing low resistance. The increase in ΔR during bending is appointed to the tunneling resistance which arises at the contact interface of two metal wires, as well as to the ratio of wires in contact/out of contact. The only place where the Al_2O_3 layer is not deposited is on the AgNWs pads as they form the electrical contact points for piezoresistive readout.
2. A film of bare metallic nanowires for force higher than 100 nN.

[0099] A system less sensitive using a thick network of nanowires is ideal for such an application.

Method of manufacture a composite structured force sensor

[0100] As depicted in Fig. 20, conductive elements 31, particularly nanowires made of silver, are arranged in or on a cantilever beam 11 in a specific pattern. When the cantilever beam 11 is bent, some sections of the beam 11 are compressed and other sections are stretched. Depending on their location and arrangement relative to one another, conductive elements 31 will remain in contact, lose contact or come into contact physically and/or electrically. The conductivity function of the trail for the described bending is a step function: at first zero (or almost zero), then constant (or almost constant) at a higher level, and then again zero (or almost zero). By superimposing several step functions every conductivity function of practical interest can be approximated. In practice the superimposition can be realized e.g. by connecting various trails or tracks (virtually) in parallel.

[0101] Additionally, the amount of bending can thereby be measured by measuring the (change in) conductivity in one or more tracks of the composite structure.

[0102] Fig. 21 illustrates a process scheme for manufacturing the above described force sensor.

Step a) A sacrificial layer 21 is deposited.

Step b) Metallic pads 30 for better subsequent electric contact are created, e.g. by vapour deposition. An example for a suitable metal is gold.

Step c) A percolation structure 31, e.g. a silver nanowire (AgNW) network, is deposited using centrifugation, drop-casting or vacuum filtration on the sacrificial layer 21 and the pads 30. Optionally, a deposition of shell material, in particular layer deposition, e.g. atomic layer deposition of aluminium oxide, can be performed. For example, the layer thickness can range from 2-3 angstroms to 50 nm.

Step d) A polymer 22, e.g. SU-8 polymer photoresist, is used as the constituent material of the cantilever beam 11. Optionally, it can be photolithographically patterned in the shape of a beam attached to a handling block 15, which makes the handling easier.

Step e) Optionally, the thickness of the handling block 15 is further increased by additional patterning

of thick SU-8 26. The increased thickness of the handling block 15 can improve the handling of the cantilever beam.

Step f) Optionally, after etching of the sacrificial layer 21, a passivation layer (such as parylene) can be deposited thermally to isolate the cantilever beam 11. The pads' 30 contact area on the hanling block 15 can be protected from the passivation layer e.g. by some cover (because it can have a rather big area, e.g. several mm^2). The figure f) shows the cantilever beam 11 from the bottom side (turned over as compared to the figures d) and e)) after etching and after deposition of the passivation layer. Therefore only the pads' 30 contact areas are visible. The percolation structure 31 is hidden under the passivation layer and the pads' 30 contact areas, respectively.

[0103] When the cantilever beam 11 is bent, the conductive elements 31, e.g. the AgNW, move relative to each other, thereby physically connecting or disconnecting and/or sliding relative to each other. Note that in the case of an aluminium oxide coating at the interface between two conductive elements 31, the elements do not physically touch but are physically close. They can therefore exchange electric charges, this phenomenon is known as the tunnel-effect.

[0104] In an embodiment, it can be the case that conductive elements 31 initially physically touch. In conventional Atomic Force Microscopy (AFM) applications the strain is typically low, e.g. 5% or smaller. Therefore for such an application the shell's thickness can be tailored with a steep function (resistance dependant on tunnelling effect dependant on shell's thickness).

[0105] An optical image of the resulting device is displayed in figure 22. The process only differs from figure 23 in the sense that there are no metallic pads, instead the NW network 31 is patterned and etched using a sacrificial photoresist. Holes 32 were created to minimize the gap between filled structures in order to accelerate the release. As seen in figure 23, silver nanowire pads 31 are glued together with a conductive silver epoxy 35 to gold flexible wires 34 for electrical contact.

Optical and Fluidic Performances

[0106] The developed process was highly successful for the realization of hollow AFM cantilevers 100 made entirely of SU-8, integrating mm-long and μm thick robust channels 12. As shown in Figure 2A, the positive resist 24 could truly help to confine the copper growth and define sharp channel walls. Channels 12 were generally defined, starting 5 μm away from the edges of the SU-8 cantilevers. In Fig. 2B and 2C, SEM pictures reveal the cross-section of the microchannel 12 using an open cantilever design; bottom 22 and SU-8 layers 26 were specifically shorter than the copper layer itself at the end of the cantilever for channel imaging. One can observe in Fig. 2C that the bottom of the channel (corresponding to top copper layer of Figure 1) is not completely straight because of the granular copper growth. Its curved profile follows the topography of a trench after copper electroplating fill process. Thicknesses of bottom 22 and top SU-8 layers 26 were 5 and 7 μm respectively. Channel 12 dimensions from inlet to outlet were: 1800 μm long, 10-50 μm wide and 3 μm thick.

[0107] Each probe was then fixed and glued on a probeholder to assess its watertightness: a FITC-based fluorescent solution did fill the microchannel and came out only from the micro aperture after plasma treatment (Fig. 2D).

[0108] Fluidic robustness was obtained as the optimized result of several interdependent parameters :

- Reduced UV exposure and baking time of the SU-8 bottom layer 22,
- Deposition of the copper seed layer 23 using thermal evaporation at minimal current for low UV radiation,
- Use of a positive photoresist 24 for the copper plating to avoid direct UV exposure onto the channel walls surface,
- Important overexposure of the top 26 and chip SU-8 layers 28.

[0109] One important point was to save sufficient amount of oligomers in the bottom SU-8 22 before the patterning of the SU-8 top layer 26. Polymerization was only completed once top layer 26 was patterned accordingly. The hydrostatic strength or fluidic robustness was proved by applying repeated times high continuous overpressure of 1 bar to release yeasts from the cantilever. Furthermore, using a FITC dye within the channel, no leakage was optically detected for an overpressure higher than 6 bars showing extremely high resistance.

[0110] Native SU-8 is highly hydrophobic. However, the possibility to enhance its hydrophilic surface properties by using oxygen plasma or ceric ammonium nitrate etchant has already been demonstrated. This leads to the increase of C=O and COO groups at the surface. By performing several oxygen plasma steps as well as prolonged chromium etching in ceric ammonium nitrate solution, SU-8 channel surface was made hydrophilic. It facilitated the filling of the cantilever, as pointed out in Fig. 2E by the low contact angle of the liquid meniscus. The cantilevers presented laminar flow showing linear relation of flow rate at the aperture for pressure range applied onto the device (Fig. 2F).

[0111] Showing the versatility of the technology, different cantilever designs could be fabricated on the same wafer with a thickness ranging from 10 μm to 50 μm thickness, lengths varying from 100 mM to 50 mm, widths from 1 μm to 50 μm, apertures from 4 to 20 μm diameter corresponding to channel volumes from 10 to 50 pL. Those different geometries allow targeting wide spring constants range of 0.01 to 1,000 N/m calibrated via Sad-

er's method for resonance frequencies measured from 10 to 5 MHz. These soft cantilevers are considered to have a range of spring constants relevant for biological applications, such as imaging of biological samples or single-molecule force spectroscopy applications.

[0112] Fig. 11 depicts the two types of cantilevers used for the proof of concept experiments described below. The micropipette-like cantilever of Fig. 11A was realized by patterning the positive photoresist 24 in a way that the SU-8 became shorter in length than the sacrificial copper layer 25, opening the cantilever on the front plane. The second design of Fig. 11 B used for the physical confinement of single-cell patterning applications was simply defined by patterning the 6 μm thick bottom SU-8 layer 22 with a circular aperture ranging from 20 to 35 μm in diameter. The typical spring constant of such cantilevers was calculated to range from 150 to 500 N/m according to the different lengths and widths of the cantilevers, with an average of 300 N/m. Based on calculations, the difference in the spring constants of plain and hollow cantilevers is less the 10%, due to the small channel size as compared to the full cross section of the cantilevers.

Cell Adhesion Studies using Force Spectroscopy

[0113] The microfabricated devices can potentially be used as micropipettes with or without force-feedback. To prove their functionality in AFM conditions, the SU-8 cantilevers were mounted on an AFM controller and connected to a fluidic system.

[0114] Cell adhesion forces can be measured with hollow AFM cantilevers, aspiring a single cell by applying negative pressure at the aperture while overcoming and measuring the immobilization or adhesion forces of the cell on the substrate. This method presents significant advantages over the more conventional approach which consists in gluing irreversibly one cell per cantilever. The latter approach is time-consuming but also limits through investigation of cell adhesion behavior as a function of time for life cycle analysis. Furthermore, cell fixation forces on the cantilever are often too low to detach entire cells from the surface of interest. Therefore, SCFS represents the right approach to validate the AFM capability of the manufactured hollow tipless SU-8 cantilevers. In this study, adhesion forces of *Saccharomyces cerevisiae* were measured by performing force spectroscopy with a single SU-8 hollow probe on more than 100 cells without fouling the aperture. No clogging or leaking issue at the cantilever level was observed highlighting the maturity of the process.

[0115] *S. cerevisiae* is a yeast species, which is extensively exploited in baking and brewery fermentation processes and one of the most investigated eukaryotic model organism. The adhesion of microbial cells to abiotic or biotic surfaces is mediated by a complex and dynamic process of interactions affecting cell development and survival. It also plays an active role in the infection process and is furthermore of relevance in biotechnological processes, making necessary a deeper understanding of the ongoing cell to substrate interactions. Here, we performed a proof of concept measuring the yeast adhesion both on bare glass and on glass coated with polydopamine (PDA). This polymer is inspired from the 3,4-dihydroxy-L-phenylalanine, which is naturally secreted from mussels and commonly used for irreversible cell immobilization to the cantilever in conventional AFM measurements.

[0116] In the present configuration, the modus operandi was rather straightforward. First, force-approach curves were measured with a hollow cantilever onto a glass surface in air and liquid environment showing elastic and reversible mechanical behavior of SU-8 within the range of applied forces. Examples of forces curves obtained with a SU-8 cantilever in A) air and B) liquid environment on glass substrate (Fig. 4). In this configuration, only the end of the cantilever was touching the substrate as shown in Fig 4. Then, the cantilever was positioned optically with the aperture over a single yeast cell and approached the cantilever on it using systematically the same set point, as shown in Figure 3A. The approach was followed by a contact pause where the single yeast was aspired at the aperture before complete retraction of the cantilever (Fig. 3B). For future biological applications targeting mammalian cells, surface modification with an antifouling layer of SU-8 for enhanced biofunctionality could be considered. In the current case, mechanical overpressure was shown sufficient for the release of yeast cells from the aperture.

[0117] Adhesion forces of *S. cerevisiae* to glass and PDA-coated glass surface were compared at room temperature using a soft cantilever presenting a spring constant of 1.2 N/m. Fig. 4 shows the spring constant calibration of a SU-8 cantilever (with 500 μm length 40 μm width and 10 μm thickness) via Sader method in air environment using JPK SPM software. The latter was chosen to measure the low adhesion force range. Considering the formula for the spring constant of a cantilever with respective length, width and thickness of 500 μm, 50 μm and 12 μm, the theoretical spring constant is 0.8 N/m. From calculations, the influence of the hollow channel on the total spring constant is limited to 0.1% because of its relative ly low thickness. Fig. 4C shows an example of a typical force-distance curve obtained for single yeast on glass substrate with adhesion forces of 15.8 nN. Averaged adhesion forces were 15 ± 7.6 nN on glass and 33 nN ± 11.9 nN on PDA showing twofold higher adhesion of S. cerevisiae on PDA substrate (Fig. 4D). Adhesion on glass was found similar to other studies [9, 50] whereas adhesion on PDA was quantified hereby for the first time, showing the expected behavior.

[0118] Cell elasticity and cell adhesion to the substrate could be decoupled: based on our calculations, elasticity of *S. cerevisiae* is found to be out of range by 3 orders of magnitude and should not interfere with the range of adhesion forces, if one considers average surface modulus or yeast elasticity of 11.1 N/m and yeast adhesion

measured of 58 mN/m with 14 nN force for a detachment distance of 240 nm (Fig. 3C). Adhesion studies were also shown to be dependent on the loading rate (applied force set point and tip speed) but also the contact time. However, the influence of these parameters was not further investigated.

Controlled single-cell deposition and patterning by the highly flexible hollow cantilevers of the invention

[0119] Fig. 5 illustrates the different approaches used and developed in order to evaluate the newly developed hollow SU-8 polymeric cantilevers for the application of single-cell patterning. In a standard micropipette-like configuration demonstrated in Fig. 5A, cell deposition from the cantilever is limited by factors like: the lowest reliable external pressure possibly applied to the system, the drag force acting on the cells, as well as dynamical properties such as the response time. A first approach was taking advantage of the highly flexible polymeric cantilever. This technique has not been investigated so far because most fluidic components in printing technologies are mostly made of rigid and brittle materials. Originally inclined at 8-10°, the cantilever was significantly bent so that the cell remained confined at the aperture-level (Fig. 5B). Since the aperture was not perfectly parallel to the surface, the liquid could flow out allowing continuous fluidic circulation in the cantilever. To be immobilized and steadily stick to the surface, the cell was mechanically squeezed onto the substrate. A second approach was used to selectively detach cells originally adhering on a substrate in order to realize larger and complex patterns (Fig. 5C). This last approach was also enabled because of the possibility to geometrically confine the flow through the cylindrical hole.

[0120] Designing the aperture at the bottom of the cantilever opens up new possibilities for more precise single-cell deposition and patterning. The first approach has been demonstrated using fluorescently labeled C2C12 cells, as depicted in Fig. 6. On a PDL-coated surface filled with medium, the cantilever was approached onto the surface with cells carried in the reservoir. The approach of the cantilever was performed using fluorescent light microscopy. To this end, overpressure of 20 mbar was constantly applied to the cantilever, ejecting individual fluorescent cells while the cantilever was brought closer to the substrate by one-micrometer vertical steps. As soon as cells stopped flying away and that one cell appeared to be confined within the circular aperture, the z-position was defined at 0 with the stepper for subsequent patterning events (Fig. 6A). Pressure was then stopped before lifting up the cantilever and moving it to the next deposition spot. Same operation was performed again until the next fluorescent cell appeared. The 0-position, necessary for mechanical confinement of the cells, was actually reproducibly matching with the position of the cantilever at which it was bent 5 μm further down after only touching the surface. This specific configuration where the aperture was inclined with respect to the surface is profitable for fine patterning.

[0121] Using this configuration, myoblast cells were patterned with high resolution for the corresponding outcome displayed in Fig. 6B. At most deposition spots, a single cell was patterned. Compared to the opening contour of the cantilever represented in green, the cells appeared to be spotted with high resolution of 5 μm. For patterning of smaller or wider cells, a cantilever with respective smaller or wider aperture should be accordingly designed. During patterning, cells were mechanically squeezed and flattened, which was correlated to their apparent large diameter after patterning (generally above 20 μm). Cells came back to their original size slowly, within the next 10 min after patterning.

[0122] The main limitation of the present setup is related to cell adhesion and sedimentation. Initially contained into the reservoir of the cantilever, the cells started adhering to the surface after 30 min. The pressure required to push them out needed slowly to be higher. Cell settling within the supply compartment is a common issue observed in bioprinting techniques, which affects directly the long-term stability of the system. To prevent this, other antifouling coatings than PII-g-Peg may be used. A fluidic system may be as well set up on the back of the device to decouple the reservoir from the cantilever in order to keep a constant flow running for gentle agitation. Embedding cells in bio-inks may be an additional alternative.

[0123] So far only additive patterning techniques have been presented, however, large and complex patterns can be created also by selectively removing cells from an initially homogeneous culture, as schematized in Fig. 5C. The technology developed was successfully used as well for selective removal of a single cell or several cells simultaneously depending on the surface functionalization of the substrate, as illustrated in Fig. 7. As shown in the top panel, on a PDL-coated surface, the cantilever is approached on the cell of interest before applying underpressure of -800 mbar to detach completely the cell. One can observe that single cells can be targeted and locally removed in series without causing any disturbance in the surrounding.

[0124] On a PLL-g-PEG coated surface (bottom panel), we observed that little applied underpressure of -10 mbar to the cantilever was sufficient to remove cells in a proximity of 300 μm to the aperture (Fig. 7C and D). At higher negative pressures, hundreds of cells could be aspirated at high speeds, providing a powerful technique for systematic cell adhesion studies, which could be, for example, modulated by different cantilever-to-substrate gaps and applied pressures.

[0125] Cell patterns of primary hippocampal neurons were entirely realized on adhesive-coated surfaces. One pattern example is shown in Fig. 8 in the form of a pumpkin-like smiley. Although it was not measured, adhesion of neurons on PDL surface was relatively lower compared to myoblasts: -500 mbar of underpressure was

high enough to remove neurons in the 20 μm vicinity of the aperture contour.

[0126] For such large patterns, the cantilever was set at a sufficient height from the surface-level (~10 μm) to avoid moving away the cells on the surface by sweeping the cantilever on the surface. Since neurons easily gather and migrate together, those patterns realized on PDL-coated surface were difficult to track after more than a week in vitro.

[0127] To overcome this limitation and provide long-term restrictions on the neuronal growth of the patterned cultures, the removal process has been repeated on pre-patterned surfaces. First, smileys of 530 μm in diameter were drawn on bare glass surfaces using fluorescently labeled PDL ink and a linewidth of 15 μm. The dishes were then backfilled with PLL-g-PEG, and the neurons were seeded and incubated for 20 min. The cantilever could enable a selective removal of the unwanted cells that were located on the PII-g-Peg surface, for a better defined pattern of cells (Fig. 9B). More complex patterns, with gap interval between PDL lines down to 30 μm, could be realized such as a brain-like pattern. After 12 DIV, the pattern from B) remained intact without any cell migrating to the repulsive surface although several neurites started to grow and bridge over the PEG-coated surface. The pattern depicted in bright field D) and GFP D) constituted a loop, which was 2 mm-long with mostly one or small group up to 3 neurons connecting to each other along the circle.

[0128] The technique was also proved to be functional to fully remove unwanted neurons from the repulsive surface as well as those on the half-right of the adhesive smiley (Fig. 9E) and F)). After 12 DIV, it was unexpectedly observed in E) that no neuron appeared to move to the PDL-coated area from where cells got initially removed. It also seemed that neurites and axons could grow over one-mm length on the PDL surface without encountering another neighbour cell. The loop architecture representing the outline of the smiley would potentially help to track the novelty in the signal transmitted compared to the previous reference signal in order to assess meaningful information but also perceive the selective directionality of the given signal. Viability of those primary neural cultures was tracked by measuring fluorescent calcium activity.

[0129] In addition, the cantilever proved to be a successful tool to modify *in situ* an existing pattern of adhering and mature cell cultures. The thick cantilevers were robust enough to undergo high underpressure (nearly -900 mbar). Up to 10 sec were necessary to remove portions of the pattern where neurons started to develop a large carpet of neurites over the PEG-coated surface, as depicted in Fig. 10A), B) and C).

[0130] Similarly, the cantilever was used to dispense fresh neurons on an existing pattern. As illustrated in Fig. 10D) and E), a smiley pattern was completed by the controlled deposition of additional cells at the right-eye location. This approach could largely profit to extensive mechanical studies of neural networks. Besides, it presents a high potential to study *in situ* mechanisms of cell growth, migration and interaction over long-term studies.

Conclusion

[0131] In this work, a working process was developed based on a sacrificial copper layer deposited by electroplating to produce robust SU-8 hollow AFM cantilevers. Cantilevers of various shapes and dimensions, e.g. of 12 μm thickness with channels of 3 μm thickness, could be fabricated with various spring constants ranging from 0.01 to 1,000 N/m. Also cantilevers of 50 μm thicknesses with channels of 23 μm thickness could be manufactured.

[0132] The AFM capability of these tipless cantilevers was demonstrated in a biologically relevant application, by performing single-cell force spectroscopy of yeast cells. One main advantage of this invention is the provision of micropipette that overcome the limitation of glass micropipettes limited in terms of throughput and geometry.

[0133] Furthermore, the present work introduces a novel technology based on highly flexible hollow cantilevers for cell patterning via controlled deposition and selective removal of single cells. The flexibility of the method has been demonstrated using yeast and C2C12 cells, as well as primary hippocampal neurons. Several patterning strategies have been tested in liquid environment with the use of fully cell adhesive and patterned adhesive/repulsive flat surfaces. The key principle behind the method resulting in single-cell patterning with an accuracy of 5 μm relies on the physical cell confinement enabled by the high flexibility of the polymeric cantilevers.

[0134] It has been shown that large engineered neuron patterns can be realized with the presented method, however, for high throughput and large patterns, subtractive patterning was found to be more promising with an average removal speed of one targeted cell per second. Additive patterning is limited by an order of magnitude slower speed and the consequently smaller patterns.

[0135] Combined with surface patterning methods, the developed precise cell-patterning techniques can become essential tools for studies related to signal processing and computation in neuroscience. Providing single neuron-based networks with arbitrary topology can lead to a better understanding of the relationships between connectivity and function.

[0136] The versatility of the cantilever was proved by modifying *in situ* patterns previously realized. Additional cells could be indeed removed or deposited thanks to the robust hollow cantilever. This latter technique allows deeper studies for mechanical and cell interactions of cell networks.

[0137] In summary, the developed highly flexible hollow cantilevers represent a promising new tool for single-cell manipulations and patterning. Compared to other techniques requiring complex setups and feedback, the presented method works with simple components and

does not require laser feedback. This makes it possible to parallelize the process, and to operate in complex, highly scattering samples in liquid environment.

Photolithography process

[0138] The microfabrication process was entirely carried out in the BRNC cleanroom facilities (IBM Zurich Laboratories and ETH Zurich, CH).

[0139] First, a sacrificial release layer 21 of 5 nm chromium/ 50 nm gold/ 50 nm chromium was deposited onto a silicon wafer used as a carrier substrate (100 mm outside diameter $\times$ 500 μm thickness, SILTRONIX Silicon Technologies, France) by e-beam deposition (BAK501, Evatec, CH). Wafers were cleaned in 5 min acetone and 5 min isopropanol in ultrasonic bath (Wet bench, Ramgraber, Germany) before dehydration bake at 200 °C for 5 min (M-HP 200 Hotplate, Ramgraber). Alignment marks, for proper alignment of the different SU-8 layers, were patterned by etching away the chromium top layer only at the mark spots using MaN 1405 negative photoresist. MaN photoresist was spun at 3000 rpm for 30 s (OPTIspin SB20, Sigmatek, CH) before being baked at 120 °C for 1 min. Samples were exposed for 200 mJ/cm^2 at λ = 365 nm (MA6, Suss, Germany) followed by 30 s of development in ma-D533S solution. Alignment marks could be etched within 10 s in a chromium etchant solution (Chromium etchant, Sigma Aldrich, USA). Removal of the exposed photoresist and cleaning of the wafers were carried out by immersion in acetone and isopropanol for 5 min each before another dehydration bake at 200 °C for 5 min.

[0140] (Fig. 1A): The bottom SU-8 layer 22 was patterned with spin-coating at 3000 rpm (SU-8 2005, Microchem, USA), soft bake for 1 min at 65 °C and 2 min at 95 °C. Systematically, wafers were cooled down to 50 °C on a hot plate avoiding any thermal shock. UV exposure was performed using 160 mJ/cm^2 exposure dose at λ = 365 nm in vacuum contact mode (for a better definition of the aperture). Post-exposure bake was performed for 1 min at 65 °C and 3 min at 95 °C before development for 2 min (PGMEA, Sigma Aldrich) and rinsing with fresh isopropanol.

[0141] (Fig. 1 B): The copper seed layer 23 was deposited by thermal evaporation for a thickness of 150 nm in two steps with 75 nm each using a tilted plate at 35 degrees, an emission current of 3.6 A, a pressure of 5x10^{-7} bar and a deposition rate of 0.45 nm/s (PLS 500, Pfeiffer, CH).

[0142] (Fig. 1 C): Positive AZ4562 photoresist 24 was used to confine the growth according to the following parameters: spin-coating at 4000 rpm for 40 s, soft bake for 1 min at 65 °C and 1 min at 95 °C, exposure for 160 mJ/cm^2 at λ = 365 nm, post-exposure bake for 1 min at 65 °C and 1 min at 95 °C before development for 2 min in AZ 400K 1:3 diluted solution (MicroChemicals, Germany). Prior to electroplating, samples were plasma treated at 200 W for 1 min (GIGAbatch 310 M, PVA TePla, Germany) and dipped in sulfuric acid for 20 s at 1:9 diluted solution (99.999 % Sulfuric acid, Sigma Aldrich).

[0143] (Fig. 1 D): Copper plating 25 was performed using copper sulfate solution (InterVia Cu 8540, Rohm and Haas, USA) and commercial setup (Luder Technik AG, CH) for current and voltage applied of respectively 160 mA and 10.2 V during 3 min for copper thickness growth of 3 μm, after electrically contacting the wafer edges at eight equidistant locations. Thickness was controlled with a stylus profiler (Dektak 6M, Veeco, USA).

[0144] (Fig. 1 E): AZ4562 24 was stripped within 10 s in an acetone bath before etching of the seed copper layer 23 for another 5 s (Copper etchant, Sigma Aldrich) and rinsing for 2 min in DI-water.

[0145] (Fig. 1 F): The top SU-8 layer 26 was patterned with spin-coating at 4000 rpm for 30 s (SU-8 10, Microchem), soft bake for 3 min at 65 °C and 7 min at 95 °C, exposure for 400 mJ/cm^2 at λ = 365 nm, post-exposure bake for 1 min at 65 °C and 3 min at 95 °C, development for 3 min and rinsing with fresh isopropanol.

[0146] (Fig. 1 G): The thick block SU-8 layer 28 (SU-8 100, Microchem) was patterned with spin-coating at 1250 rpm for 40 s, break of few hours to flatten the thick layer, soft bake for 30 min at 65 °C and 75 min at 95 °C, cooling down on hot plate back to room temperature, exposure for 1200 mJ/cm^2 at λ = 365 nm, post-exposure bake for 2 min at 65 °C and 18 min at 95 °C, cooling down on hot plate back to room temperature, development for 40 min and rinsing with fresh isopropanol.

[0147] Finally, hard bake was performed to enhance adhesion between both bottom 22 and top layers 26 at 70 °C for 2 h (VT6060M, Thermo Scientific Heraeus). This step was optimized for better cross-linking and mechanical robustness of the cantilevers but also to limit their delamination from the substrate. To enhance wetting, wafers were plasma-treated with air pressure of 0.02 mbar, RF power of 18 W for 2 min (PDC-32G, Harrick Plasma, USA) before copper etching during 10 days and release from the wafer (Fig. 1 H).

[0148] For AFM applications, SU-8 cantilevers were coated with a thin reflective layer of 2 nm Cr/10 nm Au (E306A Coating System, Edwards, England). Parafilm M substrate (Bemis, USA) was used to carry the devices (excluding cantilevers bending).

[0149] Hollow SU-8 polymeric cantilevers for controlled single-cell deposition and patterning decribed above were fabricated following the protocol described above. The process based on electroplated copper as sacrificial layer was adapted for the cell-related experiments by producing cantilevers with integrated microchannels of 22 μm in height. In brief, a positive AZ4562 photoresist was patterned with a thickness of 25 μm to confine the copper growth within the channel area using the following parameters: spin-coating at 2 000 rpm for 4 sec with 1 000 rpm/sec acceleration, baking for 1 min at 65 °C and 1 min at 95 °C, exposure in 500 mJ/cm2 at λ = 365 nm, then post-exposure baking for 1 min at 65 °C and 1 min at 95 °C before development. Applying 500 mA and 10.2

V for 6 min resulted in a growth of a copper layer with a thickness of 22 μm on the wafer. Further steps of the fabrication process were identical to that of the original protocol. The resulted cantilevers had a total height of 45 μm, lengths ranging from 250 to 400 μm, and widths from 50 to 80 μm.

SEM

[0150] Scanning electron microscopic (SEM) images were taken using a Zeiss NVision 40 (Germany) with an accelerating voltage between 5 and 10 kV.

Fluidic setup

[0151] SU-8 cantilevers were glued on a PMMA clip containing a 25 μL reservoir connected to a pressure controller (Cytosurge, CH) through a tubing system allowing to apply a large range of pressure from -800 mbar to + 1000 mbar. Before use, to avoid any possible contamination of copper residues, copper etchant, or chromium etchant, the SU-8 device was completely flushed with DI-water for 15 min after plasma activation for 5 min (PDC-32G, Harrick Plasma).

[0152] The flow rate was calibrated using a digital liquid flow sensor placed close to the reservoir (LG16- 0025-D, Sensirion, CH).

[0153] Hydrostatic tests were performed using stationary gas supply from the lab connected to a pressure regulator and a manometer (pressure limited to 6 bars). An FITC dye was used to fill the cantilever and to detect any potential leaks.

AFM experiments for studying cell adhesion using force spectroscopy

[0154] The AFM experiments were carried at 23 °C with a NanoWizard® I BioAFM from JPK Instruments (Germany) mounted on an optical microscope (Axiovert 40 MAT, Zeiss). The AFM was operated with a 15 μm range piezo-stage using the force spectroscopy mode. Before performing force spectroscopy experiments, all cantilevers were kept at rest in liquid from 30 min to 1 h until voltage- deflection signal became stable. Drift is inevitable with the use of polymeric SU-8 cantilevers. However, high overexposure and baking time probably limited the voids rate within the SU-8 matrix, capable of absorbing liquid.

[0155] The SU-8 cantilever spring constant was calibrated using the thermal noise via the conventional Sader's method in air environment on glass substrate with the SPM Control Software V4 (JPK). The sensitivity deflection measured with regard to the optical lever sensitivity (OLS) followed the configuration where only the end of the cantilever was touching the substrate.

[0156] Force spectroscopy curves were obtained by selecting optically a single yeast and subsequently approaching the cantilever on top by systematically using a set point fixed at 50 nN. Approach and retraction curves were both recorded over a length of 10 μm for 5 s each (i.e. speed of 2 μm/s). Approach was followed by a contact pause of 5 s during which force was kept constant and an underpressure of -500 mbar was applied to immobilize the yeast cell at the aperture of the cantilever before subsequent retraction. Finally, every yeast was released by applying an overpressure of 1000 mbar before targeting a new yeast.

Experimental setup for controlled single-cell deposition and patterning by the highly flexible hollow cantilevers of the invention

[0157] Hollow cantilevers were connected to a pressure controller (Cytosurge, Switzerland) and mounted on an atomic force microscope (NanoWizard 1 BioScience AFM; JPK Instruments AG, Germany) for controlling their z-position with sub-μm precision (no laser force feedback has been used for the experiments). Free-hanging cantilevers had an inclination angle of 8-10° with respect to the substrate. The AFM stage was placed on an inverted microscope (Axio Observer.Z1) equipped with a Colibri LED light source system (both from Carl Zeiss AG, Switzerland), an incubation chamber, and a CCD camera (C9100-13; Hamamatsu, Japan). The temperature control of the incubation chamber has been used only for the neuron related experiments keeping the setup at 37 °C, the other experiments were performed at room temperature.

[0158] Additionally, CLSM images were taken using a LSM 510 mounted on an Axiovert 200 M motorized microscope (Zeiss), while scanning electron microscope (SEM) images were taken with the help of an NVision 40 (Zeiss) using accelerating voltages in the range of 5-10 kV.

Chemicals

[0159] Purified Milli-Q water was produced by an Elix 5 water purification system (Merck Millipore, USA). Fluorescent cell-adhesive solution was prepared by mixing 100 μg/ml Poly-D-lysine (PDL, P6407 70-150kDa; Sigma-Aldrich) with 40 μg/ml fluorescently tagged secondary antibody (anti-mouse IgG (H+L), CF 555; Sigma-Aldrich) diluted in phosphate-buffered saline (PBS, pH 7.4; Thermo Fisher Scientific AG, Switzerland). PLL-g-PEG solution was prepared from powder (PLL(20)-g[3.5]-PEG(2); SuSoS AG, Switzerland) and diluted in PBS to a final concentration of 100 μg/ml if not indicated otherwise.

Cells culturing and substrate preparation

[0160] Glass substrates (GWSB-5040, WillcoWells, NL) were plasma treated for 30 s.

[0161] PDA-coated substrates were initially plasma treated for 30 s, immersed in a 10 mM TRIS HCL solution

pH 8 containing 4 mg/mL PDA (Sigma Aldrich) for 1 h, then intensively washed with filtered PBS and dried with N_2.

[0162] Wildtype Saccharomyces cerevisiae (W303) were grown in yeast extractpeptone-dextrose medium (10 g yeast extract (Oxoid), 20 g bactopeptone (BD) and 20 g glucose (Sigma-Aldrich) in 1 L ddH_2O, with 15 g Agar (Sigma-Aldrich) for solid media). The yeasts were plated onto YPD plates and incubated for 2-3 days at 28 °C. Until the force spectroscopies were performed, colony containing plates were kept for up to three month at 4 °C.

[0163] Prior to the experiments, individual colonies were picked, resuspended in PBS medium (10010023, Life Technologies, USA) before directly letting them sediment on top of glass substrates for SCFS experiments at room temperature during 10 min. 20 μL yeasts colony solution was directly injected on top of the substrates previously filled up with 3 mL PBS.

[0164] Mouse myoblast C2C12 cells (American Type Cell Collection) were cultured in C2C12 culture medium (DMEM/F-12 supplemented with 10% fetal bovine serum and 1% antibiotic-antimycotic; all from Thermo Fischer) at 37 °C and 5% CO_2. Prior to the patterning experiments, cells were trypsinized (with TrypLE Express; Thermo Fischer) and fluorescently tagged with a PKH26 Red Fluorescent Cell Linker Kit (Sigma Aldrich).

[0165] Primary Hippocampal Neurons were prepared from E17 embryos of time-mated pregnant Wistar rats (Harlan Laboratories, NL), and cultured in neuronal culture medium (neurobasal medium mixed with 2% B-27 serum-free supplement, 1% penicillin-streptomycin, and 1% GlutaMAX; all from Thermo Fischer) at 37°C and 5% CO_2.

Cantilever preparation

[0166] Before the experiments, cantilevers were coated with PLL-g-PEG (0.5 mg/ml in PBS) for 45 min then flushed with fresh PBS to make the surface anti-adhesive. For plating experiments with yeast, individual colonies were resuspended in PBS and injected into the reservoir of the cantilevers at a concentration of 100'000 cells/ml. For plating experiments with C2C12, cells were resuspended at a concentration of 100'000 cells/ml in HBSS (Hank's Balanced Salt Solution H8264; Thermo Scientific).

Substrate preparation

[0167] Glass bottom dishes (GWSB-5040; WillCo Wells B.V., The Netherlands) were used for all the experiments. The dishes were oxygen plasma activated for 2 min at 18 W, then were either filled up with PBS, or incubated with a non-fluorescent PDL solution for 1 h, rinsed 3 times with Milli-Q water, and blow dried with nitrogen gas to create a fully adhesive surface.

[0168] Before the patterning experiments, dishes were filled with medium corresponding to the cell type used. For the subtractive patterning experiments, cells were seeded at a density of 150'000 cells/cm^2 and incubated for 20 min.

Surface patterning

[0169] Patterned cell-adhesive surfaces for neuronal cultures have been prepared with the help of a hollow cantilever as a probe. In brief, a tipless hollow cantilever was filled with the fluorescent cell-adhesive solution, connected to the pressure controller, and then mounted on a standard AFM head (FlexAFM; Nanosurf, Switzerland). Once the probe was placed on top of the dish and submerged in the PBS, 10 mbar overpressure was applied from the pressure controller to continuously push the patterning solution out of the probe. After the patterning, dishes were rinsed with Milli-Q and blow dried with nitrogen gas, and then PLL-g-PEG solution was added in order to increase the contrast between patterned and non-patterned surface regions by backfilling. After 1 h of incubation the dishes were rinsed three times with PBS, then were filled up with cell culture medium and stored in the incubator until cell seeding.

Claims

1. A method for manufacturing a device (100) comprising a flexible shank (11), and said shank (11) comprises a microfluidic channel (12) having an aperture (13), the method comprises the steps of:

   - providing a support covered by a sacrificial release layer (21), wherein particularly said sacrificial release layer (21) is **characterized by** a thickness in the range of 5 nm to 500 nm;
   - depositing a bottom layer (22) of a first photoresist onto said sacrificial release layer (21), wherein said bottom layer (22) is **characterized by** a thickness in the range of 0.5 μm to 100 μm;
   - partially curing said bottom layer (22) within a first defined pattern (22), wherein said bottom layer (22) optionally comprises said aperture (13);
   - depositing a metal seed layer (23) onto said bottom layer (22);
   - depositing a mould layer (24) of a second photoresist onto said metal seed layer (23);
   - curing said mould layer (24) within a second defined pattern (24), thereby yielding a cured mould layer (24), wherein a part (23a) of said metal seed layer (23) covering said bottom layer (22) is not covered by said cured mould layer (24);
   - depositing an additional metal layer (25) onto said part (23a) of said metal seed layer (23) not covered by said cured mould layer (24), wherein

said additional metal layer (25) is **characterized by** a thickness in the range of 0.1 μm to 30 μm;
- dissolving said cured mould layer (24) and said metal seed layer (23);
- depositing a cover layer (26) of said first photoresist onto said bottom layer (22) and said additional metal layer (25), wherein said cover layer is **characterized by** a thickness in the range of 0.5 μm to 100 μm;
- completely curing said first photoresist comprised within said cover layer (26) and said bottom layer (22) within a third defined pattern (26), thereby forming a bottomside, sidewalls and a topside of said device (100);
- dissolving said additional metal layer (25); and
- dissolving said sacrificial release layer (21) releasing said device (100) from said support.

2. The method according to claim 1, **characterized in that** a handling block layer (28, 15) is attached onto said cover layer (26), wherein said handling block layer (28, 15) comprises a through hole (16) being in fluid communication with said microchannel (12), and wherein said handling block layer (28, 15) is **characterized by** a thickness in the range of 100 μm to 300 μm, preferably 250 μm.

3. The method according to claim 1 or 2, **characterized in that** said first photoresist is a negative photoresist, particularly SU-8.

4. The method according to any one of the preceding claims, **characterized in that** said second photoresist is a positive photoresist, particularly AZ4562.

5. The method according to any one of the preceding claims, **characterized in that** said bottom layer (22), said mould layer (24) and/or said cover layer (26) are deposited by spin coating.

6. The method according to any one of the preceding claims, **characterized in that** said bottom layer (22) and said coverlayer (26) are cured such with said first defined pattern and said third defined pattern, respectively, that said shaft (11) of said device (100) comprises a tip (17) that extends along a first direction, wherein the angle between said first direction and the longitudinal axis of said shank (11) or said microfluidic channel (12) is in the range of 180° to 90°.

7. The method according to any one of the preceding claims, **characterized in that** said said bottom layer (22) and said coverlayer (26) are cured such with said first defined pattern and said third defined pattern, respectively, that said shaft (11) exhibits a curved shape, a jagged shape, a zigzag shape, or a shape comprising a step.

8. A device (100) having:

- a flexible shank (11) comprising a microfluidic channel (12) and an aperture (13) that is in fluid communication with said microfluidic channel (12), wherein said microfluidic channel (12) is delimited by at least one surface being formed by a polymer, and
- a reservoir (14) in fluid communication to said microfluidic channel (12), whereby said aperture (13) is oriented at the end of said flexible shank (12) opposite to said reservoir (14), and
- a means for measuring a mechanical force acting on said flexible shank (11) arranged on or within said flexible shank (11), and
- optionally a handling means (15) with a through hole (16) in fluid communication with said reservoir (14),

characterized in that

- said polymer forming said at least one surface delimiting said microfluidic channel (12) is integrally formed in one piece, and particularly said polymer is **characterized by** an elasticity of 1 GPa to 10 GPa, preferably 4 GPa to 5 GPa, more preferable 4.5 GPa, and
- said microfluidc channel (12) is configured to pass a fluid stream with pressure of up to 6 bar (a), and particularly is fluid tight up a pressure of 6 bar(a), and
- said flexible shank (11) is **characterized by** spring constant in the range of 0.01 $N*m^{-1}$ to 1,000 $N*m^{-1}$.

9. The device according to claim 8, **characterized in that** said polymer forming at least one surface delimiting said microfluidic channel (12) exhibits a homogenous structure.

10. The device according to claim 8 or 9, **characterized in that** said polymer is a cured photosensitive polymer, particularly SU-8.

11. The device according to any one of claims 8 to 10, **characterized in that**

- said microfluidic channel (12) has a length in the range of 0.1 mm to 50 mm and/or a width in the range of 1 μm to 50 μm and/or a height in the range of 0.1 μm to 30 μm; and/or
- said shank (11) has a thickness in the range of 10 μm to 50 μm, and/or a width in the range of 20 μm to 80 μm.

12. The device according to any one of claims 8 to 11, **characterized in that** said means for measuring a mechanical force acting on said flexible shank (11)

is formed by

- a metal layer consisting of at least one noble, non-toxic metal, whereby said metal layer is able to changes its resistance in dependence of a mechanical force acting on said metal layer; or
- a sensing layer comprising a plurality of nanowires (31) made of metal, wherein said nanowires (31) are partially coated with an isolator such that at least a part of said nanowires (31) are in conductive contact to each other when no mechanical force is acting on said shank (11), and said at least one part of said nanowires (31) in conductive contact to each other decreases with increase of an mechnical forces acting on said shank, wherein particularly said nanowires (31) are **characterized by** a thickness in the range of 40 nm to 60 nm and/or a length in the range of 5 μm to 50 μm;
- a sensing layer comprising a plurality of nanowires (31) made of metal, wherein said nanowires (31) are arranged such within the sensing layer that at least a part of said nanowires (31) are in conductive contact to each other when no mechanical force acts on said shank (11), and said at least one part of said nanowires (31) in conducting contact to each other decreases with increase of an mechnical forces acting on said shank, wherein particularly said nanowires (31) are **characterized by** a thickness in the range of 40 nm to 60 nm and/or a length in the range of 5 μm to 50 μm;
- a part of said shank (11) being optically transparent, wherein said part of said shank (11) is configured to change its optical properties, particularly its refractive or diffractive properties, in dependence of a mechanical force acting on said part of said shank (11).

13. The device according to any one of claims 8 to 12, **characterized in that** said aperture (13) is comprised within a tip (17) of said shank (11), wherein said tip (17) extends along a first direction, and the angle between said first direction (R) and the longitudinal axis of said shank (11) or said microfluidic channel (12) is in the range of 180° to 90°, and wherein said tip (17) has a tapered shape or a cylindrical shape.

14. The device according to any one of claims 8 to 13, **characterized in that** said shank (11) exhibits a curved shape, a jagged shape, a zigzag shape or a shape comprising a step, wherein said curved shape, said jagged shape, said zigzag shape or said shape comprising a step extends within a plane being parallel to said first direction.

15. The device according to any one of claims 8 to 14, **characterized in that** said device (100) or said flexible shank (11) is designed as a cantilever or a micropipette, wherein said micropipette optionally comprises a re-usable tip (17) comprising a plurality of segments extending from said shank (11), wherein each segment is **characterized by** a tapered shape, and between each segment a portion of said tip is arranged, and wherein at least one of said portions arranged between said segments is designed as predetermined breaking point.

Fig 1

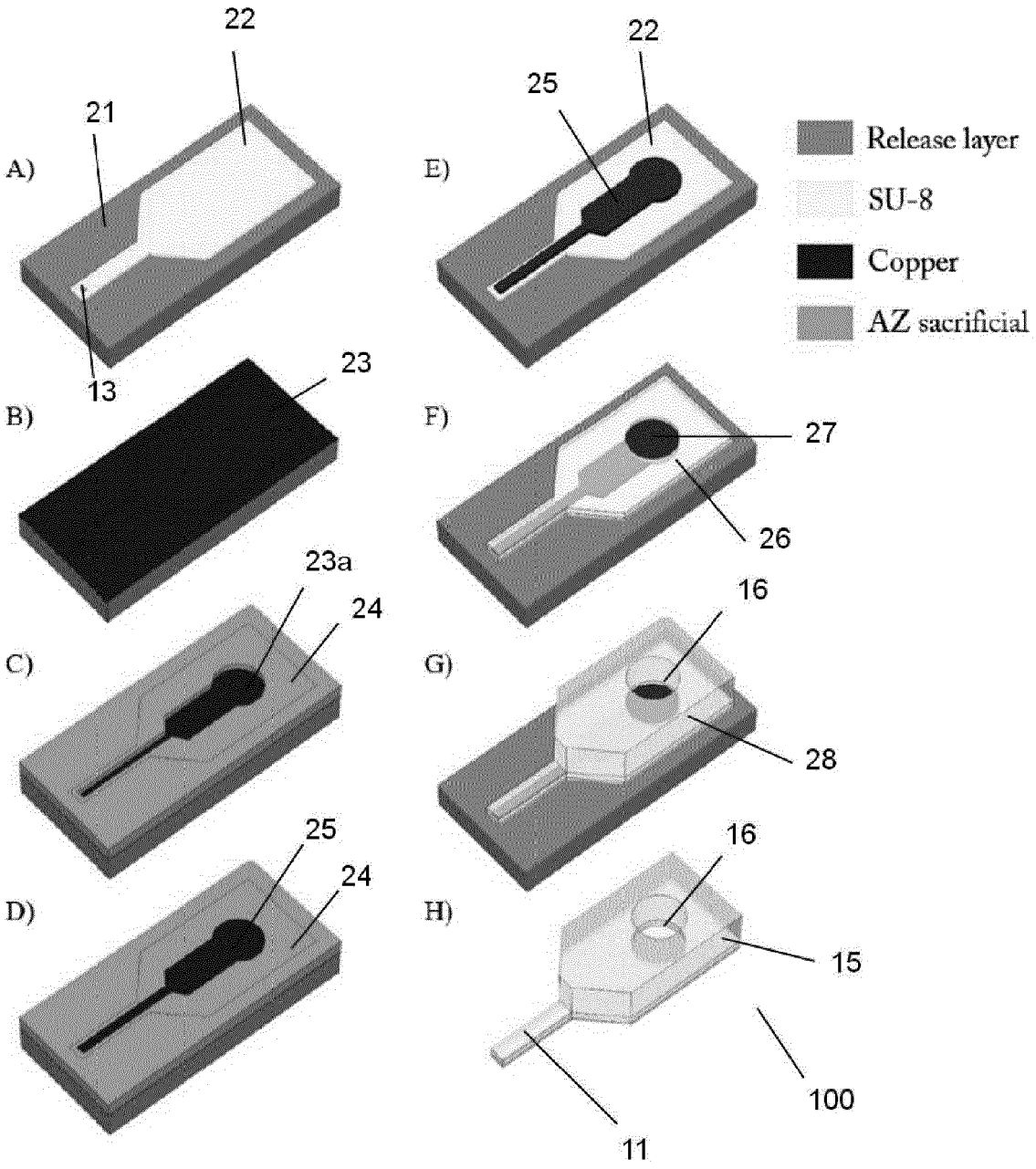
A)
21
22
13
B)
23
C)
23a
24
D)
25
24
E)
25
22
F)
27
26
G)
16
28
H)
16
15
100
11
Release layer
SU-8
Copper
AZ sacrificial

Fig. 2

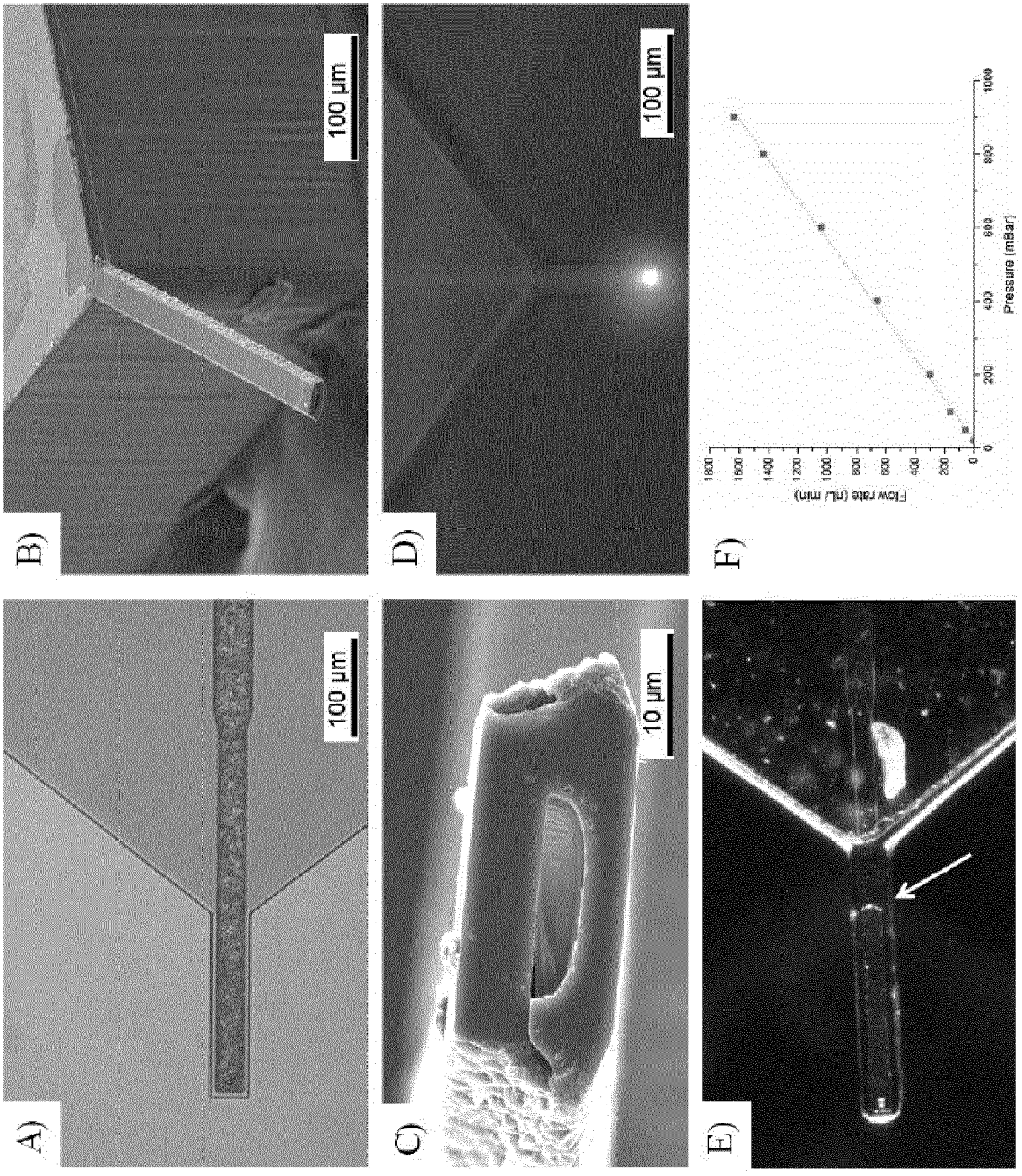
A)
100 µm
B)
100 µm
C)
10 µm
D)
100 µm
E)
F)
Flow rate (nL/ min)
Pressure (mBar)
0
200
400
600
800
1000
1200
1400
1600
1800

Fig. 3

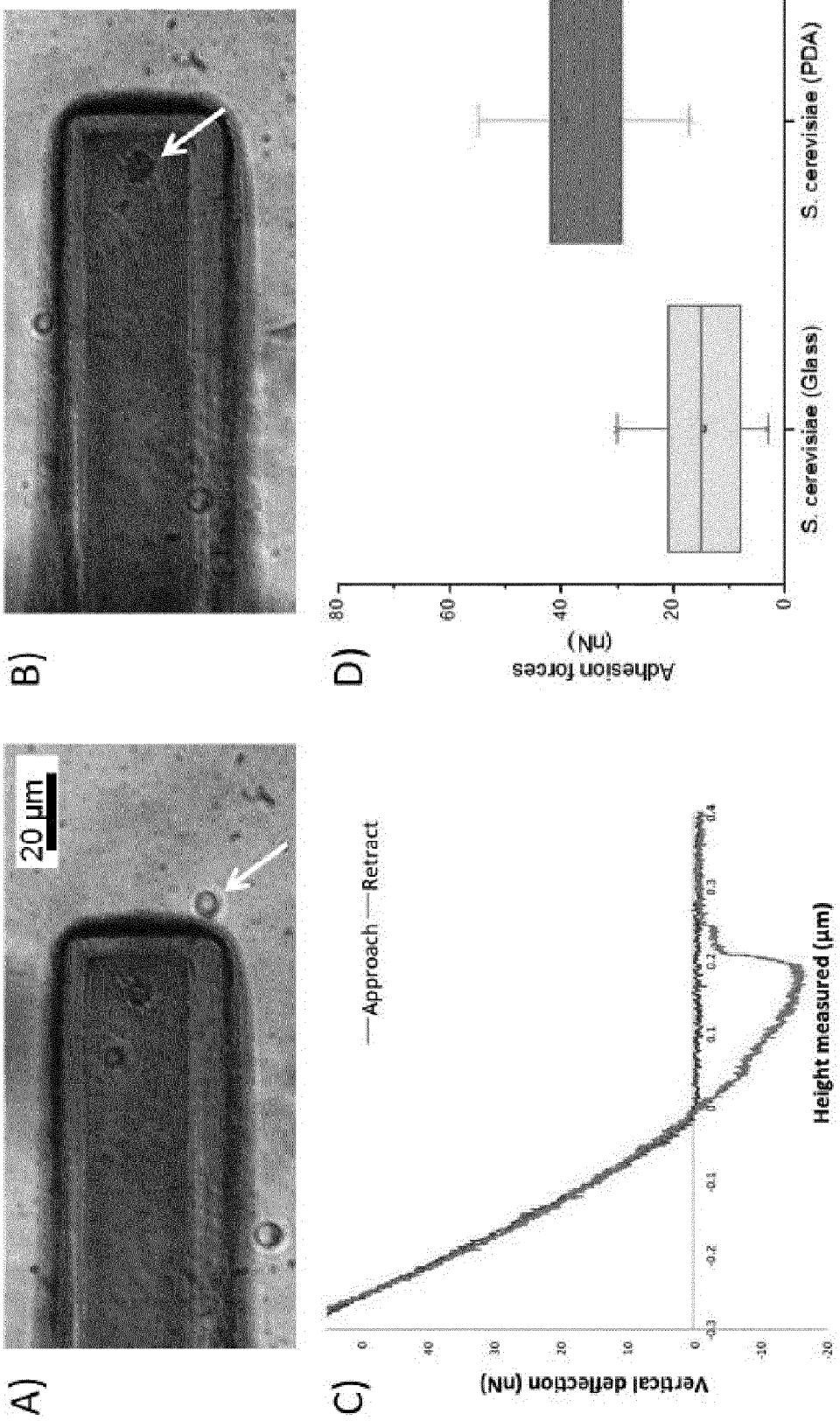
A)
20 µm
B)
C)
Approach
Retract
Vertical deflection (nN)
Height measured (µm)
D)
Adhesion forces (nN)
S. cerevisiae (Glass)
S. cerevisiae (PDA)

Fig. 4

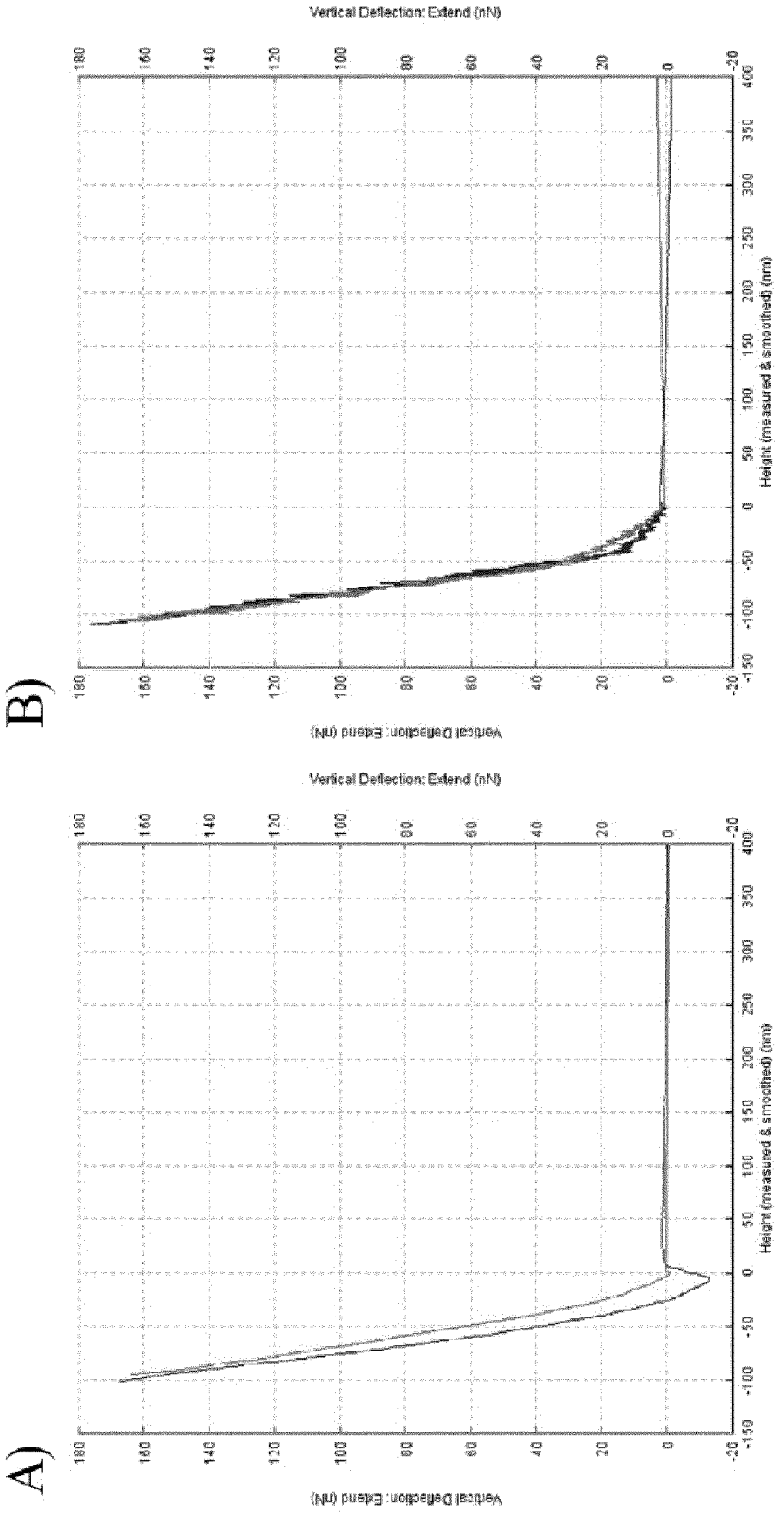
B)
Vertical Deflection: Extend (nN)
Height (measured & smoothed) (nm)
A)
Vertical Deflection: Extend (nN)
Height (measured & smoothed) (nm)

Fig. 5

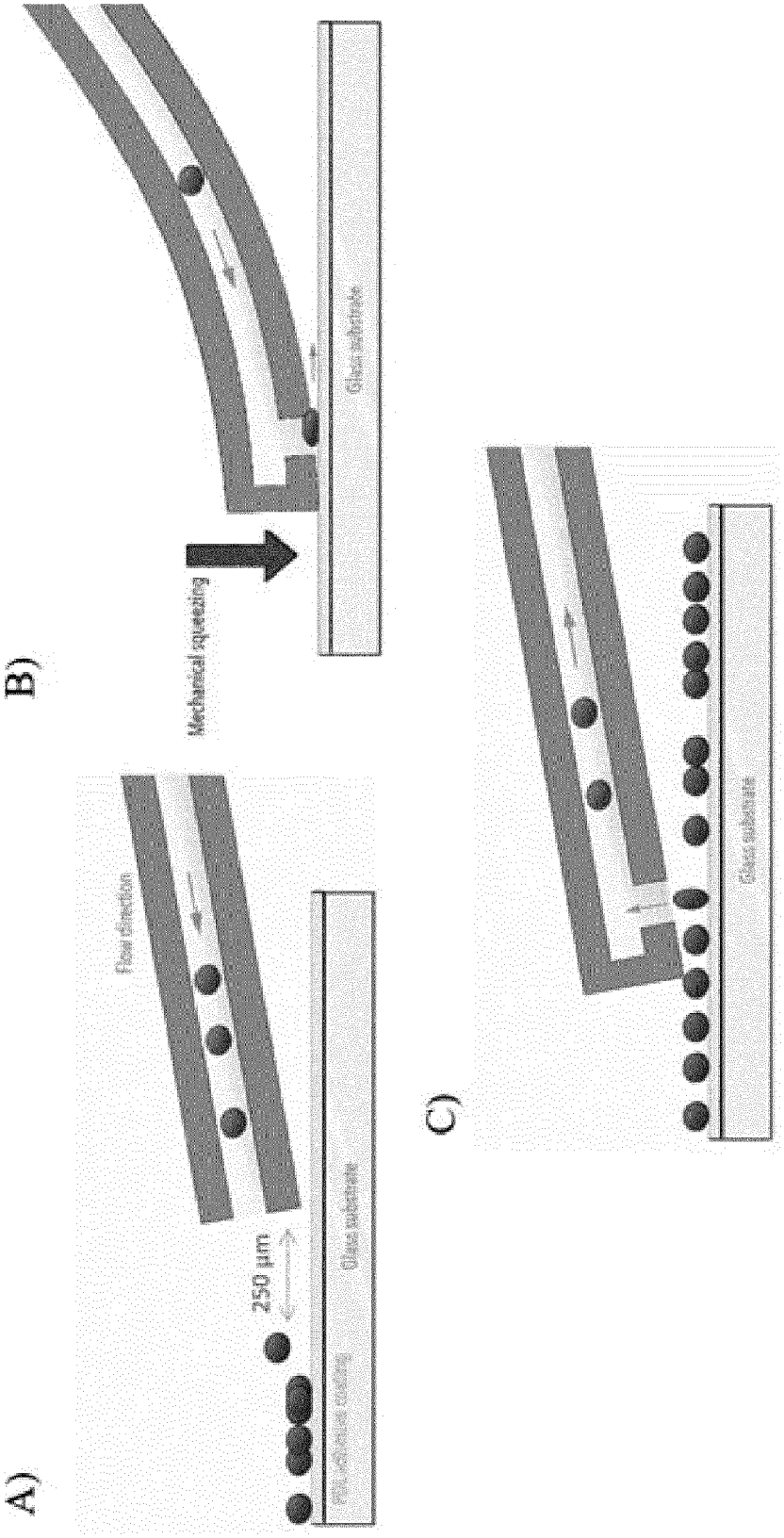
A)
Flow direction
250 µm
Glass substrate
B)
Mechanical squeezing
Glass substrate
C)
Glass substrate

Fig. 6

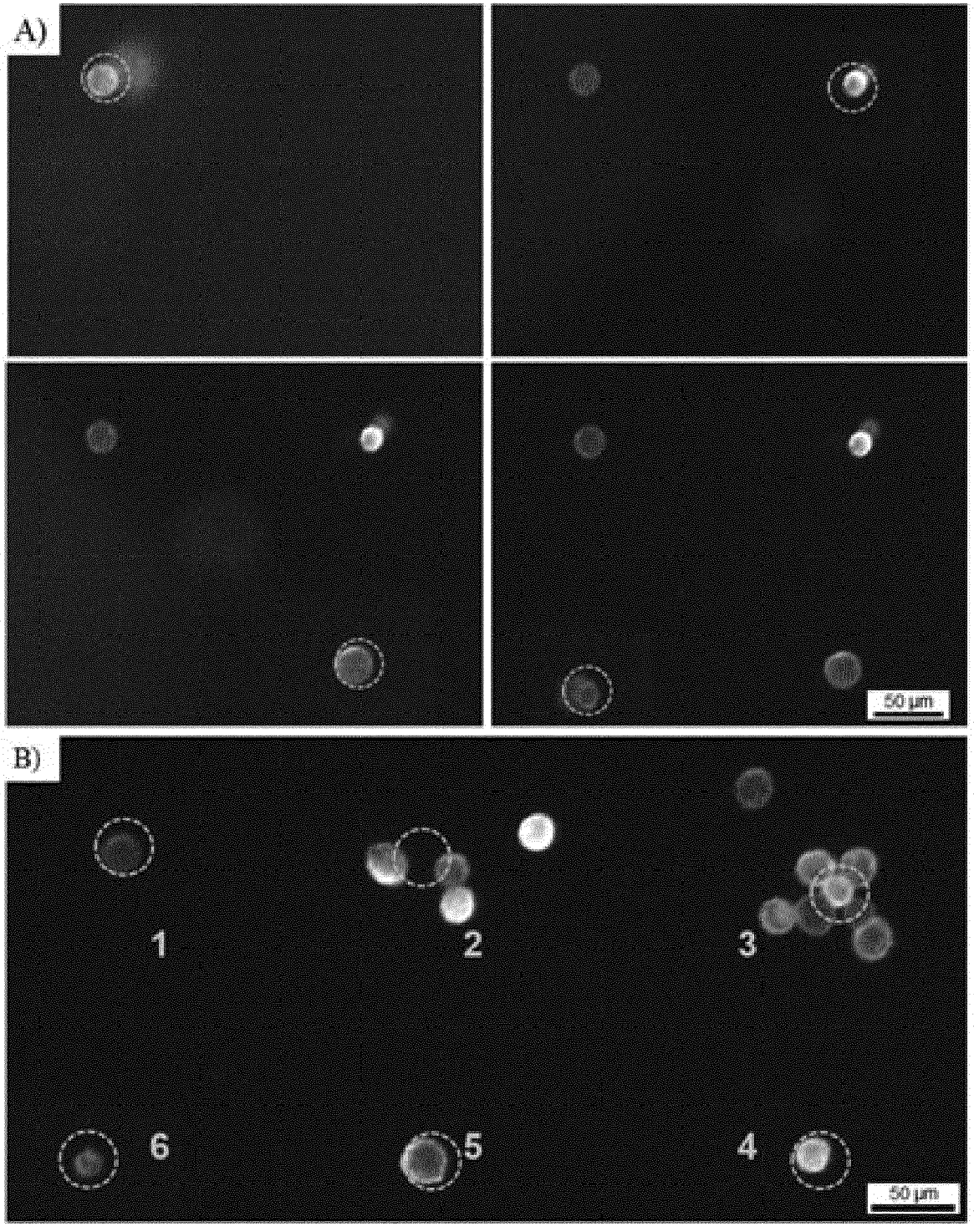

Fig. 7

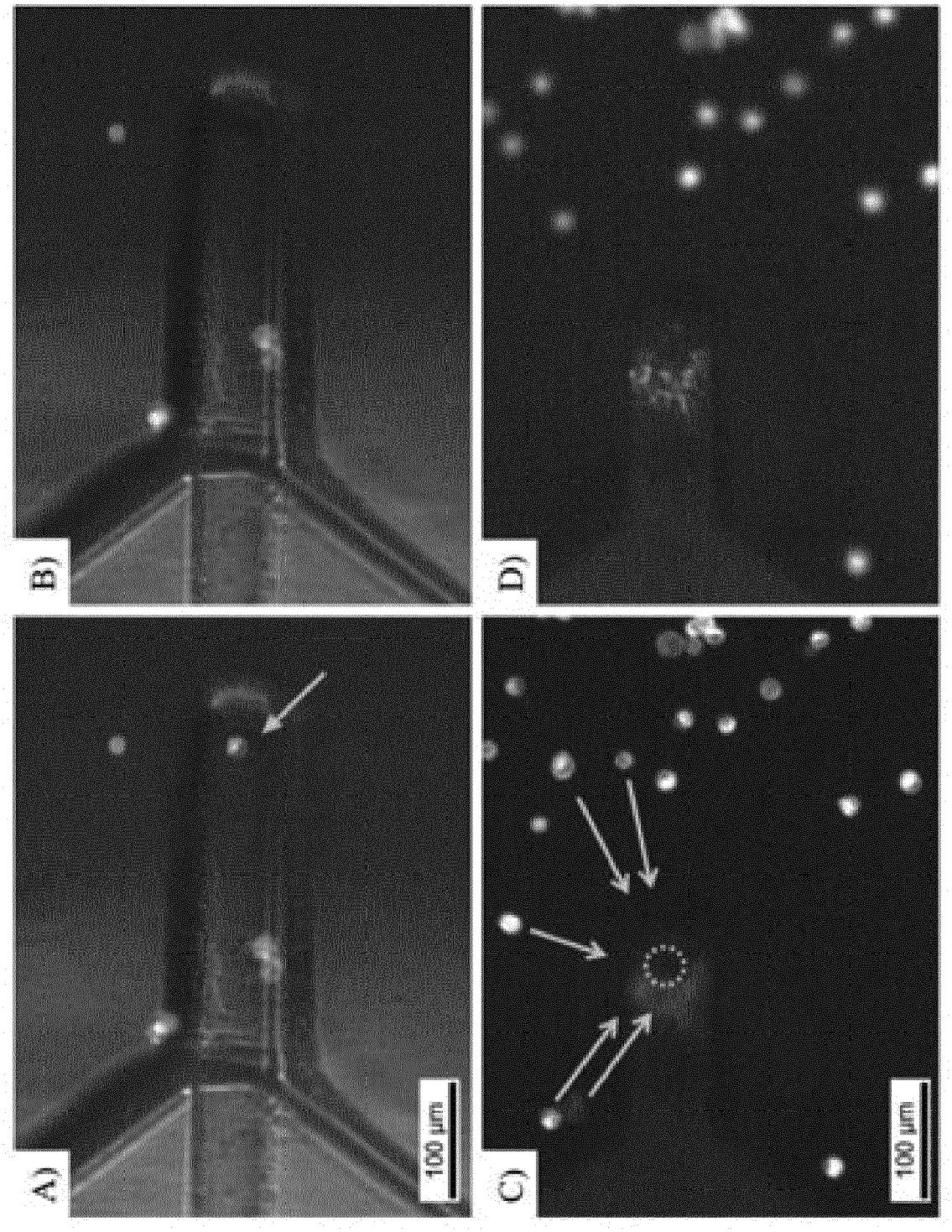

Fig. 8

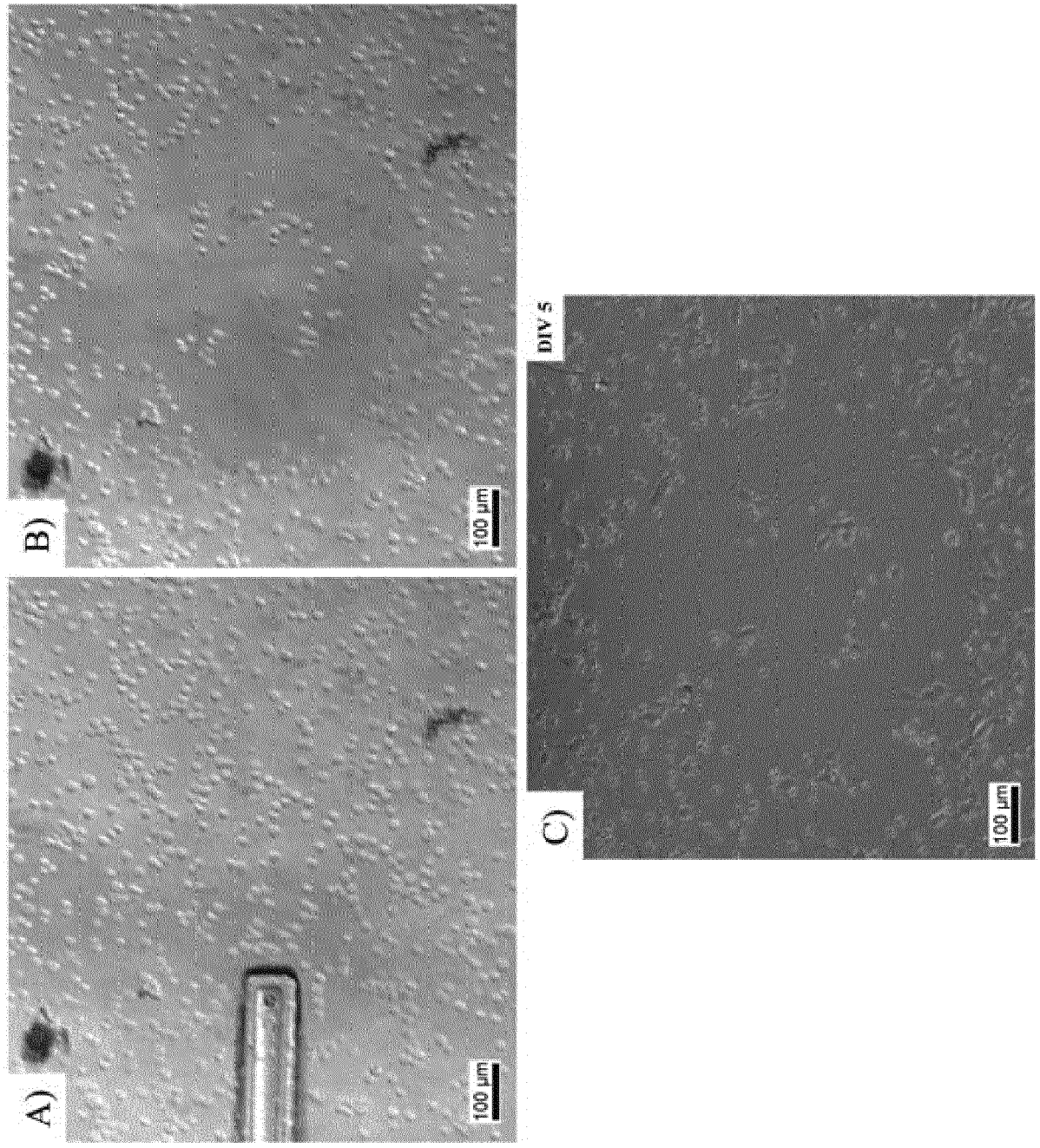

Fig. 9

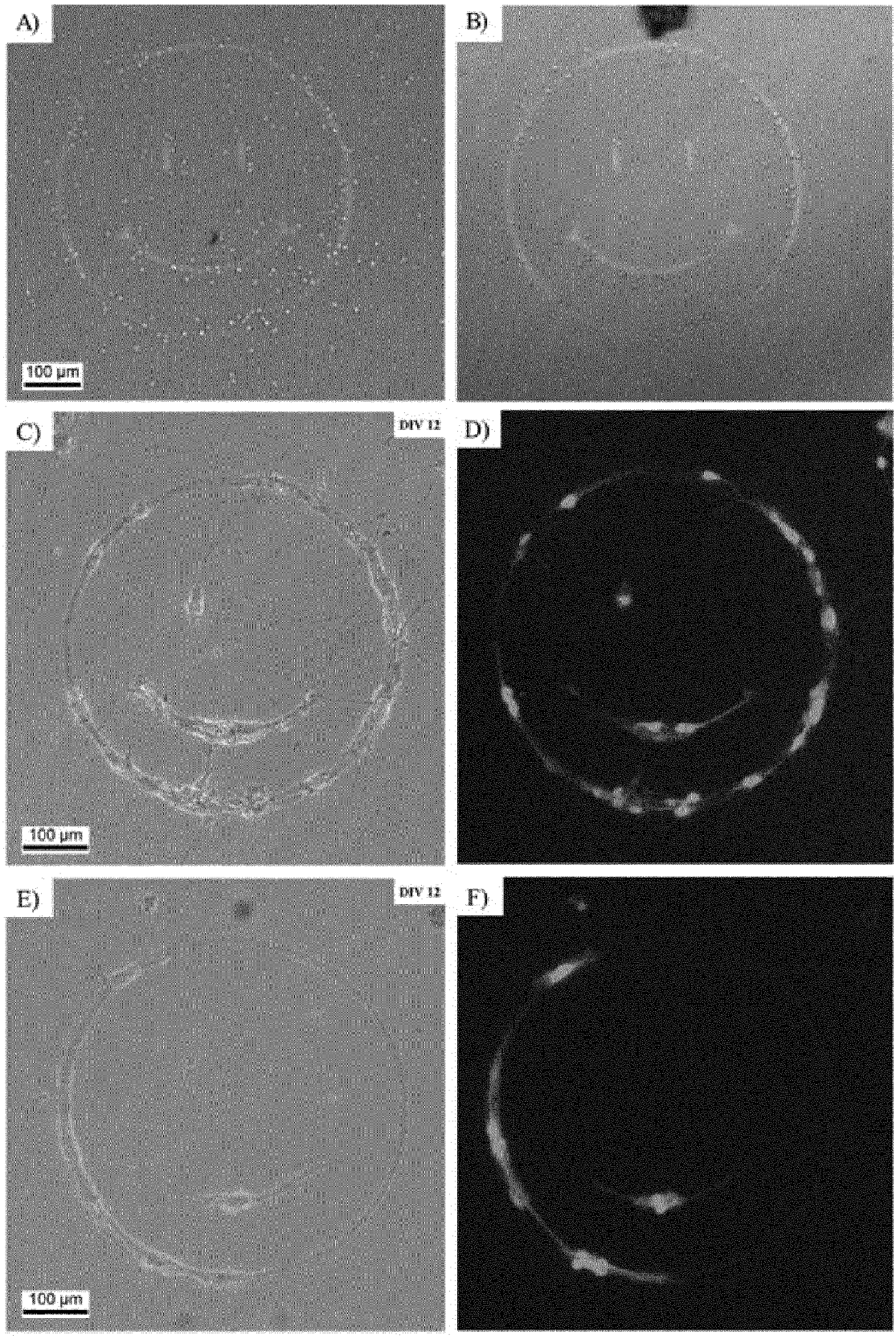

Fig. 10

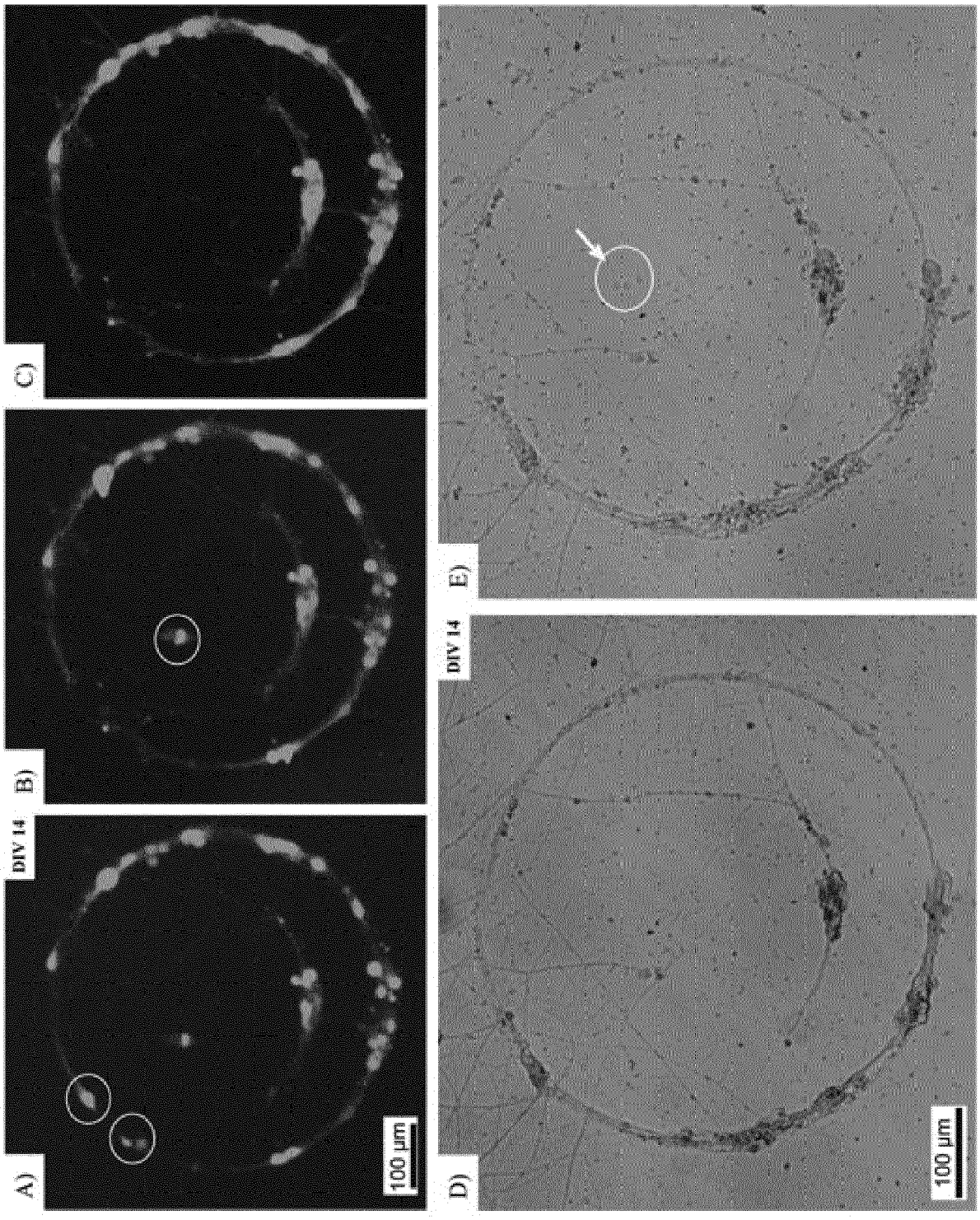

Fig. 11

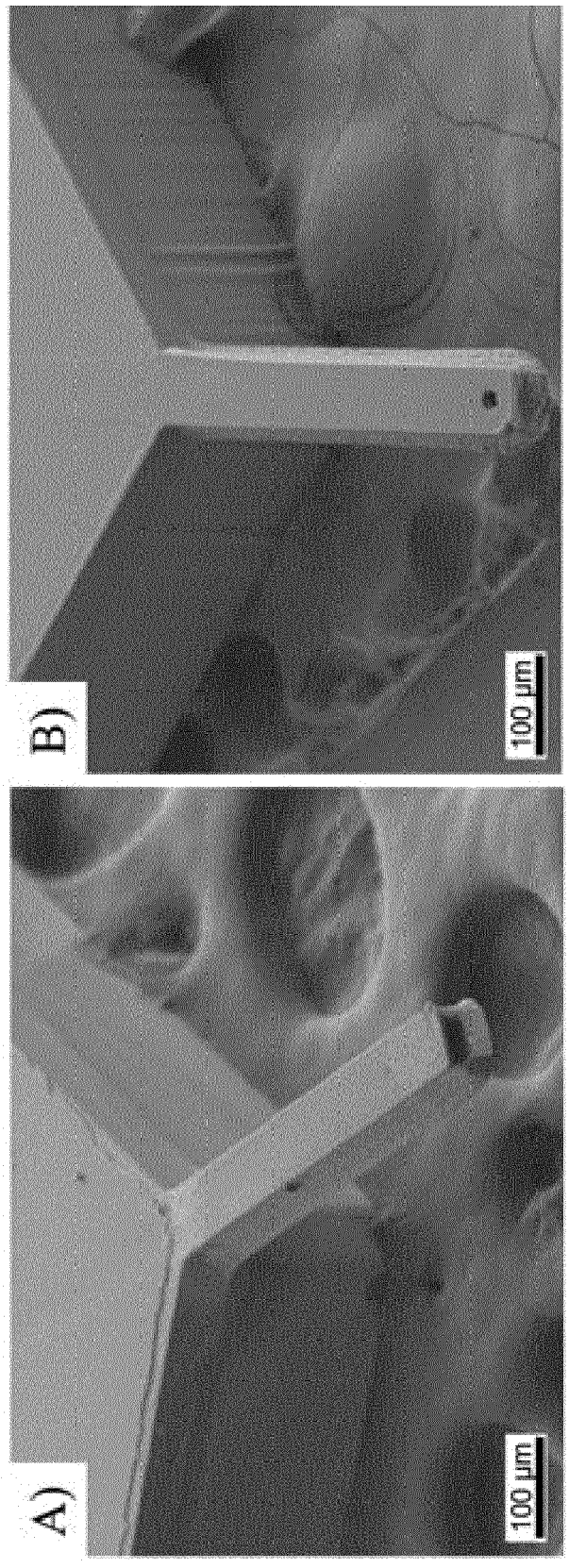

Fig. 12

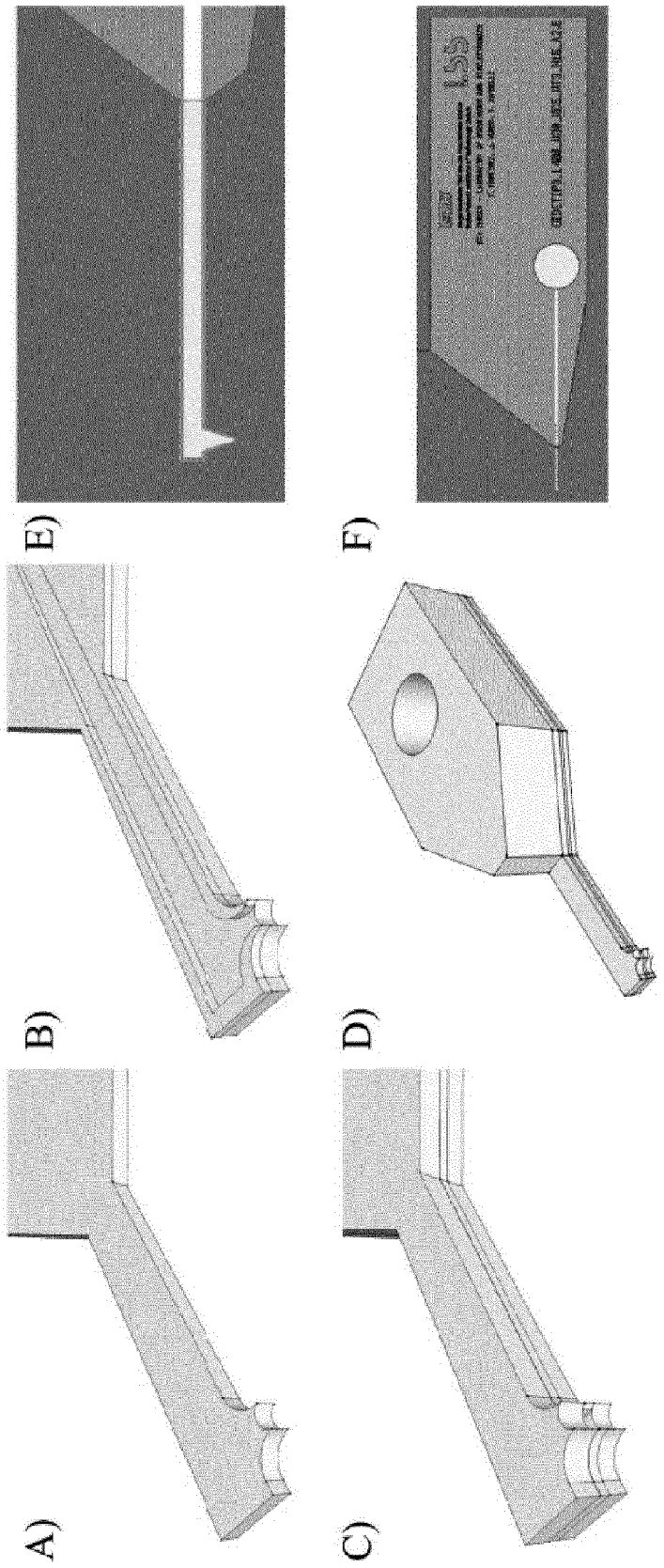

Fig. 13

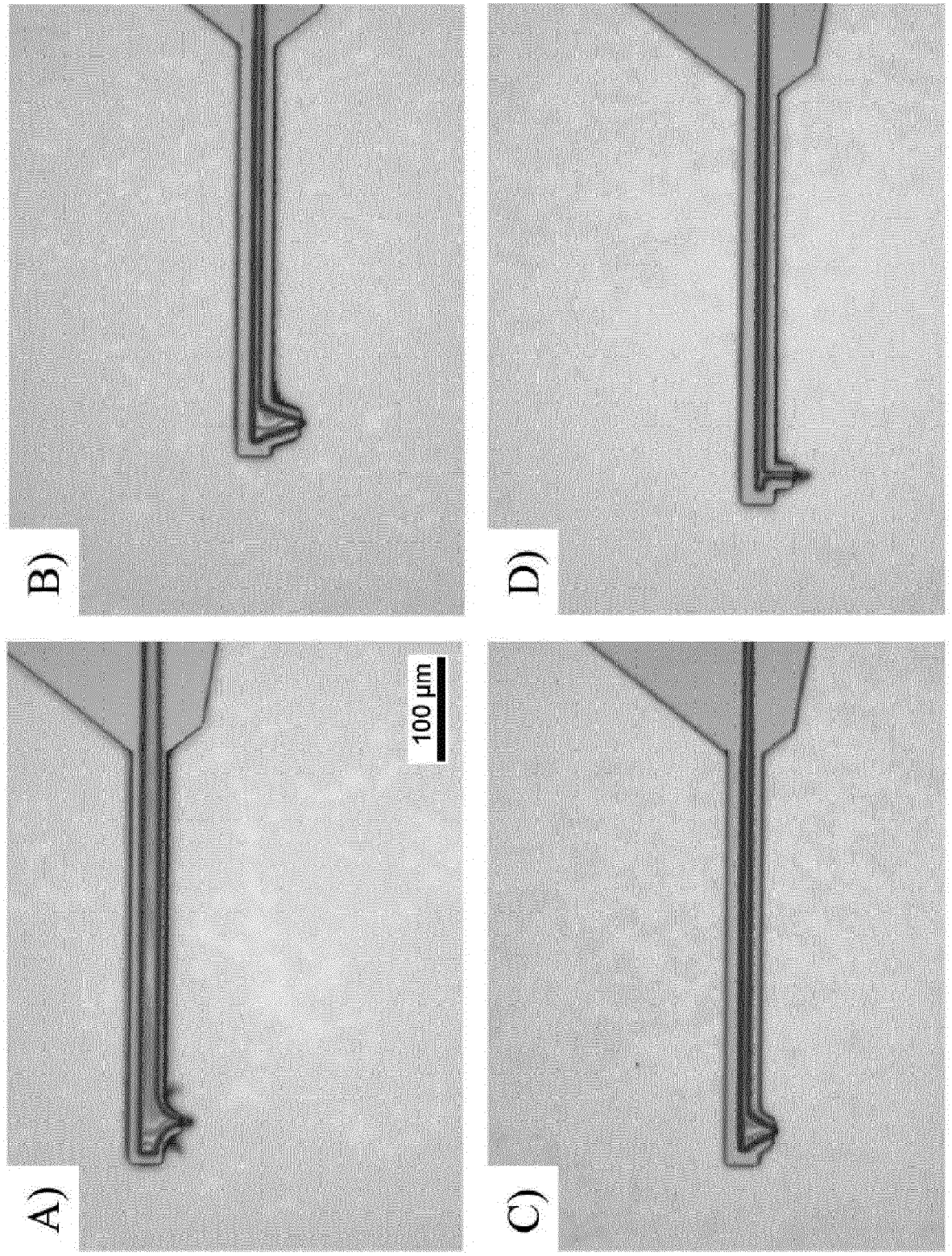

Fig. 14

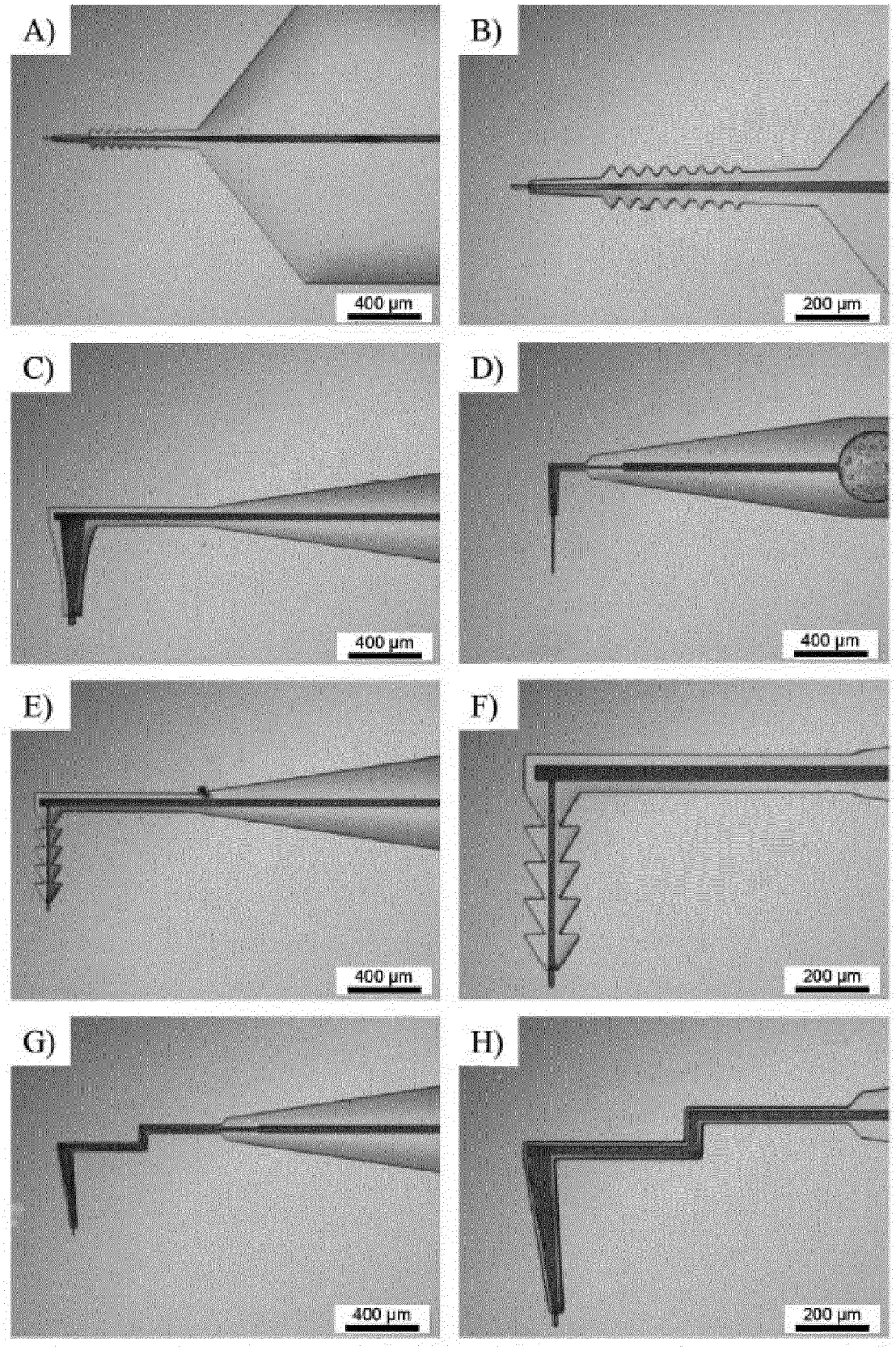

Fig. 15

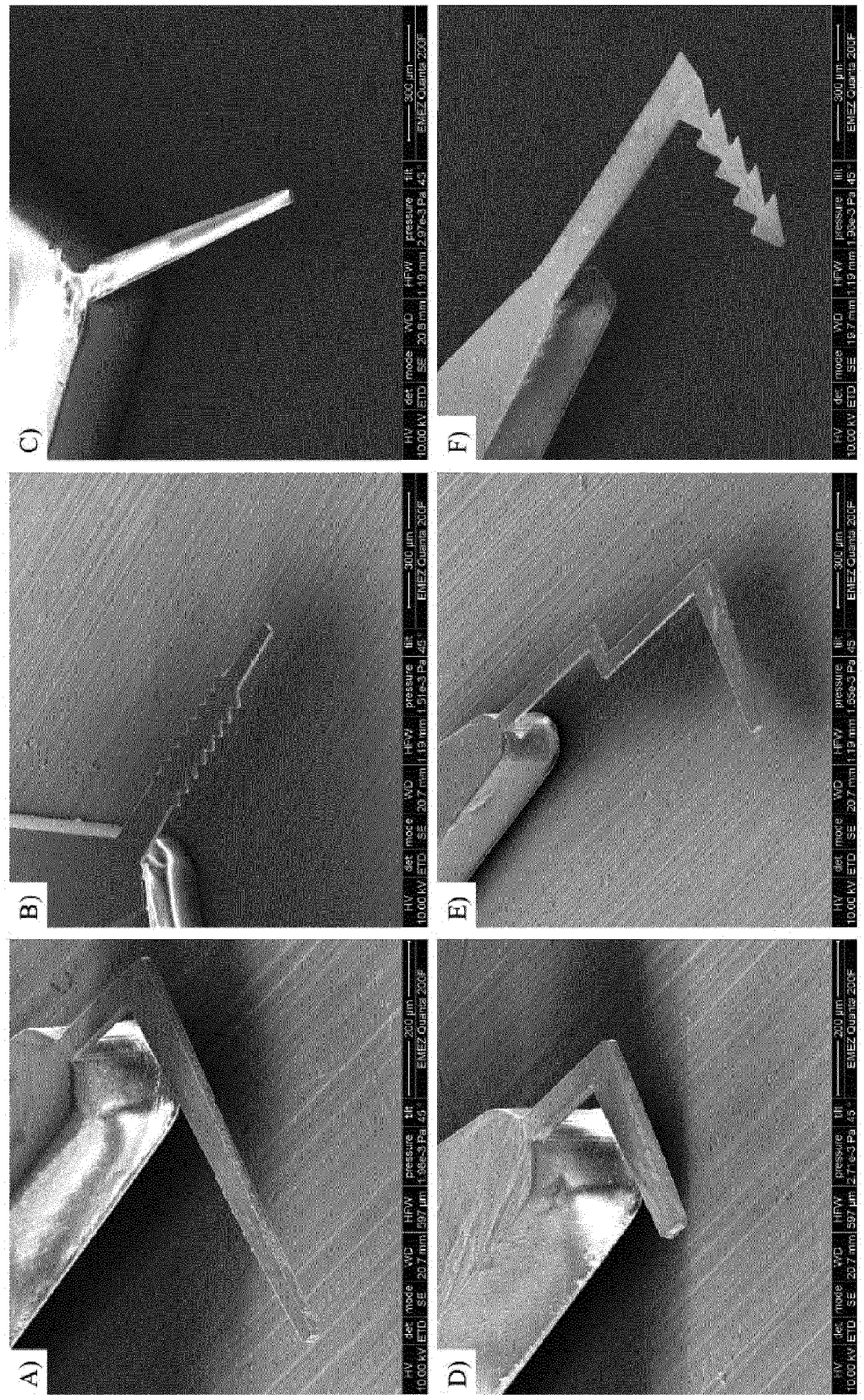

Fig. 16

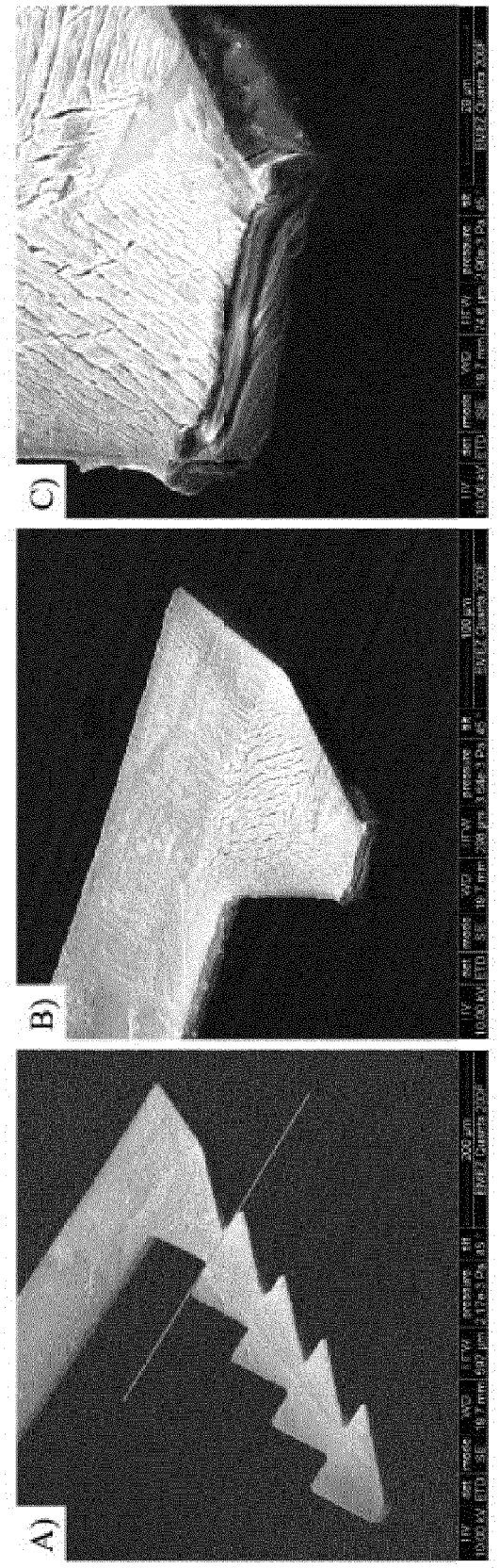

Fig. 17

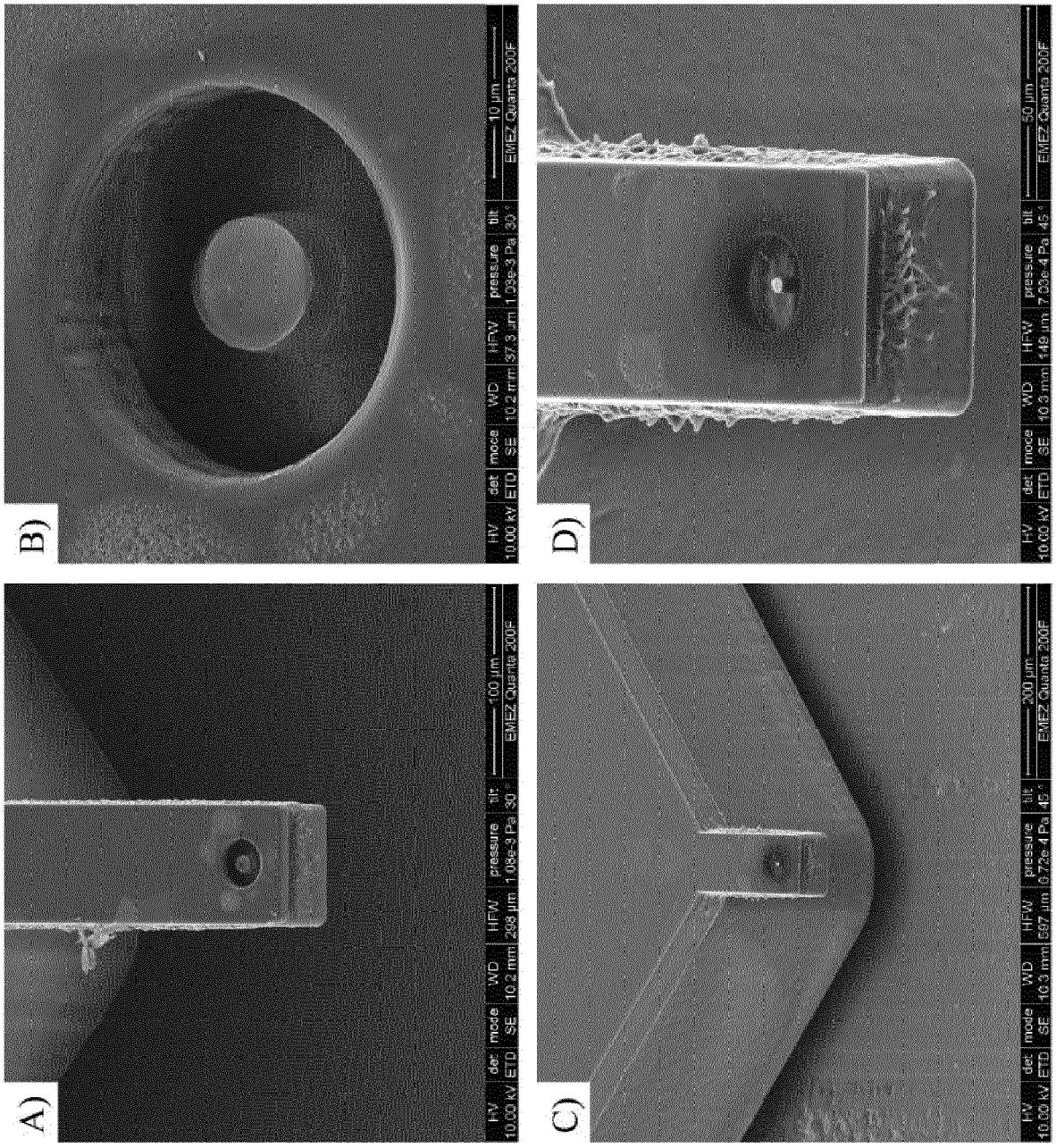

Fig. 18

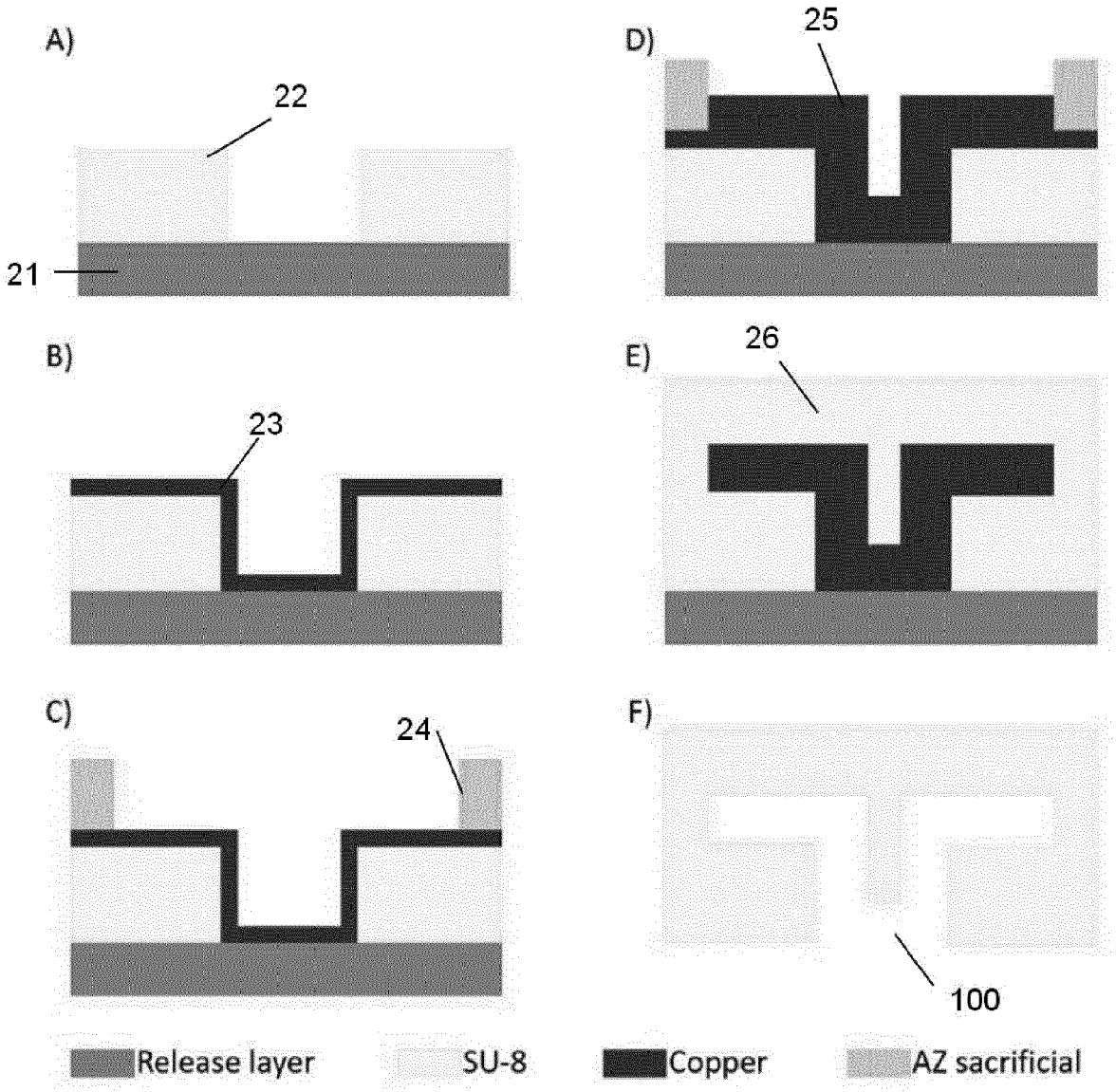
A)
22
21
B)
23
C)
24
D)
25
E)
26
F)
100
Release layer
SU-8
Copper
AZ sacrificial

Fig. 19

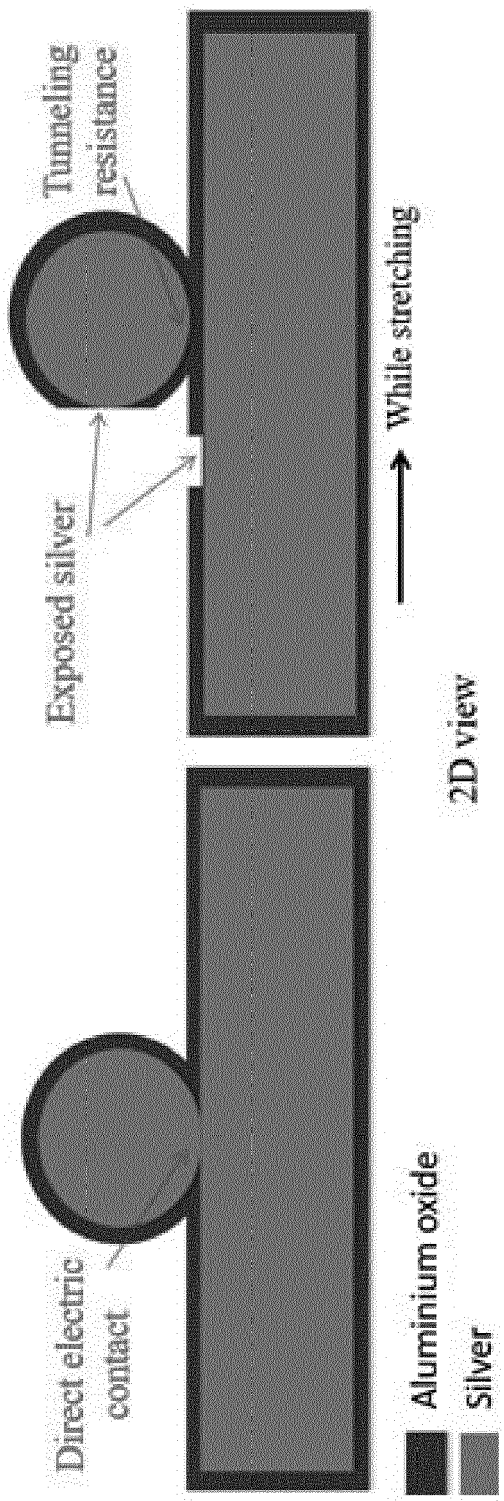
Tunneling resistance
Exposed silver
While stretching
2D view
Direct electric contact
Aluminium oxide
Silver

Fig. 20

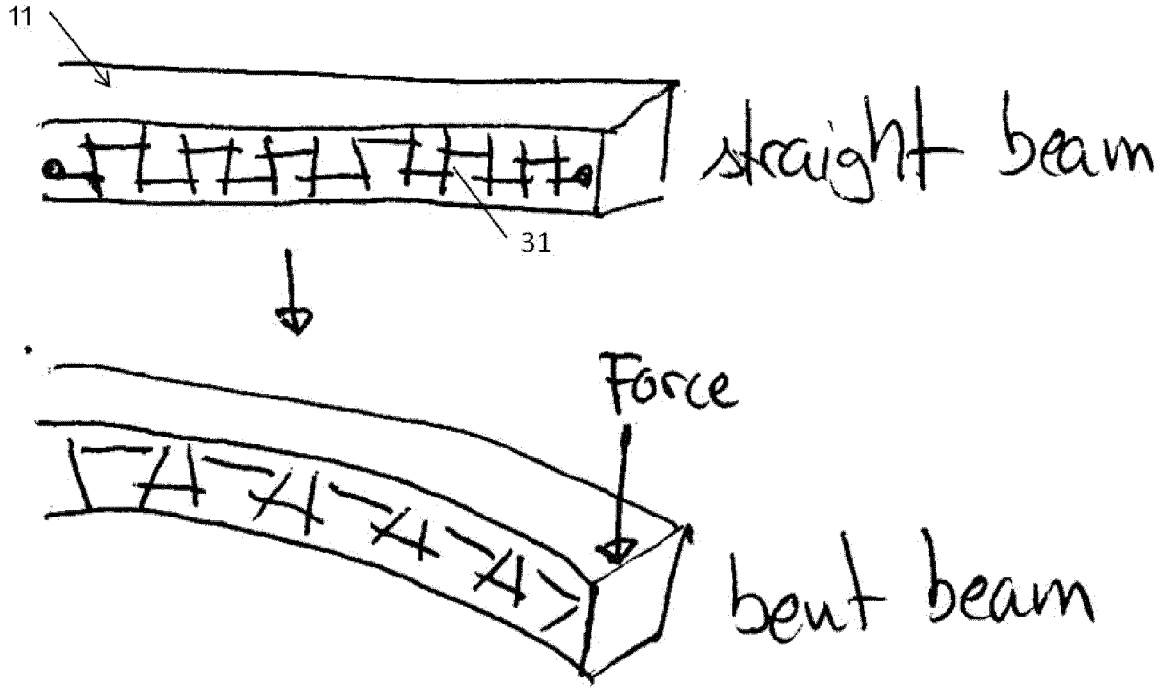

Fig. 21

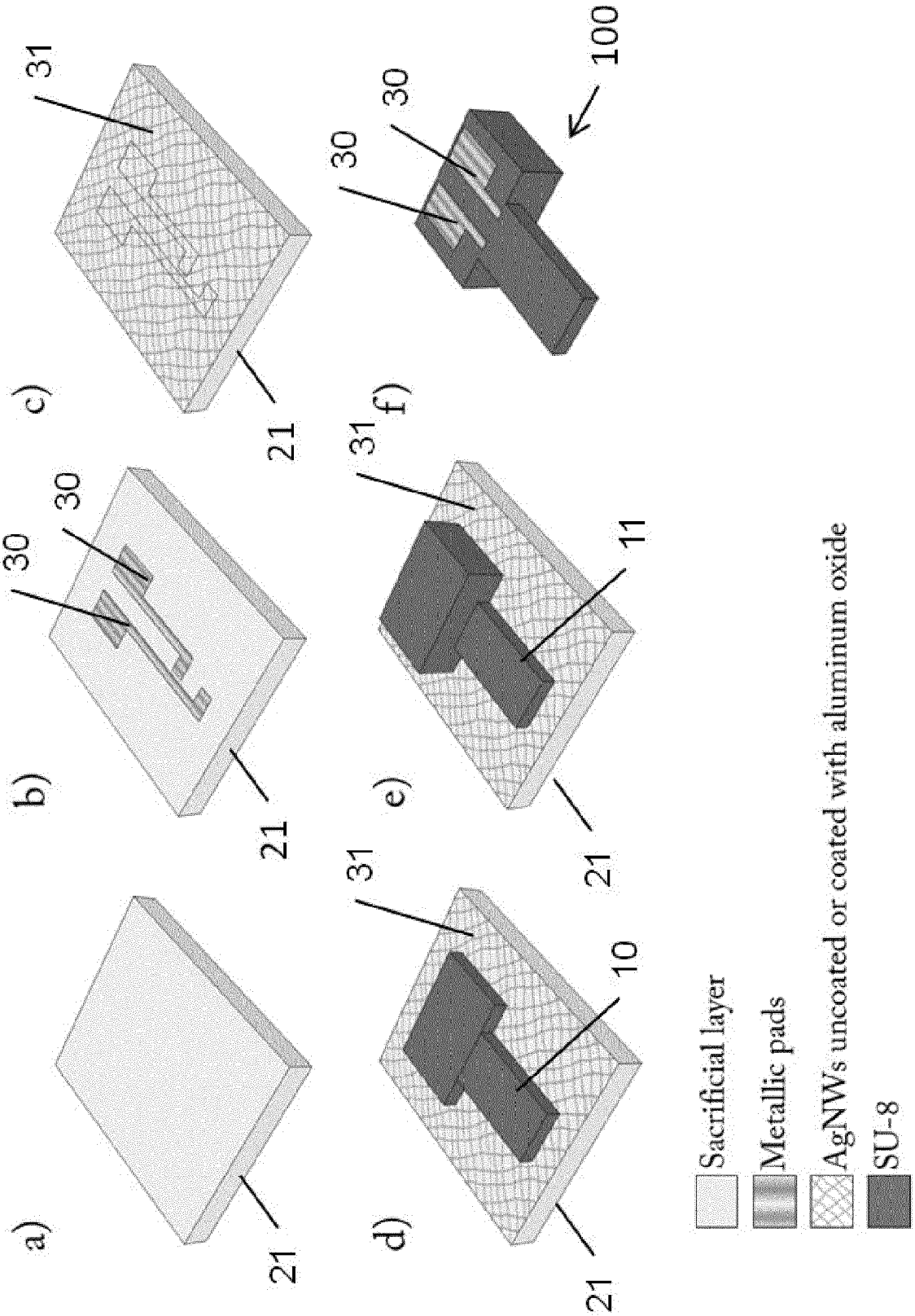
a)
21
b)
30
30
21
c)
31
21
d)
31
10
21
e)
31
11
21
f)
30
30
100
Sacrificial layer
Metallic pads
AgNWs uncoated or coated with aluminum oxide
SU-8

Fig. 22

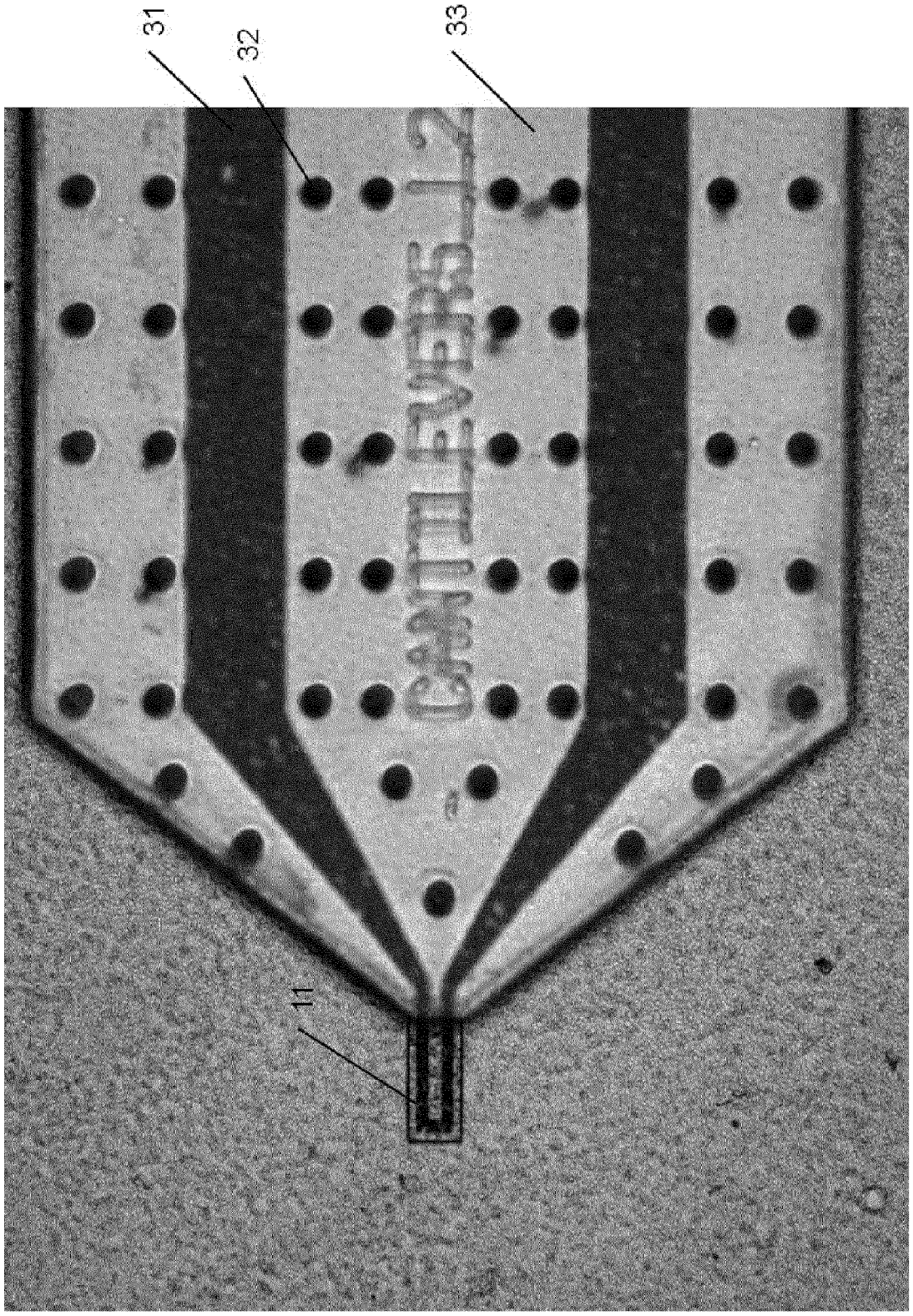

Fig. 23

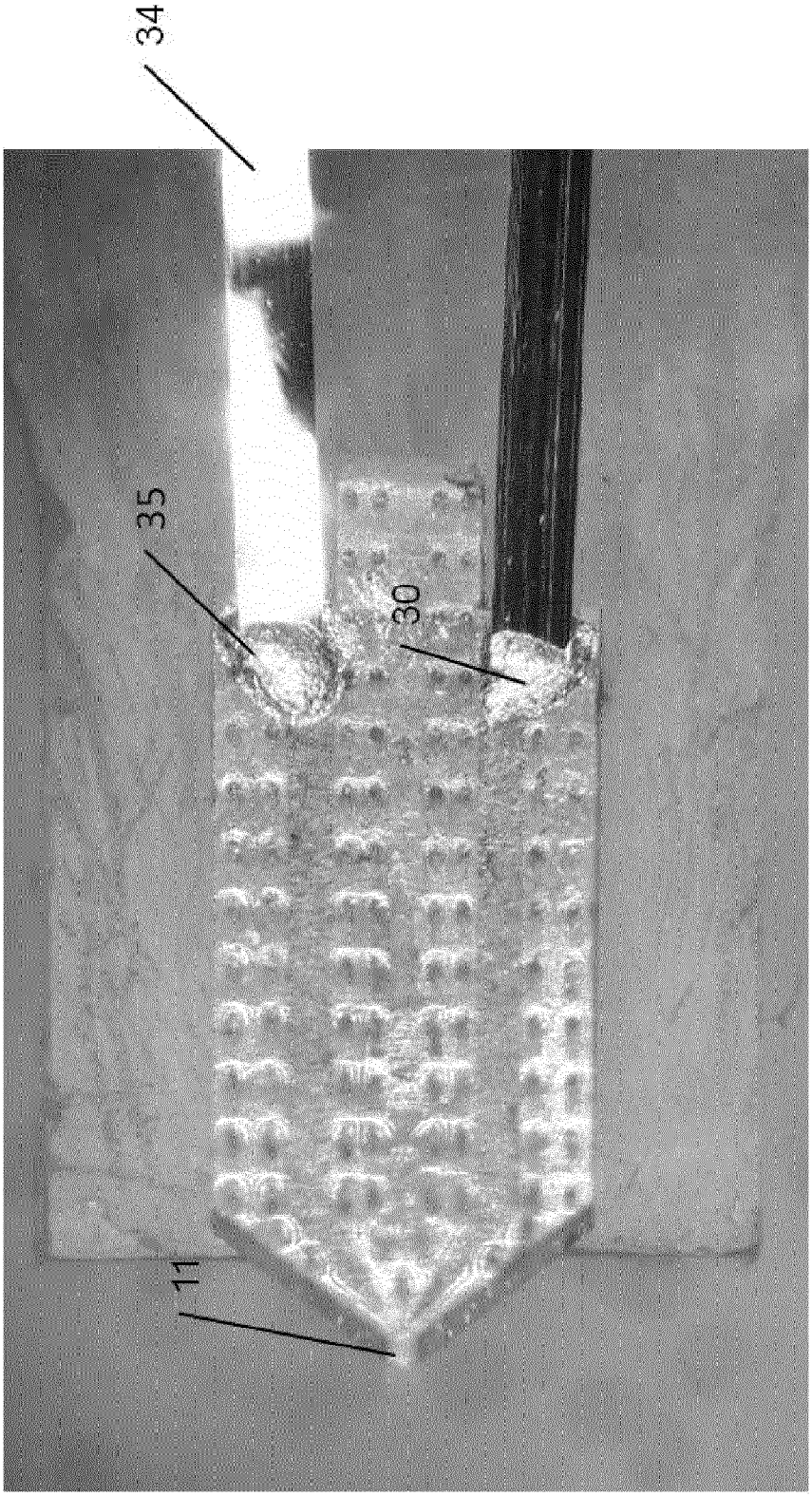

Fig. 24A

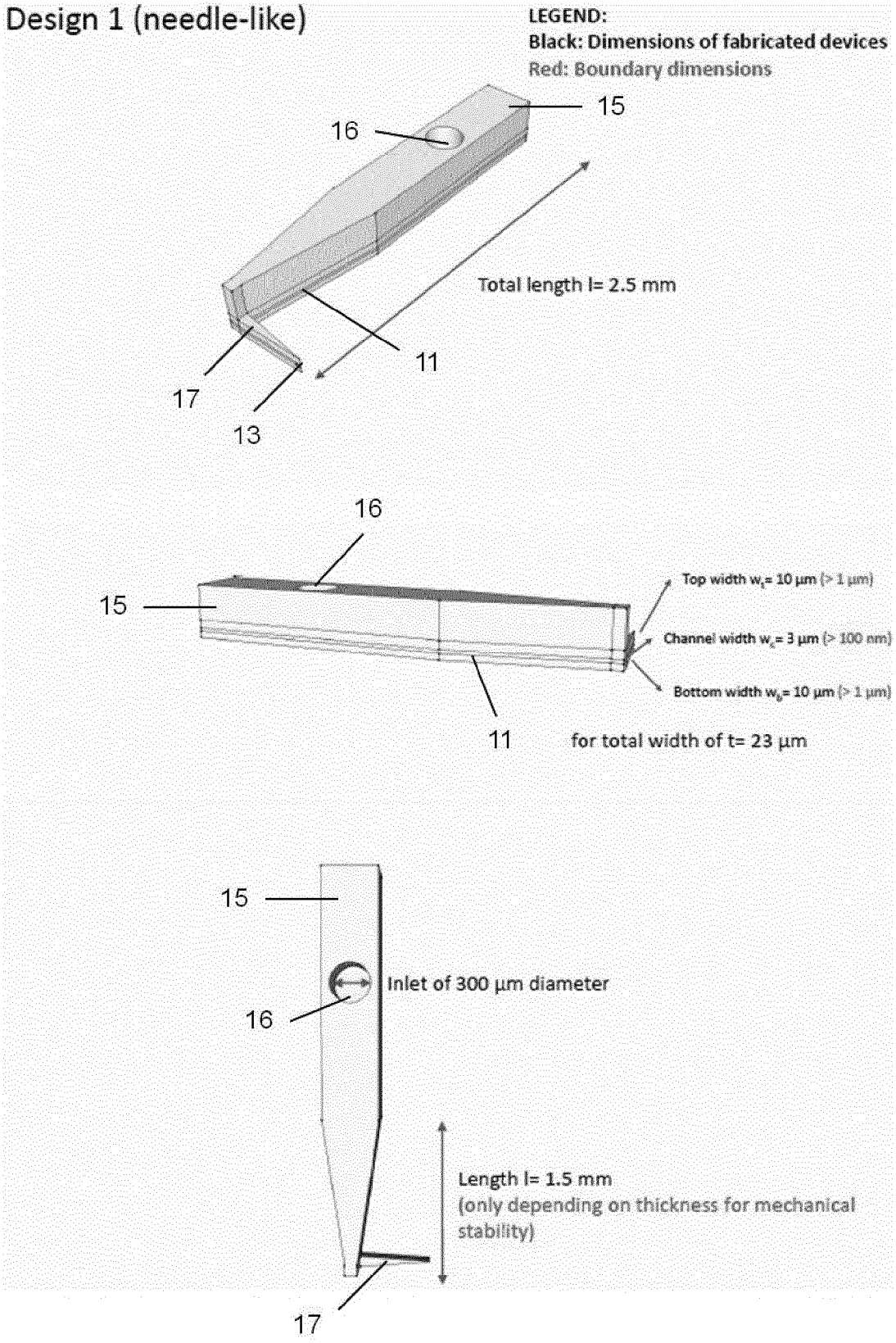
Design 1 (needle-like)
LEGEND:
Black: Dimensions of fabricated devices
Red: Boundary dimensions
15
16
Total length l= 2.5 mm
11
17
13
16
15
Top width w_t= 10 µm (> 1 µm)
Channel width w_c= 3 µm (> 100 nm)
Bottom width w_b= 10 µm (> 1 µm)
11
for total width of t= 23 µm
15
Inlet of 300 µm diameter
16
Length l= 1.5 mm
(only depending on thickness for mechanical stability)
17

Fig. 24B

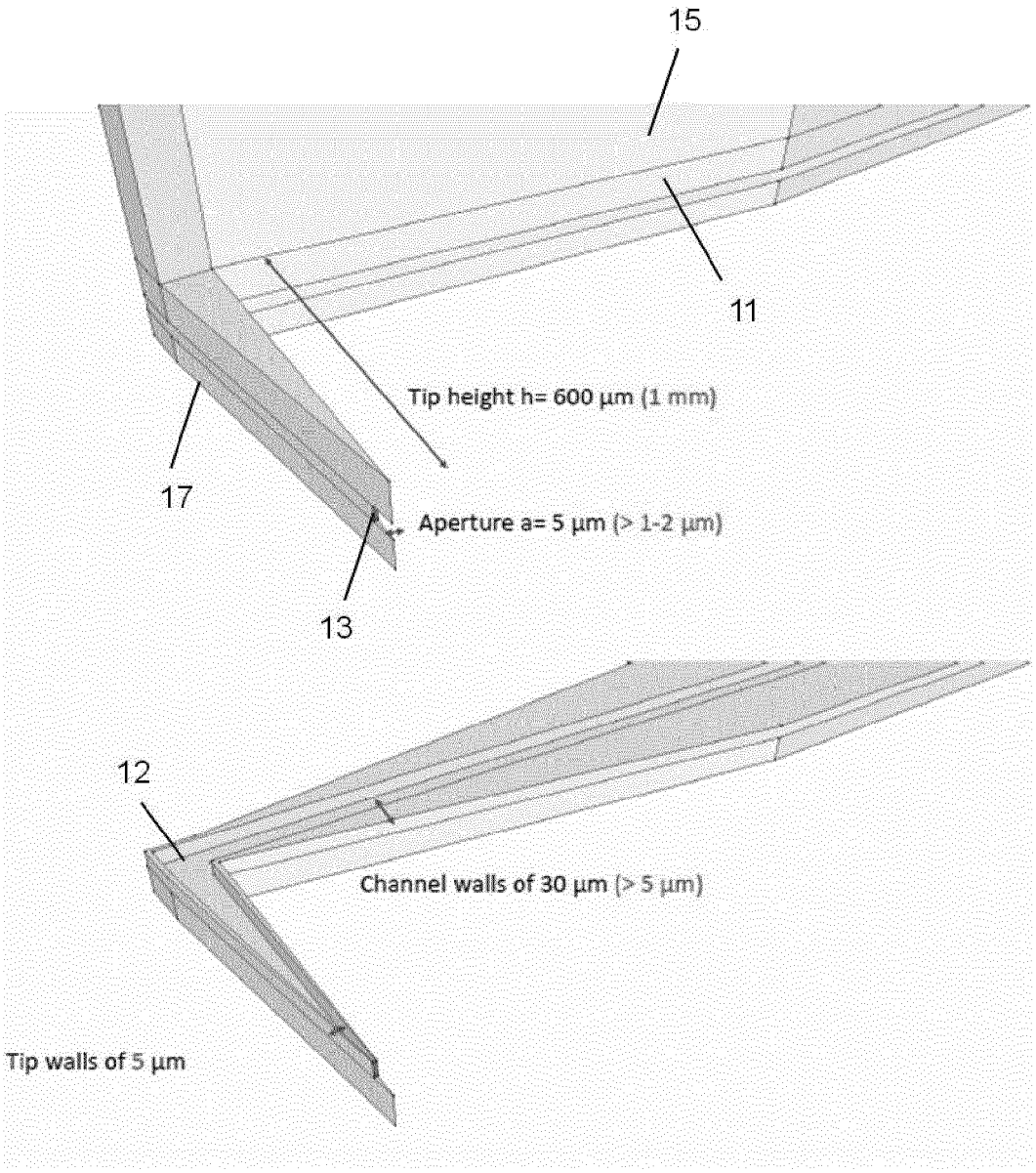
15
11
Tip height h= 600 µm (1 mm)
17
Aperture a= 5 µm (> 1-2 µm)
13
12
Channel walls of 30 µm (> 5 µm)
Tip walls of 5 µm

Fig. 25A

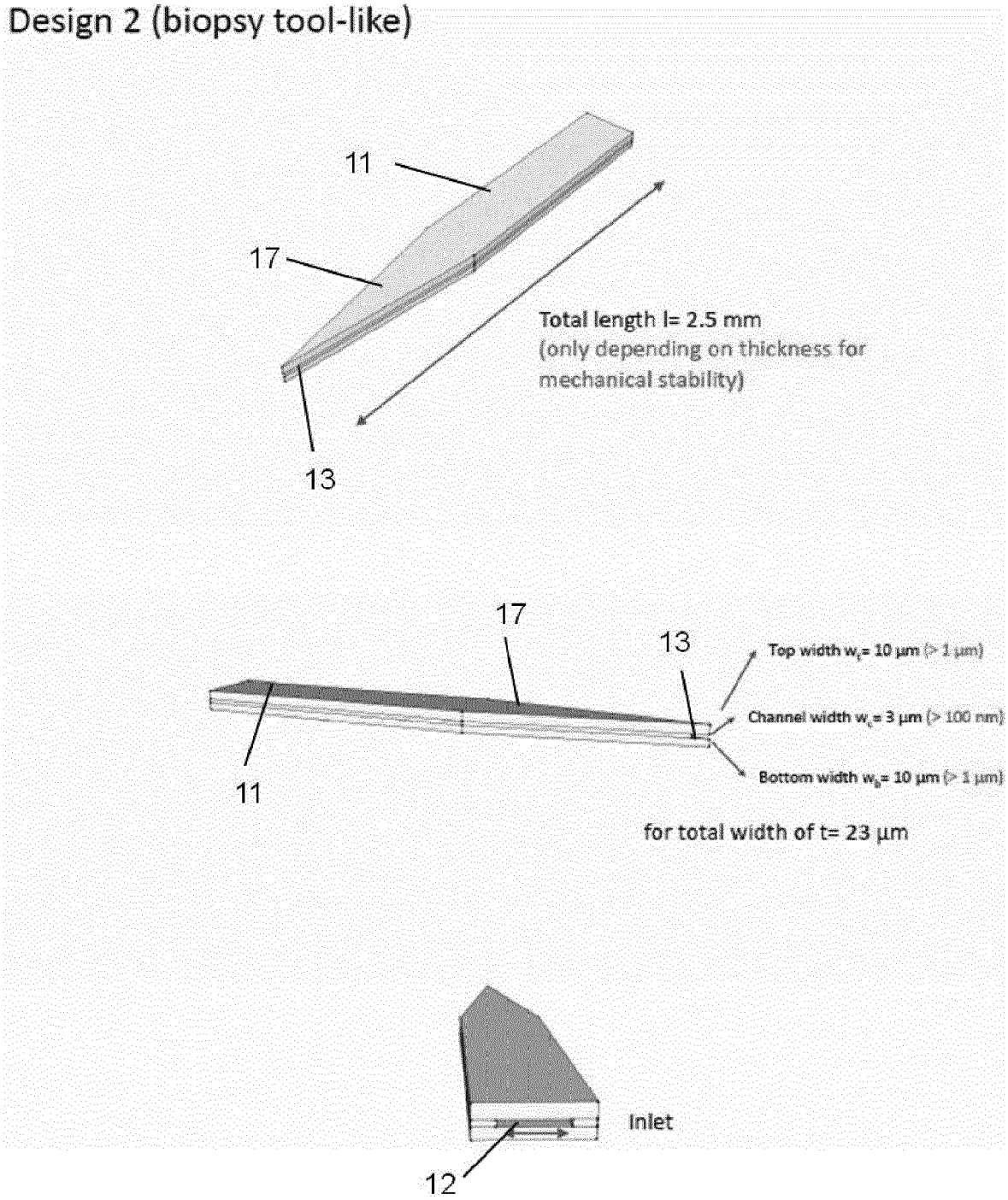
Design 2 (biopsy tool-like)
11
17
13
Total length l= 2.5 mm
(only depending on thickness for mechanical stability)
17
13
11
Top width w_t= 10 µm (> 1 µm)
Channel width w_c= 3 µm (> 100 nm)
Bottom width w_b= 10 µm (> 1 µm)
for total width of t= 23 µm
Inlet
12

Fig. 25B

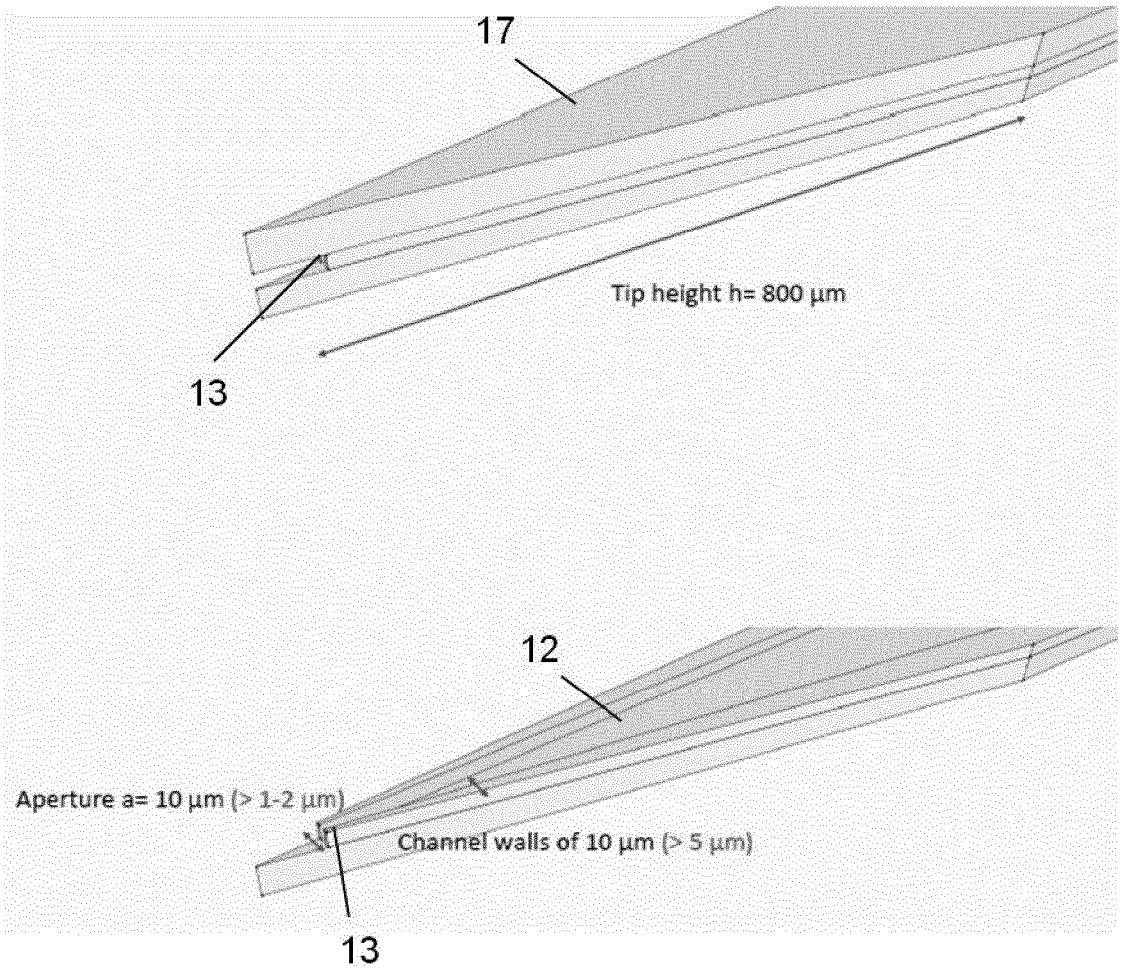
17
Tip height h= 800 µm
13
12
Aperture a= 10 µm (> 1-2 µm)
Channel walls of 10 µm (> 5 µm)
13

Fig. 26A

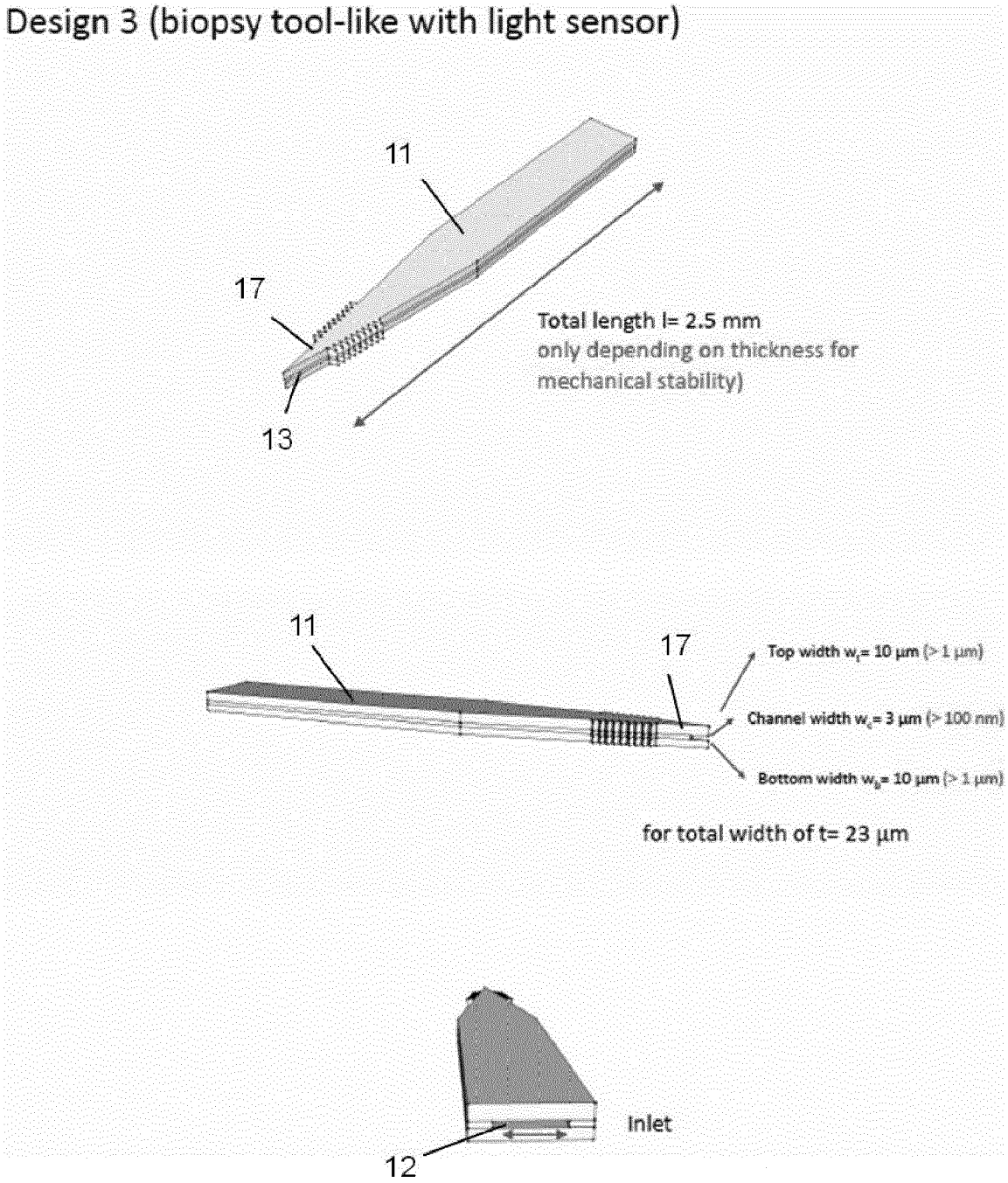
Design 3 (biopsy tool-like with light sensor)
11
17
13
Total length l= 2.5 mm
only depending on thickness for
mechanical stability)
11
17
Top width w_t= 10 µm (> 1 µm)
Channel width w_c= 3 µm (> 100 nm)
Bottom width w_b= 10 µm (> 1 µm)
for total width of t= 23 µm
Inlet
12

Fig. 26B

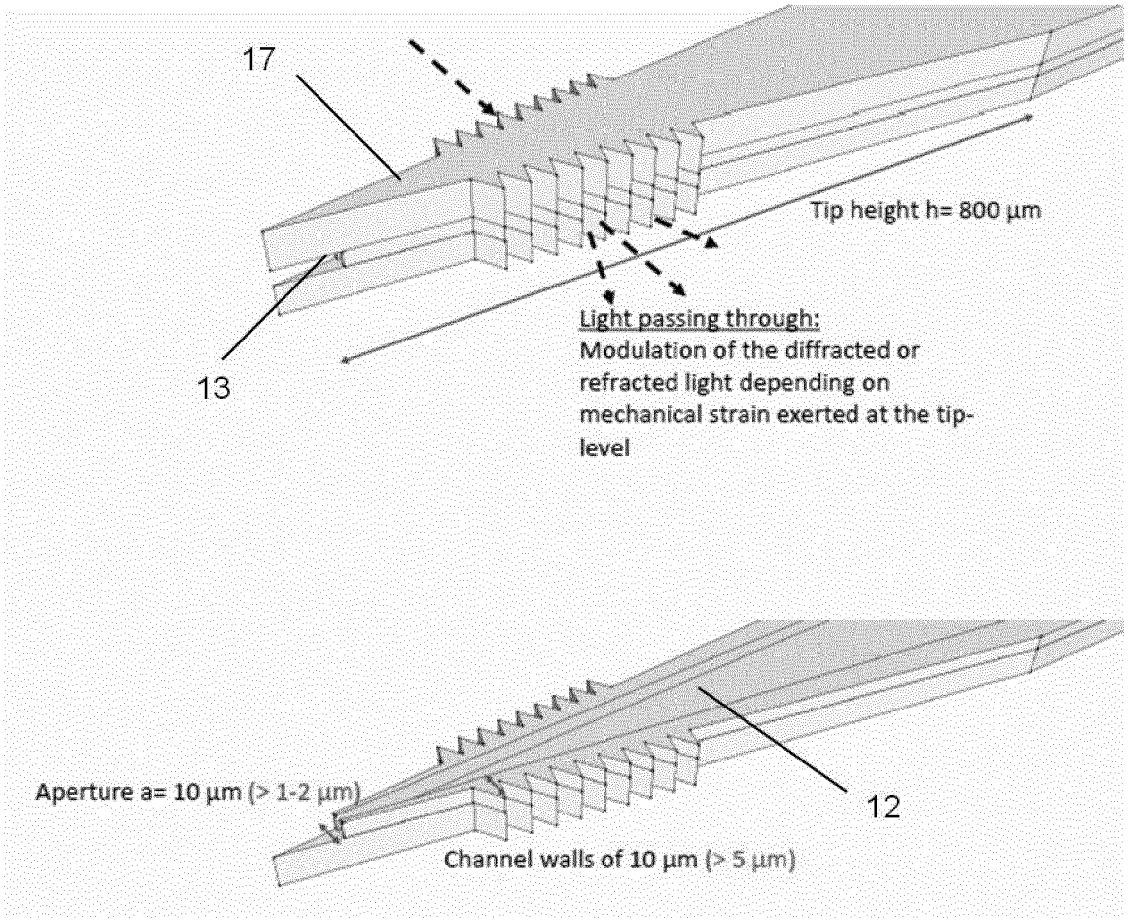
17
Tip height h= 800 µm
13
Light passing through:
Modulation of the diffracted or refracted light depending on mechanical strain exerted at the tip-level
Aperture a= 10 µm (> 1-2 µm)
12
Channel walls of 10 µm (> 5 µm)

Fig. 27A

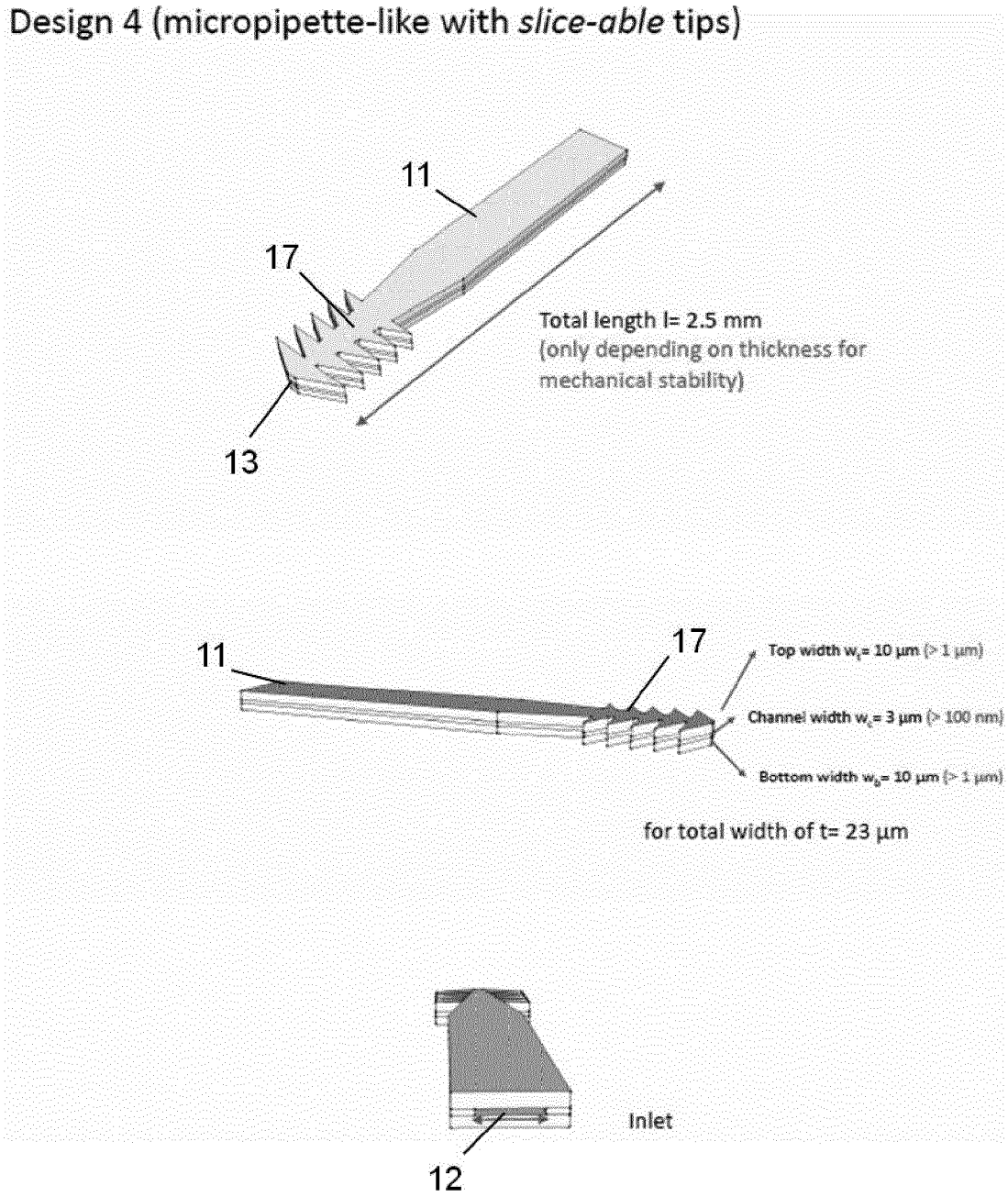
Design 4 (micropipette-like with *slice-able* tips)
11
17
13
Total length l= 2.5 mm
(only depending on thickness for
mechanical stability)
11
17
Top width w_t= 10 µm (> 1 µm)
Channel width w_c= 3 µm (> 100 nm)
Bottom width w_b= 10 µm (> 1 µm)
for total width of t= 23 µm
Inlet
12

Fig. 27B

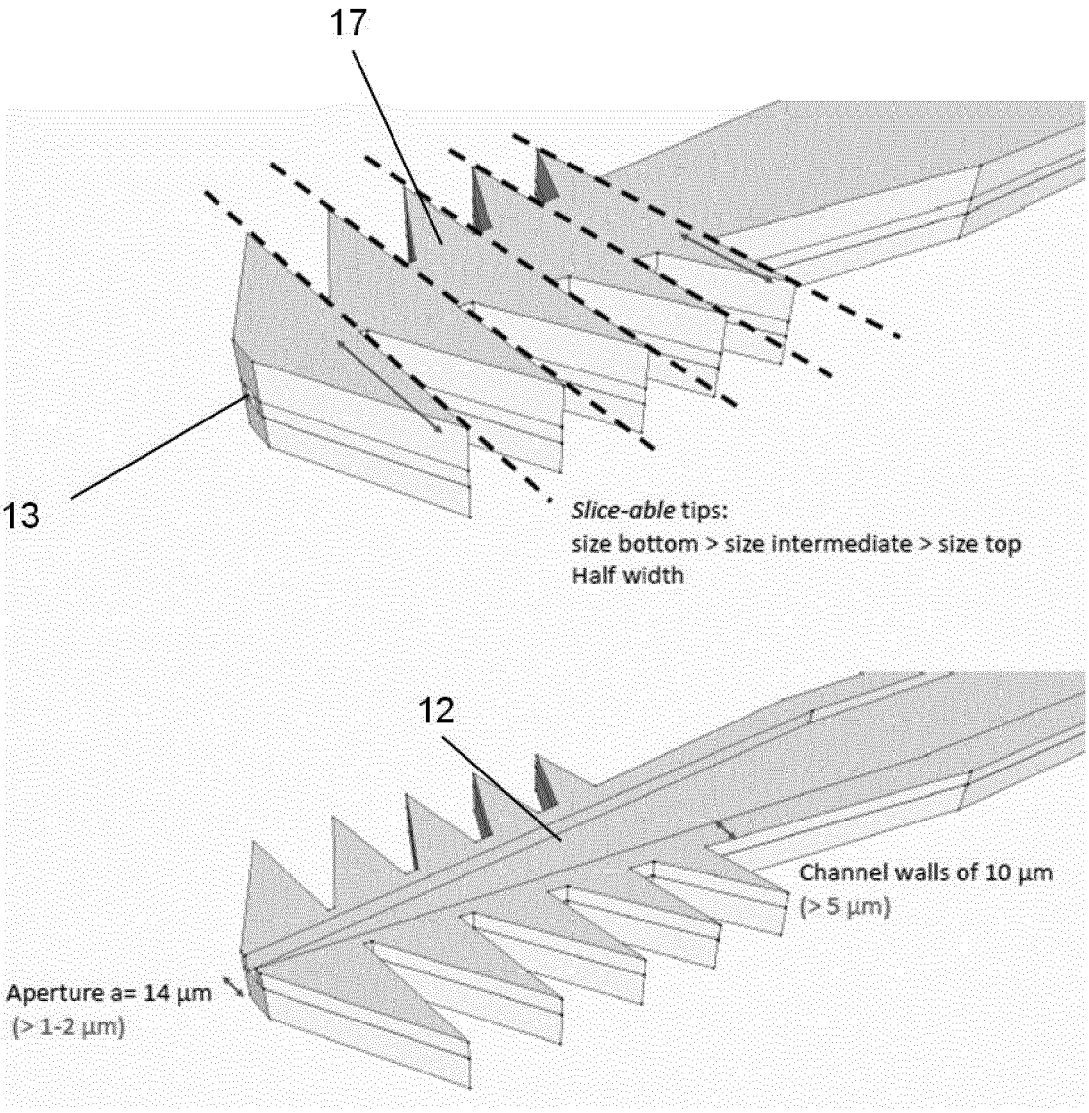
17
13
Slice-able tips:
size bottom > size intermediate > size top
Half width
12
Channel walls of 10 µm
(> 5 µm)
Aperture a= 14 µm
(> 1-2 µm)

Fig. 28A

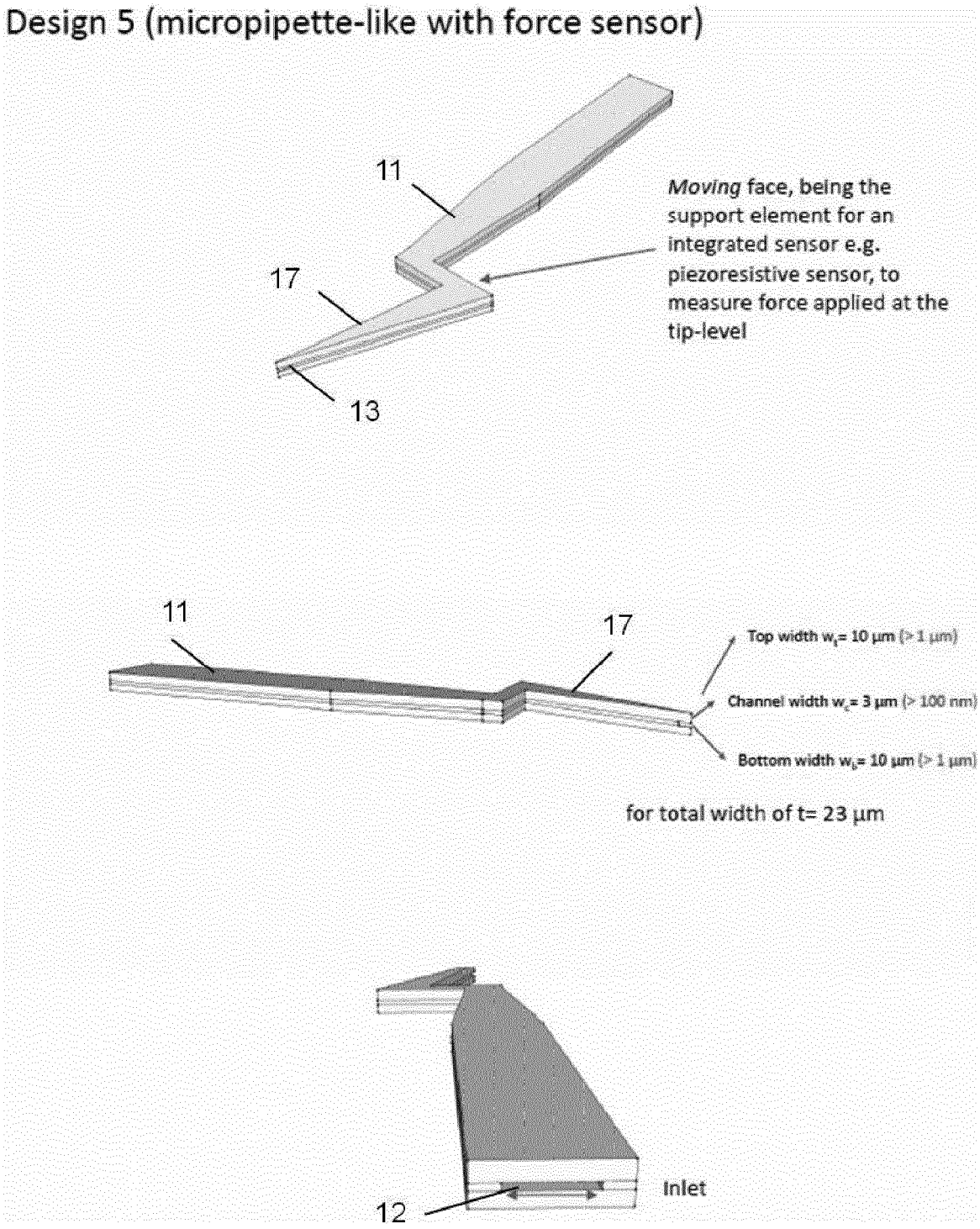
Design 5 (micropipette-like with force sensor)
11
17
13
Moving face, being the support element for an integrated sensor e.g. piezoresistive sensor, to measure force applied at the tip-level
11
17
Top width w_t= 10 µm (> 1 µm)
Channel width w_c= 3 µm (> 100 nm)
Bottom width w_b= 10 µm (> 1 µm)
for total width of t= 23 µm
12
Inlet

Fig. 28B

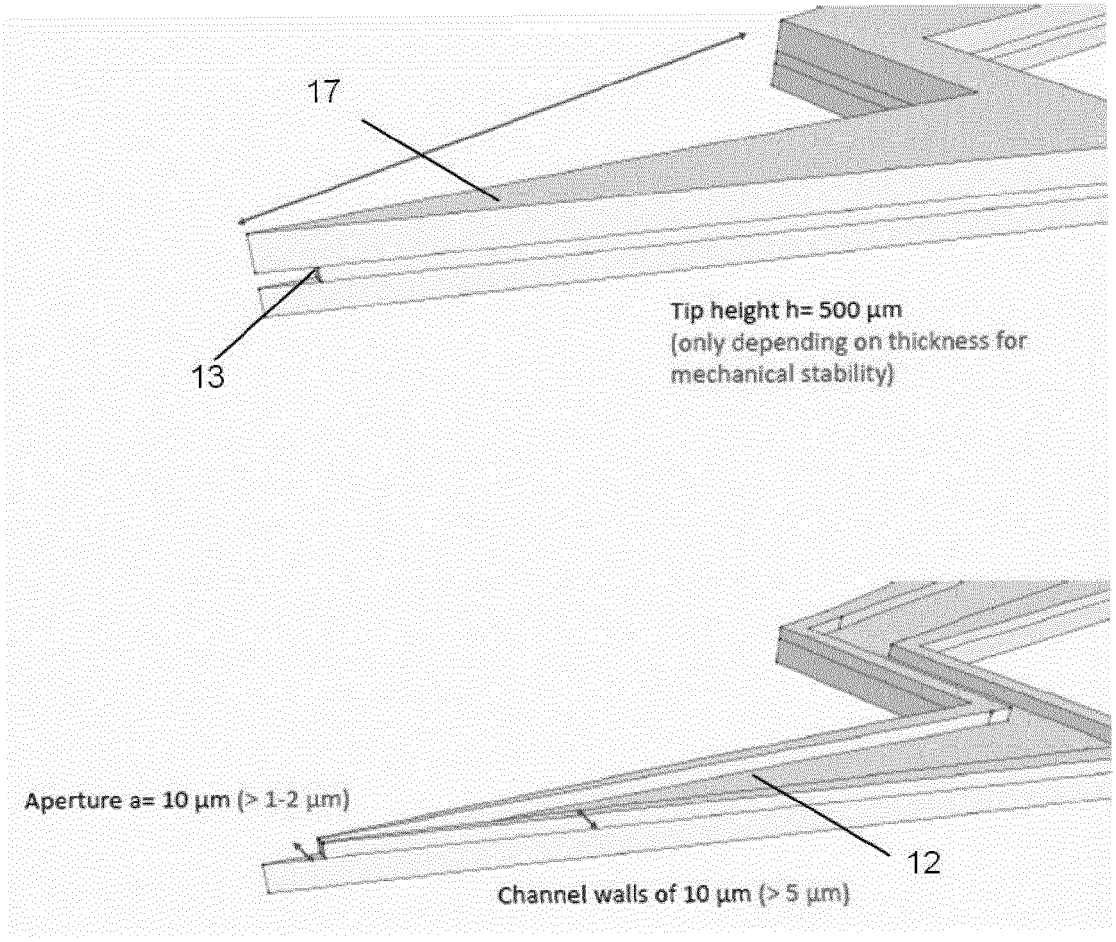
17
13
Tip height h= 500 µm
(only depending on thickness for
mechanical stability)
Aperture a= 10 µm (> 1-2 µm)
12
Channel walls of 10 µm (> 5 µm)

Fig. 29A

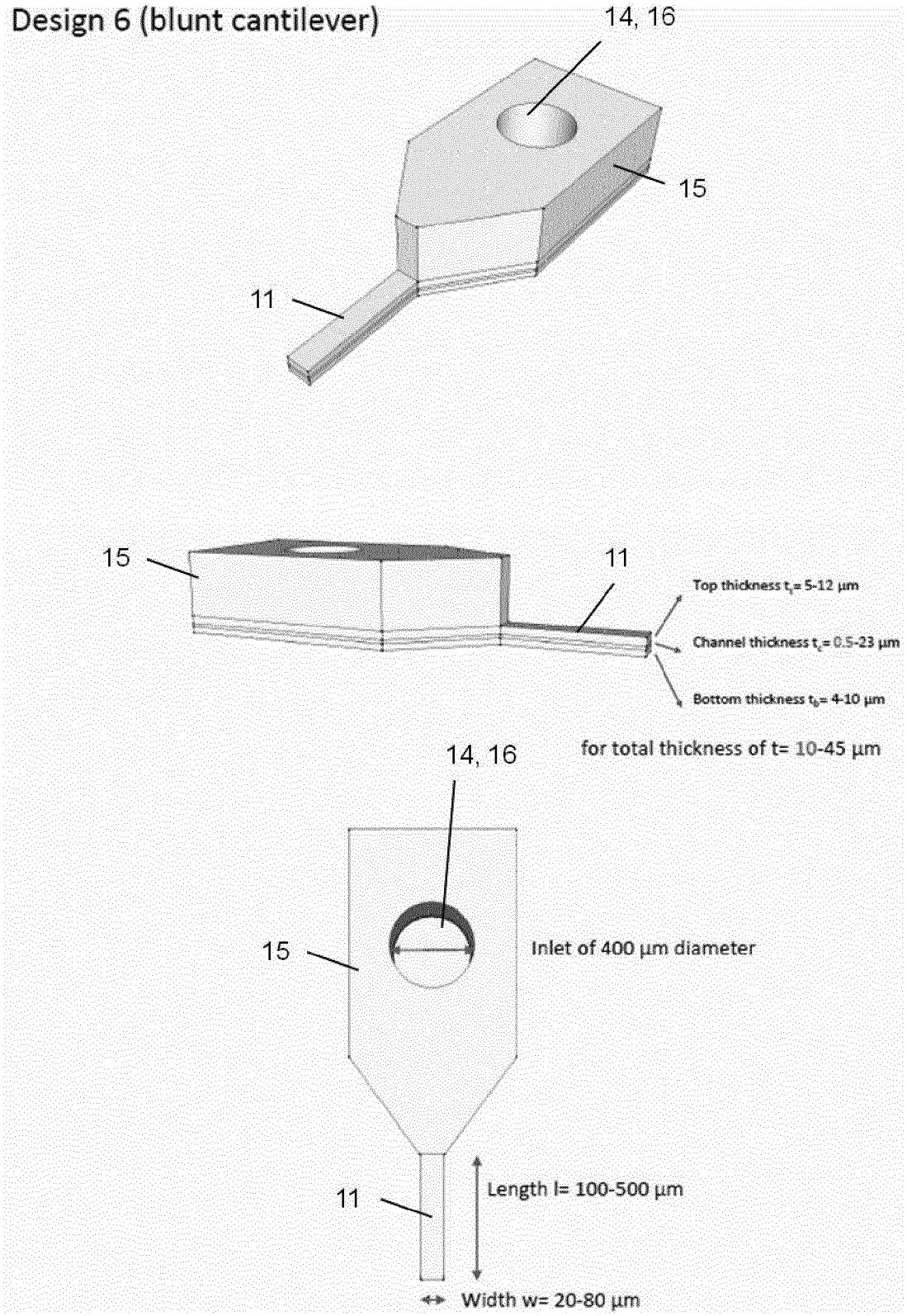
Design 6 (blunt cantilever)
14, 16
15
11
15
11
Top thickness t_t= 5-12 µm
Channel thickness t_c= 0.5-23 µm
Bottom thickness t_b= 4-10 µm
for total thickness of t= 10-45 µm
14, 16
15
Inlet of 400 µm diameter
11
Length l= 100-500 µm
Width w= 20-80 µm

Fig. 29B

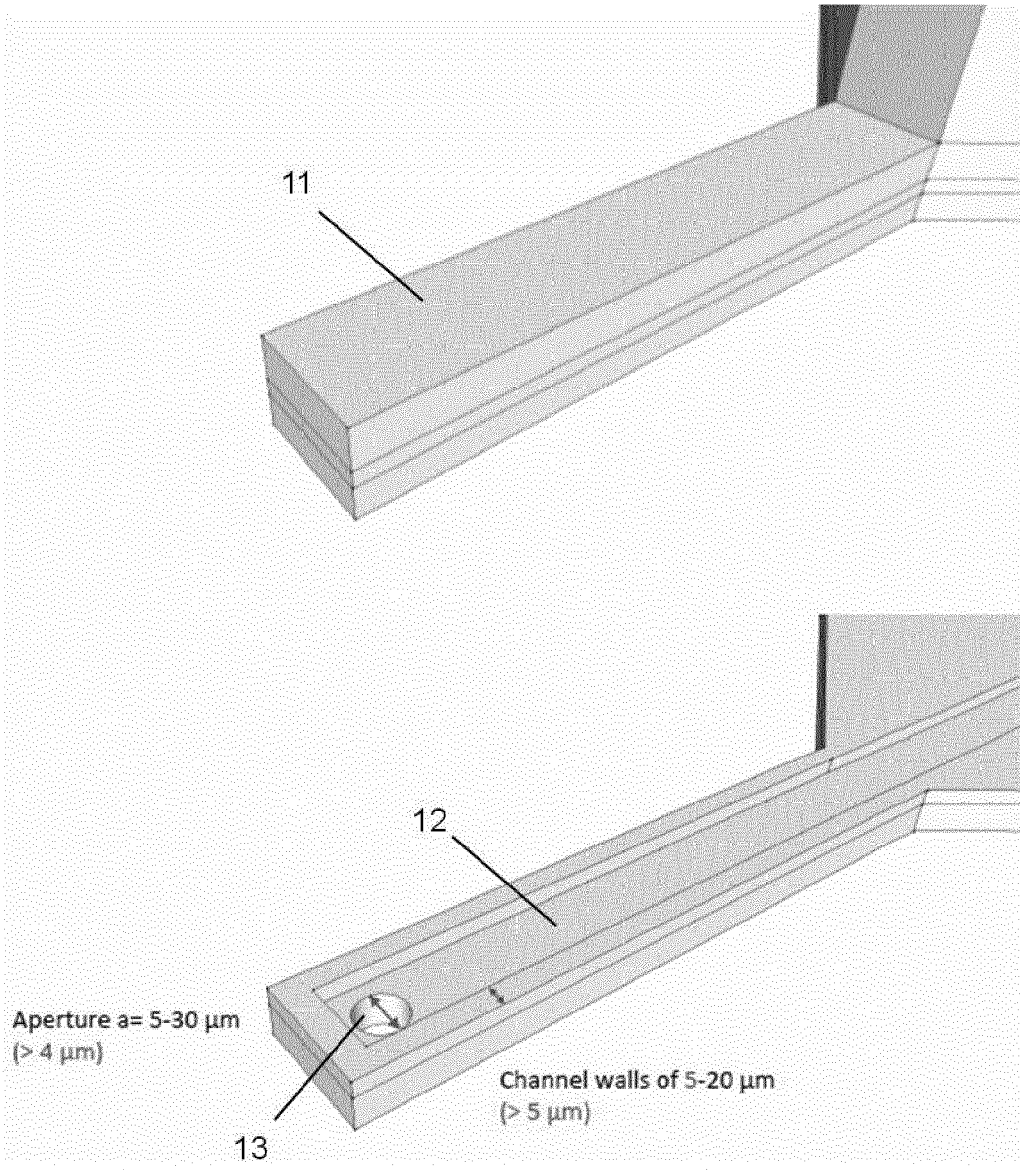

Fig. 30A

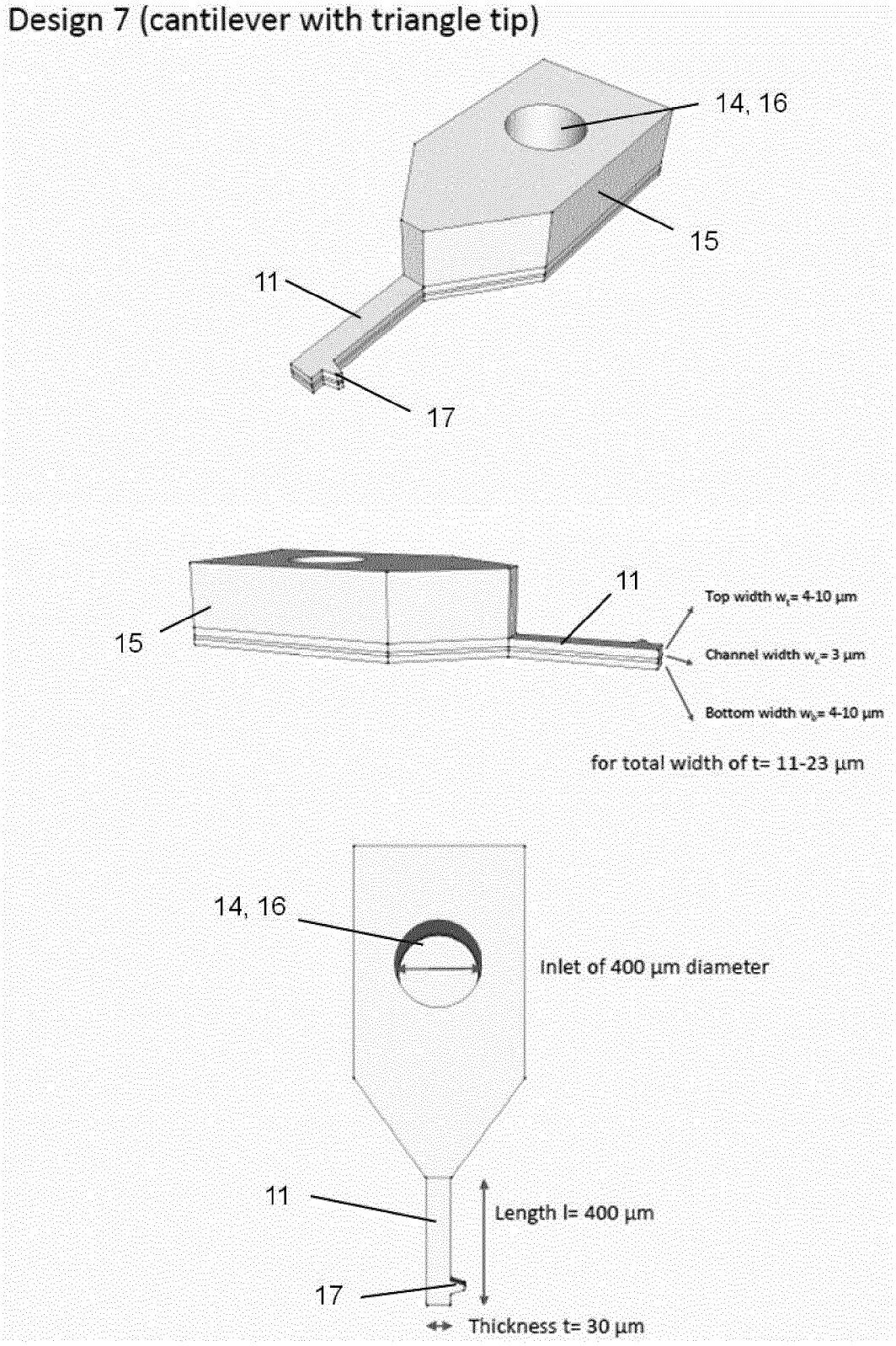
Design 7 (cantilever with triangle tip)
14, 16
15
11
17
11
15
Top width w_t= 4-10 µm
Channel width w_c= 3 µm
Bottom width w_b= 4-10 µm
for total width of t= 11-23 µm
14, 16
Inlet of 400 µm diameter
11
Length l= 400 µm
17
Thickness t= 30 µm

Fig. 30B

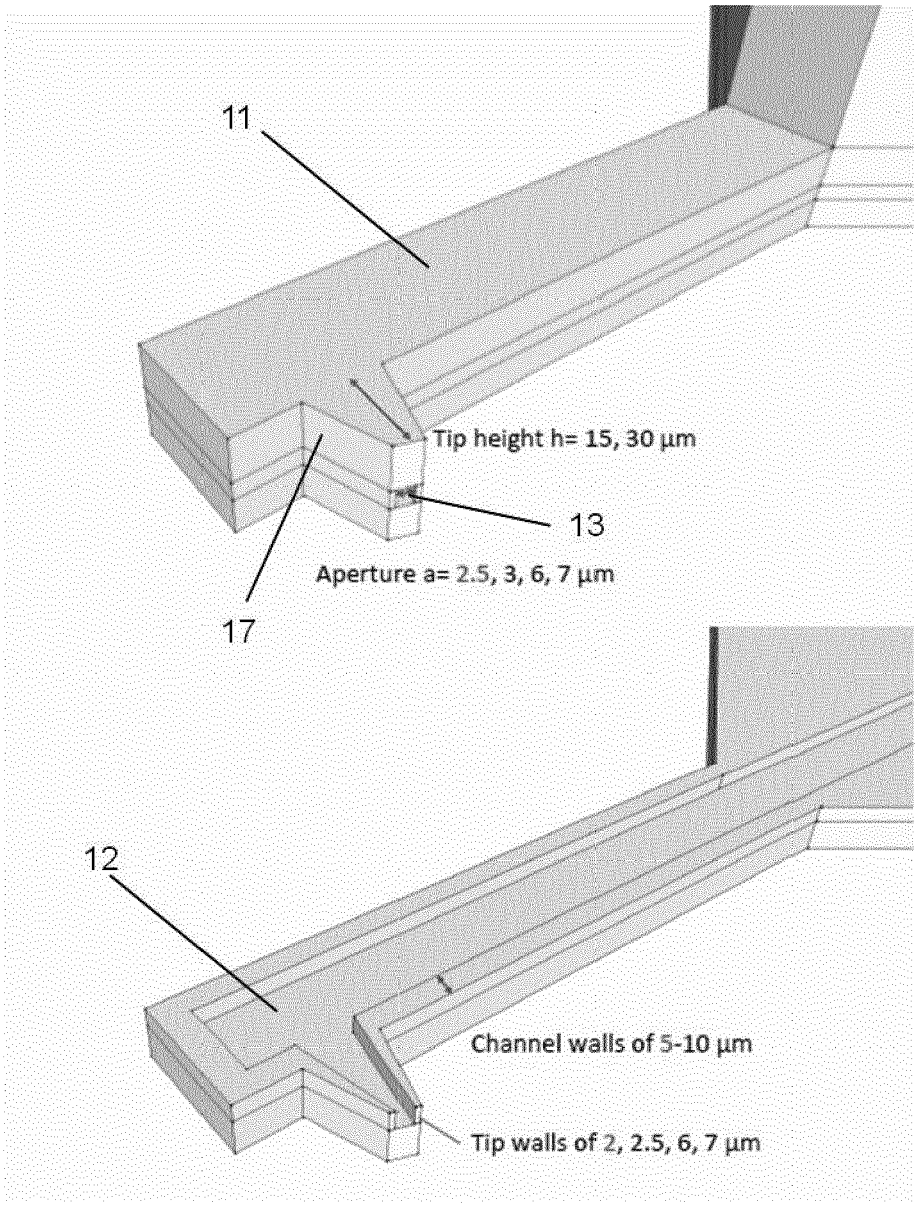
11
Tip height h= 15, 30 µm
13
Aperture a= 2.5, 3, 6, 7 µm
17
12
Channel walls of 5-10 µm
Tip walls of 2, 2.5, 6, 7 µm

Fig. 31A

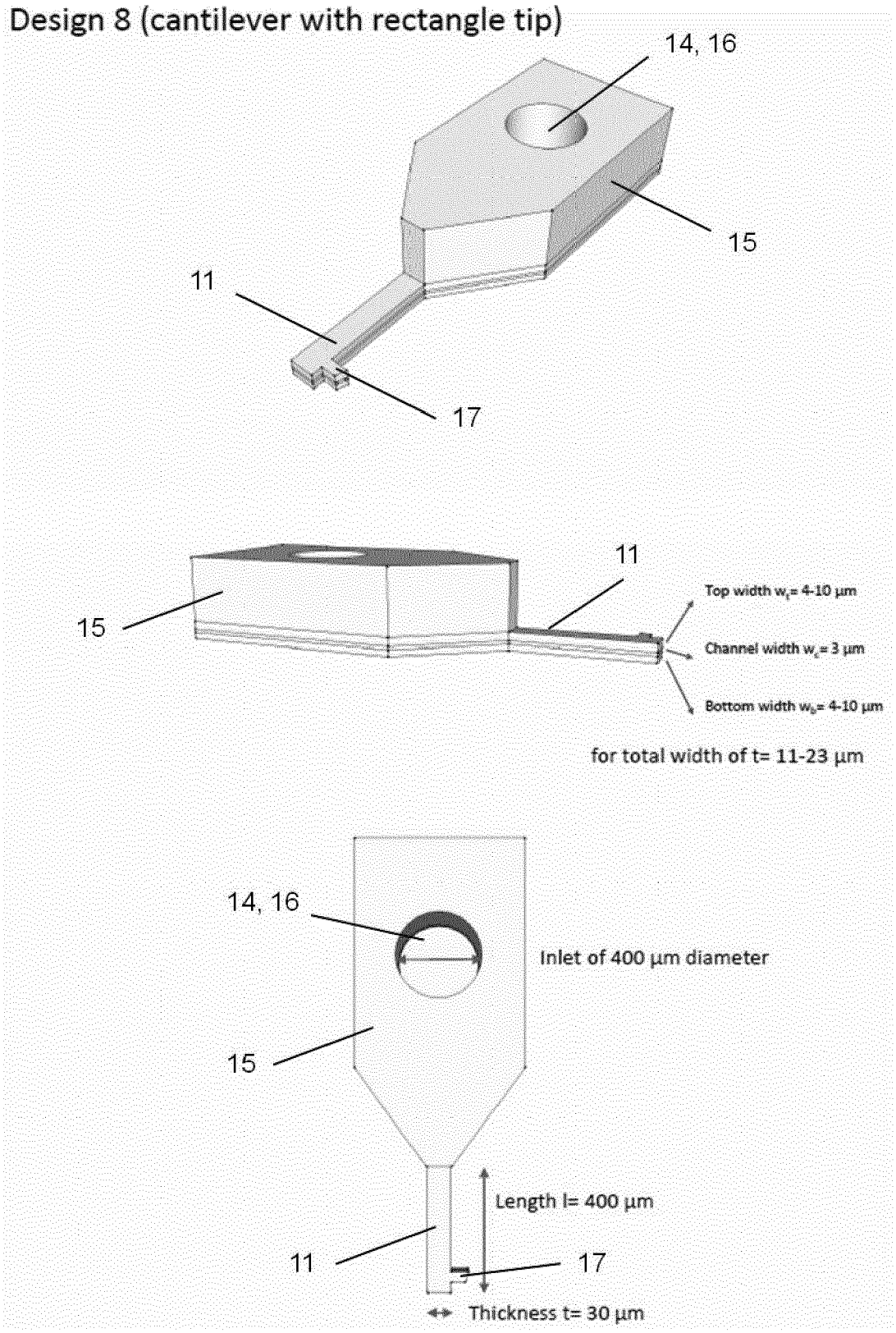
Design 8 (cantilever with rectangle tip)
14, 16
15
11
17
11
15
Top width w_t= 4-10 µm
Channel width w_c= 3 µm
Bottom width w_b= 4-10 µm
for total width of t= 11-23 µm
14, 16
Inlet of 400 µm diameter
15
Length l= 400 µm
11
17
Thickness t= 30 µm

Fig. 31B

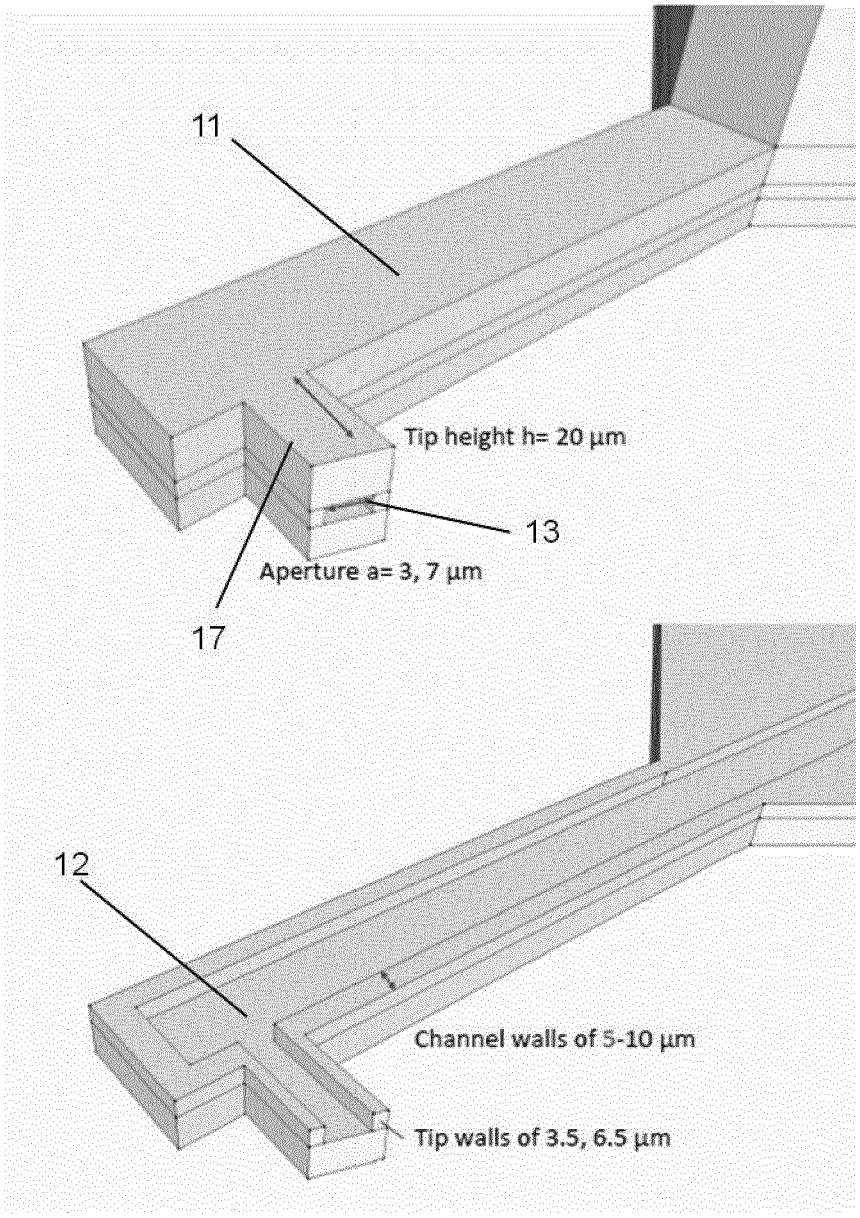
11
Tip height h= 20 µm
13
Aperture a= 3, 7 µm
17
12
Channel walls of 5-10 µm
Tip walls of 3.5, 6.5 µm

Fig. 32A

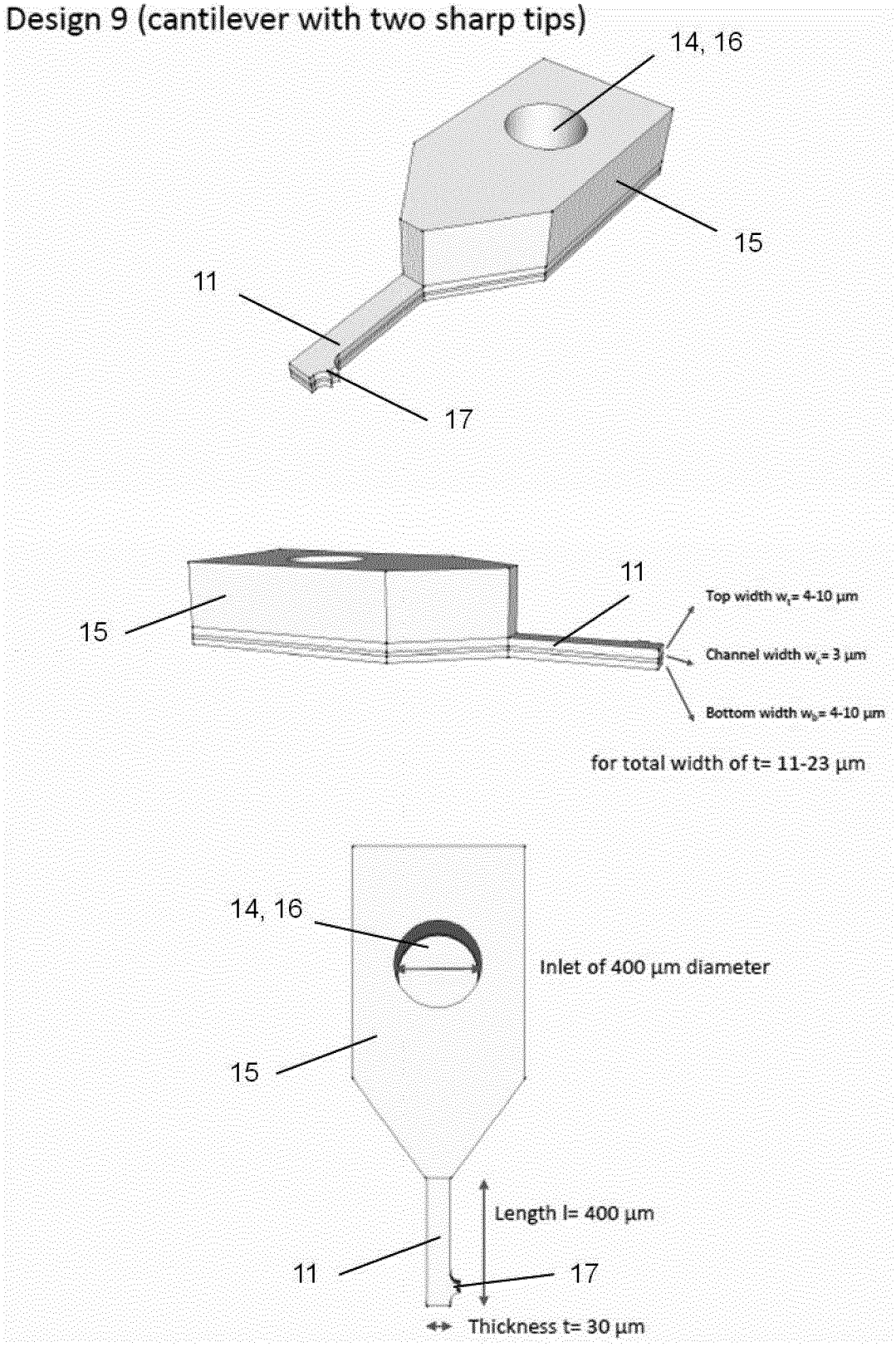
Design 9 (cantilever with two sharp tips)
14, 16
15
11
17
11
15
Top width w_t= 4-10 µm
Channel width w_c= 3 µm
Bottom width w_b= 4-10 µm
for total width of t= 11-23 µm
14, 16
Inlet of 400 µm diameter
15
Length l= 400 µm
11
17
Thickness t= 30 µm

Fig. 32B

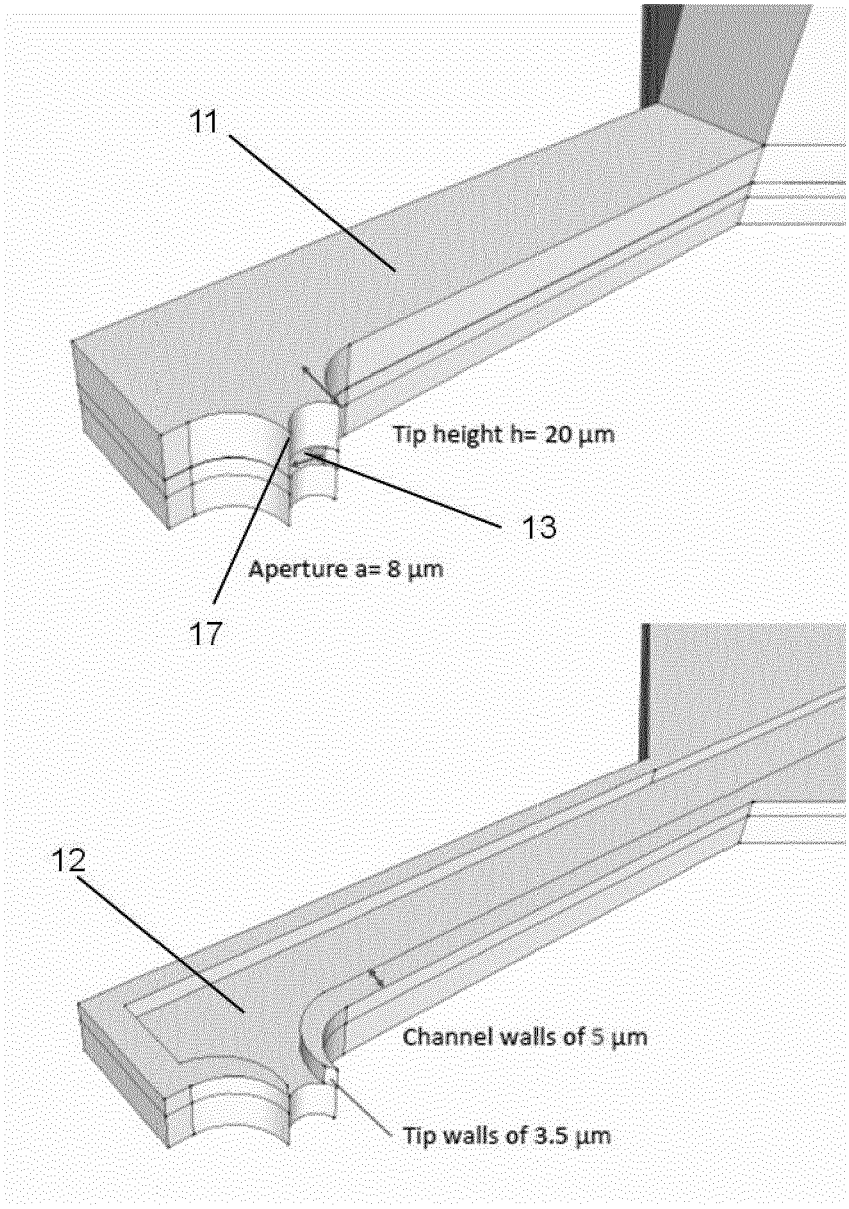
11
Tip height h= 20 µm
13
Aperture a= 8 µm
17
12
Channel walls of 5 µm
Tip walls of 3.5 µm

Fig. 33A

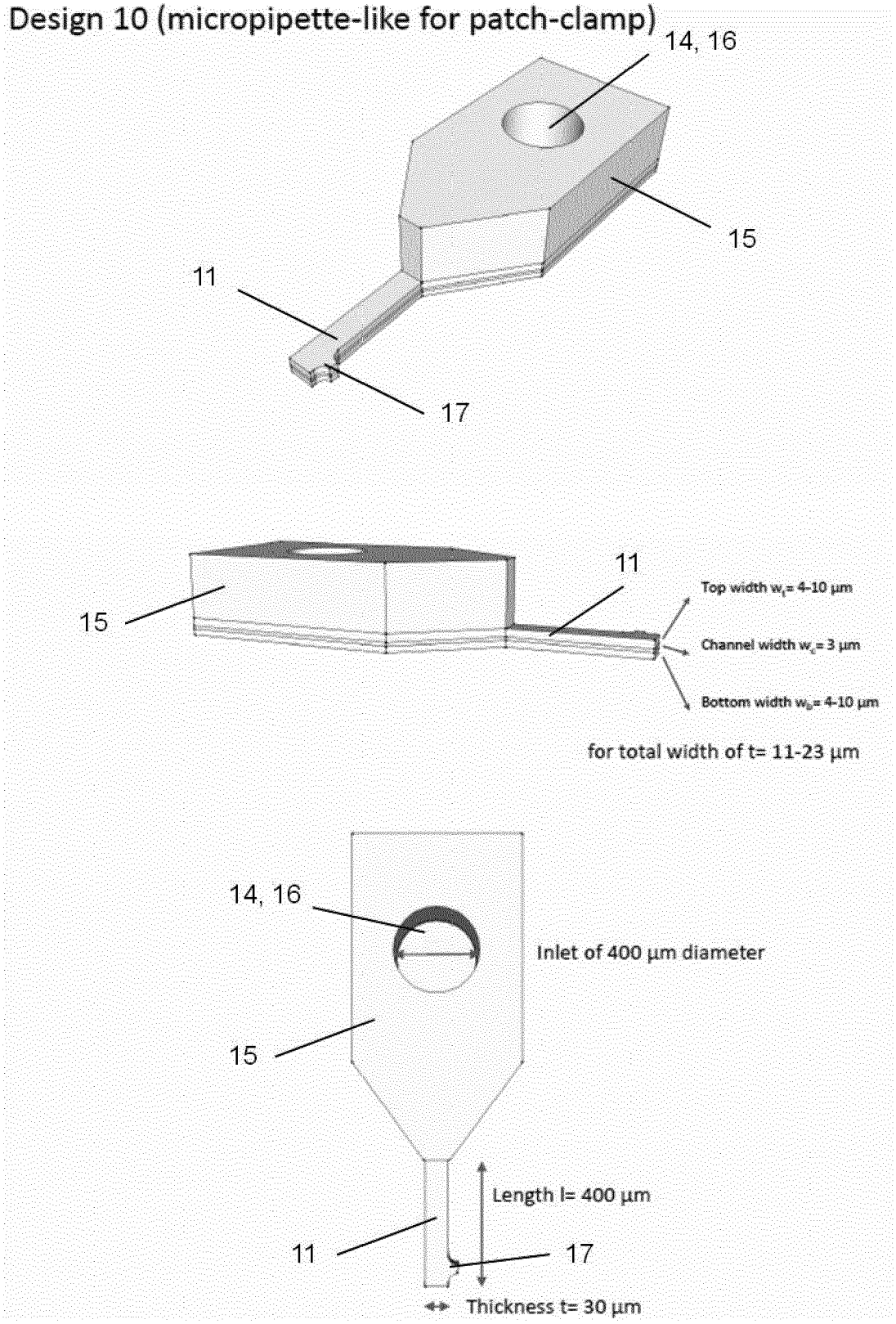
Design 10 (micropipette-like for patch-clamp)
14, 16
15
11
17
11
15
Top width w_t= 4-10 µm
Channel width w_c= 3 µm
Bottom width w_b= 4-10 µm
for total width of t= 11-23 µm
14, 16
Inlet of 400 µm diameter
15
Length l= 400 µm
11
17
Thickness t= 30 µm

Fig. 33B

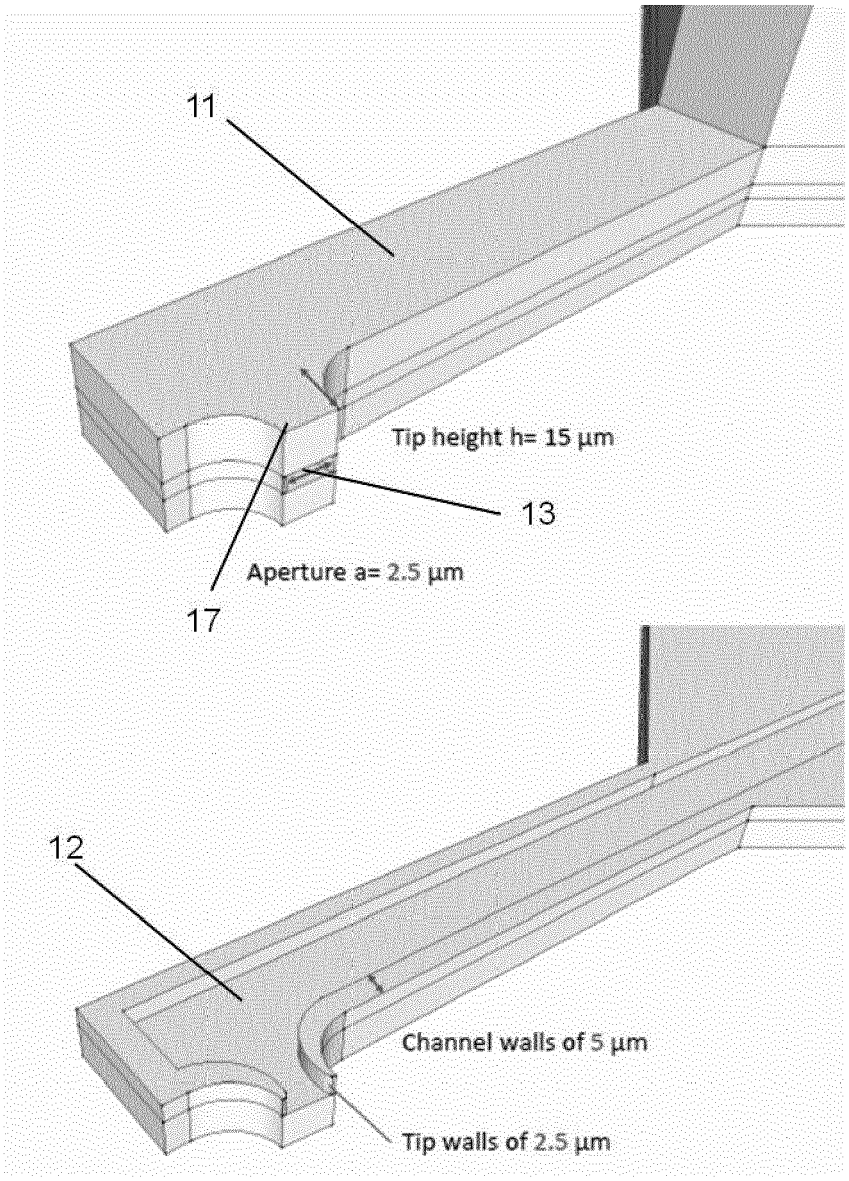
11
Tip height h= 15 µm
13
Aperture a= 2.5 µm
17
12
Channel walls of 5 µm
Tip walls of 2.5 µm

Europäisches Patentamt
European Patent Office
Office européen des brevets

EUROPEAN SEARCH REPORT

Application Number
EP 16 16 1648

DOCUMENTS CONSIDERED TO BE RELEVANT

Category	Citation of document with indication, where appropriate, of relevant passages	Relevant to claim	CLASSIFICATION OF THE APPLICATION (IPC)
A	WO 2014/139031 A1 (UNIV CONCORDIA [CA]) 18 September 2014 (2014-09-18) * the whole document *	1-15	INV. B01L3/00
X	ANGELO GAITAS ET AL: "SU-8 microcantilever with an aperture, fluidic channel, and sensing mechanisms for biological and other applications", JOURNAL OF MICRO/NANOLITHOGRAPHY, MEMS, AND MOEMS, vol. 13, no. 3, 15 September 2014 (2014-09-15), page 030501, XP055300803, US ISSN: 1932-5150, DOI: 10.1117/1.JMM.13.3.030501 * the whole document *	1-7 8-15	
X	VINCENT MARTINEZ ET AL: "Controlled single-cell deposition and patterning by highly flexible hollow cantilevers", LAB ON A CHIP: MINIATURISATION FOR CHEMISTRY, PHYSICS, BIOLOGY, MATERIALS SCIENCE AND BIOENGINEERING, vol. 16, no. 9, 9 February 2016 (2016-02-09), pages 1663-1674, XP055300678, GB ISSN: 1473-0197, DOI: 10.1039/C5LC01466B * abstract * * page 1664 - page 1665 * * figures S1A, S1B *	8-15	TECHNICAL FIELDS SEARCHED (IPC) B01L

-/--

The present search report has been drawn up for all claims

Place of search	Date of completion of the search	Examiner
The Hague	12 September 2016	Sinn, Cornelia

CATEGORY OF CITED DOCUMENTS

X : particularly relevant if taken alone
Y : particularly relevant if combined with another document of the same category
A : technological background
O : non-written disclosure
P : intermediate document

T : theory or principle underlying the invention
E : earlier patent document, but published on, or after the filing date
D : document cited in the application
L : document cited for other reasons

& : member of the same patent family, corresponding document

EPO FORM 1503 03.82 (P04C01)

Europäisches Patentamt
European Patent Office
Office européen des brevets

EUROPEAN SEARCH REPORT

Application Number
EP 16 16 1648

DOCUMENTS CONSIDERED TO BE RELEVANT

Category	Citation of document with indication, where appropriate, of relevant passages	Relevant to claim	CLASSIFICATION OF THE APPLICATION (IPC)
T	VINCENT MARTINEZ ET AL: "SU-8 hollow cantilevers for AFM cell adhesion studies", JOURNAL OF MICROMECHANICS & MICROENGINEERING, INSTITUTE OF PHYSICS PUBLISHING, BRISTOL, GB, vol. 26, no. 5, 5 April 2016 (2016-04-05), page 55006, XP020302064, ISSN: 0960-1317, DOI: 10.1088/0960-1317/26/5/055006 [retrieved on 2016-04-05] * the whole document * -----		

TECHNICAL FIELDS SEARCHED (IPC)

The present search report has been drawn up for all claims

Place of search	Date of completion of the search	Examiner
The Hague	12 September 2016	Sinn, Cornelia

CATEGORY OF CITED DOCUMENTS

X : particularly relevant if taken alone
Y : particularly relevant if combined with another document of the same category
A : technological background
O : non-written disclosure
P : intermediate document

T : theory or principle underlying the invention
E : earlier patent document, but published on, or after the filing date
D : document cited in the application
L : document cited for other reasons

& : member of the same patent family, corresponding document

EPO FORM 1503 03.82 (P04C01)

ANNEX TO THE EUROPEAN SEARCH REPORT ON EUROPEAN PATENT APPLICATION NO. EP 16 16 1648

This annex lists the patent family members relating to the patent documents cited in the above-mentioned European search report. The members are as contained in the European Patent Office EDP file on
The European Patent Office is in no way liable for these particulars which are merely given for the purpose of information.

12-09-2016

Patent document cited in search report	Publication date	Patent family member(s)	Publication date
WO 2014139031 A1	18-09-2014	CA 2906237 A1	18-09-2014
		US 2016033403 A1	04-02-2016
		WO 2014139031 A1	18-09-2014

EPO FORM P0459

For more details about this annex : see Official Journal of the European Patent Office, No. 12/82

REFERENCES CITED IN THE DESCRIPTION

This list of references cited by the applicant is for the reader's convenience only. It does not form part of the European patent document. Even though great care has been taken in compiling the references, errors or omissions cannot be excluded and the EPO disclaims all liability in this regard.

Patent documents cited in the description

- EP 15171419 A **[0069]**